Enhancing Traffic Control Systems to Reduce Emissions and Fuel Consumption

Date: June 2016

Andrew P. Nichols, PhD, Professor, Marshall University
Montasir Abbas, PhD, Associate Professor, Virginia Tech
Byungkyu Brian Park, PhD, Associate Professor, University of Virginia
Hesham A. Rakha, PhD, P.Eng, Professor, Virginia Tech

Prepared by:
Marshall University
One John Marshall Drive
Huntington, WV 25755

Prepared for:
Virginia Center for Transportation Innovation and Research
530 Edgemont Road
Charlottesville, VA 22903

1. Report No.	2. Government Accession No.	3. Recipient's Catalog No.
4. Title and Subtitle Enhancing Traffic Control Systems to Reduce Emissions and Fuel Consumption		**5. Report Date** **6. Performing Organization Code**
7. Author(s) Andrew P. Nichols, Montasir Abbas, Byungkyu Brian Park, Hesham A. Rakha		**8. Performing Organization Report No.**
9. Performing Organization Name and Address Marshall University One John Marshall Drive Huntington, WV 25755		**10. Work Unit No. (TRAIS** **11. Contract or Grant No.** DTRT13-G-UTC33
12. Sponsoring Agency Name and Address US Department of Transportation Office of the Secretary-Research UTC Program, RDT-30 1200 New Jersey Ave., SE Washington, DC 20590		**13. Type of Report and Period Covered** Final 7/1/14 – 6/10/16 **14. Sponsoring Agency Code**

15. Supplementary Notes

16. Abstract

This report contains four sub-reports on research tasks that were completed related to the enhancement of traffic control to reduce emissions and fuel consumption. The first task looks at the type of control to implement at an intersection, based on minimizing emissions. Assuming that an intersection is signalized, the second tasks look at the optimal cycle length that should be selected to minimize emissions and fuel consumption. Once a signalized intersection has been deployed, the third and fourth tasks look at new ways to evaluate traffic signal performance related to emergency vehicle preemption using high resolution data and optimizing timing plans based on emissions.

17. Key Words	18. Distribution Statement
traffic signal warrant, MUTCD, emissions, mobility, VISSIM microscopic traffic simulation, cycle length, optimization, fuel consumption, high resolution data, performance measures, emergency vehicle preemption, Classifier; Regression; Discriminant analysis; VT-Micro; AnyLogic; Flowchart; Traffic flow; Simulation; Offset; Acceleration; Speed	No restrictions. This document is available from the National Technical Information Service, Springfield, VA 22161

19. Security Classif. (of this report)	20. Security Classif. (of this page)	21. No. of Pages	22. Price
Unclassified	Unclassified	124	

Executive Summary

This report contains four sub-reports on research tasks that were completed related to the enhancement of traffic control to reduce emissions and fuel consumption. The first task looks at the type of control to implement at an intersection, based on minimizing emissions. Assuming that an intersection is signalized, the second tasks look at the optimal cycle length that should be selected to minimize emissions and fuel consumption. Once a signalized intersection has been deployed, the third and fourth tasks look at new ways to evaluate traffic signal performance related to emergency vehicle preemption using high resolution data and optimizing timing plans based on emissions.

Task 1. Exploring Environmentally Sustainable Traffic Signal Warrant for Planning Application. With the concerns over the greenhouse gas (GHG) emissions associated with the surface transportation, the environmentally sustainable traffic signal warrant is essential to provide guidelines for making environmentally conscious decisions about control types at intersections. A pilot study was conducted on developing CO2 emissions-oriented traffic signal warrants. Intersection control types that were analyzed for this study include two-way stop, four-way stop, traffic signal and roundabout. Two environmentally sustainable traffic signal warrants were proposed: Type I (without roundabout) and Type II (with roundabout). The proposed traffic signal warrants were compared with the existing mobility-oriented traffic signal warrant of the Manual on Uniform Traffic Control Devices (MUTCD) in terms of CO2 emissions and total delay. The measurements were collected and estimated using a microscopic traffic simulation tool, VISSIM. The environmentally sustainable traffic signal warrants show that the annual CO2 emissions of the ground transportations in the USA were reduced by 7.15% with Type I warrant and 13.75% with Type II warrant.

Task 2. Optimizing Isolated Traffic Signal Timing Considering Energy and Environmental Impacts
Traffic signal cycle lengths are typically designed to minimize the intersection vehicle delay using the Webster formula. The objectives of this study are two-fold. First, it validates the Webster formula using simulated data. Second, it develops new formulations to compute the optimum cycle length considering other measures of effectiveness, including vehicle fuel consumption levels and tailpipe emissions. The microscopic simulation software, INTEGRATION, is used to simulate an isolated intersection controlled by a two-phase traffic signal over a range of cycle lengths, traffic demand levels, and signal timing lost times. Intersection delay, fuel consumption levels, and hydrocarbon, carbon monoxide, oxides of nitrogen, and carbon dioxide emissions were derived from the simulation model. The cycle lengths that minimized the measures of effectiveness were then used to develop the proposed models. The first effort entailed re-calibrating the Webster model to the simulated data. The second effort entailed enhancing the Webster model by incorporating an additional intercept term. The model estimates produce shorter cycle lengths when compared to the Webster model and also considers fuel consumption and Green House Gas (GHG) emissions in the optimization procedure.

Task 3. Characterizing Emergency Vehicle Operation Using High Resolution Traffic Signal Event Data

This research proposes the use of a signal phase spectrum (SPS) plot to analyze high resolution traffic signal event data. Specifically, the controller performance related to emergency vehicle preemption operation is characterized in an effort to identify performance measures that will allow a traffic engineer to better understand the impact that various configurations have on intersection operations. Performance measures for individual intersections in coordinated systems including preemption duration, transition duration, and total interruption time. Performance measures for networks are based on an emergency vehicle re-identification process for deriving an emergency vehicle's trajectory through a network, and the results can further be used to estimate travel time, travel speed, and origin-destination. These performance measures are illustrated using a simulated signal system in Morgantown, WV. Transition modes are varied in the simulation network to determine the relative performance measures. Case studies are presented for using high resolution data to troubleshoot field preemption operation using the Morgantown, WV and Huntington, WV signal systems.

Task 4. Emissions-Based Performance Assessment of Traffic Control Using High Resolution Data

This study presents the outcome of efforts to leverage high resolution data to develop online models that can be used to assess the performance of control strategies in terms of vehicle emissions. The proposed model was developed and implemented in the AnyLogic framework to simulate a network in WV-705 corridor in Morgantown, WV, with four coordinated intersections. The simulation was also used to calculate vehicle CO, HC, NOx emissions with the aid of the VT-Micro microscopic emission model. Offset variation was run to determine the optimal offsets for this particular road network with traffic volume, signal phase diagram and vehicle characteristics. Significant combination of attributes of HRD were utilized to develop robust statistical classifiers. The developed classifiers were able distinguish between set of timing plans that produce maximum emissions from those that result in minimum emissions. In addition, two flowcharts were developed to model the presence of Emergency Vehicle Preemption (EVP) in the system. Three scenarios were implemented and evaluated, namely, No-EVP, EVP, and EVP with traffic yielding the right-of-way to EV. Emission results of these scenarios were analyzed and compared to find out whether EV affect vehicle emissions on the road network and what the level of this influence is, if any.

Sub-report Task #1

Exploring Environmentally Sustainable Traffic Signal Warrant for Planning Application

Prepared by:

Seongah Hong
Research Assistant
University of Virginia

Jia Hu, Ph.D.
Research Associate
Turner Fairbank Highway Research Center

Byungkyu Brian Park, Ph.D.
Associate Professor
University of Virginia

Acknowledgments

The authors would like to thank a research group at the Turner-Fairbank Highway Research Center including Taylor W. P. Lochrane, Dr. Joe Bared, Dr. Daniel J. Dailey and Dr. Wei Zhang, and Dr. Nopadon Kronprasert at Virginia Tech for providing the simulation model of roundabout which was used to build a part of the simulation testbeds of this research. This research project was in part supported by the Global Research Laboratory Program through the national Research Foundation of Korea (NRF) funded by the Ministry of Science, ICT & Future Planning (2013K1A1A2A02078326) as well as Mid-Atlantic Transportation Sustainability University Transportation Center.

Disclaimer

Table of Contents

List of Figures

List of Tables

1. Problem

Transportation sector accounts for about 28 percent of greenhouse gas (GHG) emissions in the United States (U.S. Department of Transportation, 2015) and about 25 percent of the total energy consumption in developed countries (World Energy Council, 2007). GHG emissions have become a major cause of environmental pollutants that could lead to global warming and human health problems. Among different types of GHGs such as carbon dioxide (CO2), methane, nitrous oxide (NOx), etc., CO2 imposes major impacts on world climate due to its largest quantity present in the air, the longest atmospheric lifetime, and the most rapid increase rate (US EPA, 2014). In 2011, CO2 accounted for about 73% of total GHG emissions and Annual Greenhous Gas Index (AGGI) which measures greenhouse effect indicated that CO2 was at 1.3 while the other types of emissions remained less than 0.5 (NOAA, 2012).

In a roadway network, most CO2 emissions come from controlled intersections where the most speed variations take place when vehicles stop and accelerate. According to the Manual on Uniform Traffic Control Devices (MUTCD) (FHWA, 2009), traffic signal is a device for controlling vehicular and pedestrian traffic by assigning the right-of-way to various traffic movements. Many studies proposed strategies in terms of intersection control devices to improve environmental sustainability performances, such as optimizing vehicles' approaching behaviors (van Katwijk and Gabriel, 2015), determining signal phases and timing scheme (Park and Kamarajugadda, 2007; Park et al., 2009; Khalighi and Christofa, 2015; Lee et al., 2015), intelligent cooperation between signal control and approaching vehicles (Hu et al., 2014; Hu et al., 2015), and refining lane configurations (Bing et al., 2014). Although they all showed their merits in reducing emissions, the point that was indiscreetly presumed was that they accepted the current intersection control types as it was. One question to ask before one tries to invent a complicated application is this: Has the appropriate intersection control type been chosen?

There are different types of intersection control strategies, including but not limited to 2-way stop control (2WSC), 4-way stop control (4WSC), traffic signal and roundabout. To provide guidance to engineers and other practitioners in terms of determination of intersection control types, various traffic signal warrants have been developed throughout the world. The first framework of traffic signal warrant was published by American Association of State Highway Officials (AASHO) in 1935 by the name of MUTCD (AASHO, 1935). It has been continuously revised to construct current framework which has been most widely adopted both in the US and abroad (FHWA, 2009). The countries that do not use the MUTCD traffic signal warrant include United Kingdom, New Zealand, Canada and South Africa (Sampson, 1999), yet those traffic signal warrants use similar criteria as the MUTCD warrant; they consider either mobility, safety or a combination of the two criteria. This report adopted the MUTCD traffic signal warrant as a baseline to be compared with the proposed traffic signal warrant, since it could be a fair representation of various traffic signal warrants around the globe.

Since the MUTCD traffic signal warrant was developed, there have been many efforts to propose alternative traffic signal warrants utilizing various quantitative criteria, such as gap-based criterion (Neudorff, 1985), peak-hour conflicting turning movement volumes (Bretherton and Elhaj, 1994), and average queue length (Sampson, 1999). In addition, the Highway Capacity Manual (HCM) guideline (TRB, 2010) introduced the traffic signal warrant that was developed

based on the peak hour volumes and several mobility measurements such as delay, volume to capacity (v/c) ratio and average queue length (Marek et al., 1997). Nevertheless, these alternative traffic signal warrants proposed the criteria that heavily relied on mobility. No emission-oriented warrant has been invented, while it has been shown that environmental sustainability performances do not always comparable with mobility performance and improving mobility could sometimes lead to sacrificing in emissions (Park et al., 2009; Guo and Zhang, 2014).

2. Approach

Therefore, the objective of this research is to develop a pilot guideline of traffic signal warrant using environmental sustainability criteria of CO_2 emissions, which is applicable at the planning level. Through this effort, the research team aims to demonstrate the significant difference between the emission-based warrant and the mobility-based warrant and quantify the benefits of environmental sustainability and effects on mobility.

3. Methodology

A traffic signal warrant developed based on CO2 emissions was explored and evaluated by comparing the developed traffic signal warrant to the existing MUTCD traffic signal warrant. The scope of this report was limited to the four intersection control types including 2WSC, 4WSC, traffic signal control, and roundabout. Two types of signal warrants were developed, i.e., Type I environmentally sustainable traffic signal warrant which did not include roundabout control and Type II environmentally sustainable traffic signal warrant that included roundabout control. Type I traffic signal warrant was included for a fair comparison with the baseline traffic signal warrant of MUTCD which did not include a roundabout. The measures of effectiveness (MOEs) adopted were CO2 emissions and total vehicle delay, which were collected from the microscopic traffic simulation software, called VISSIM (Verkehr In Stadten – SIMulationsmodell). Minimum sample size requirements were examined for both MOEs. Statistical tests were conducted to ensure statistical significance of the conclusions drawn. Detailed information is provided in the following subsections.

3.1. Baseline Signal Warrant

The existing MUTCD guidelines contain the nine different traffic signal warrants using various criteria. Among them, the three warrants (i.e., Warrant 1 through Warrant 3) use traffic volumes as their criteria with different temporal scopes of consideration (i.e., 8-hour, 4-hour and a peak hour). This research adopted the peak-hour volume warrant (i.e., Warrant 3) as the baseline to emphasize on the most critical period for operations. As shown in Figure 1, the Warrant 3 provides the volume thresholds to warrant a traffic signal. That is, if the traffic volume scenario falls above the correspondent threshold curve, the need for the traffic signal control shall be considered. It should be noted that the major street volume is represented as the total volume of both approaches and the minor street volume is represented as the higher volume between the two opposing approaches. Appropriate curve shall be referred to depending on the number of lanes of intersection approaches. For comparison and evaluation purposes, the baseline traffic signal warrant was reformatted into as in Figure 2 to match the format of the proposed

environmentally sustainable traffic signal warrant. In Figure 2, both x-axis and y-axis represent the total volumes of the opposing approaches.

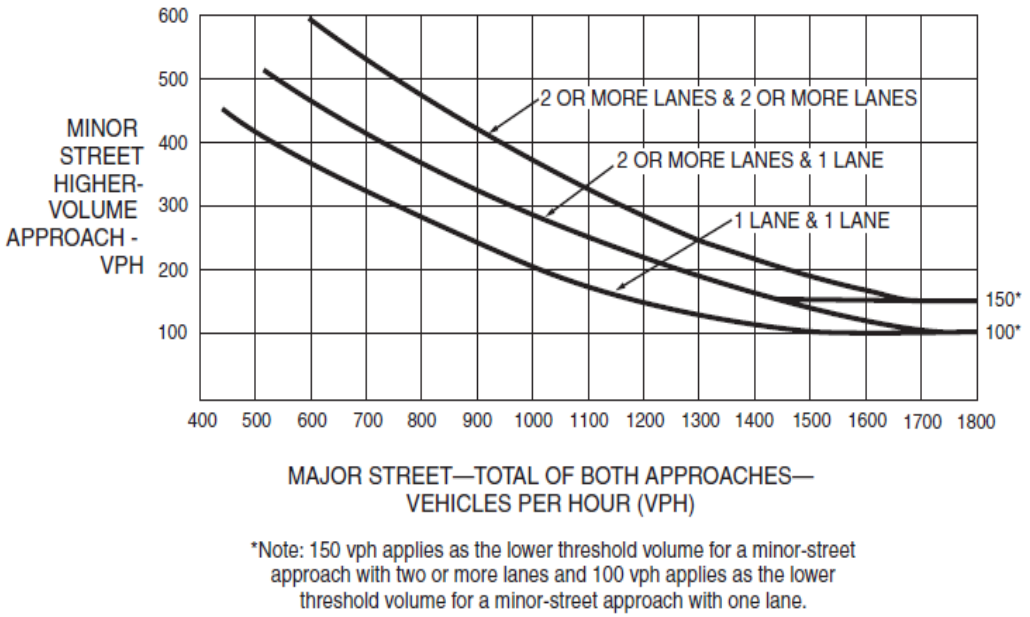

Figure 1 MUTCD signal Warrant 3

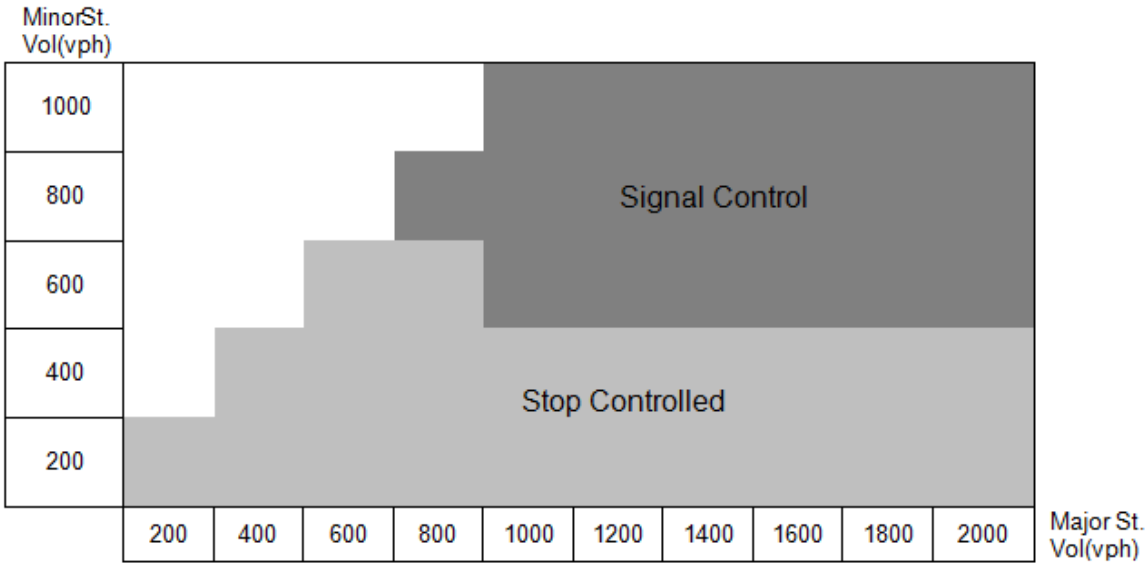

Figure 2 Representation of the existing MUTCD traffic signal warrant

3.2. Development of Testing Scenarios

A set of 40 scenarios with various traffic volumes was tested. As shown in Figure 3, the traffic volumes in the major street ranged from 200 to 2,000 veh/hr and the traffic volumes in the minor street ranged from 200 to 1,000 veh/hr with the 200 veh/hr of increments for both. Again, these volumes represent the summations of both directions. Through the remainder of this report, each

scenario was referred to by its traffic volume levels. For example, for the scenario with 600 veh/hr on major street and 200 veh/hr on minor street, the scenario was referred to as (600, 200).

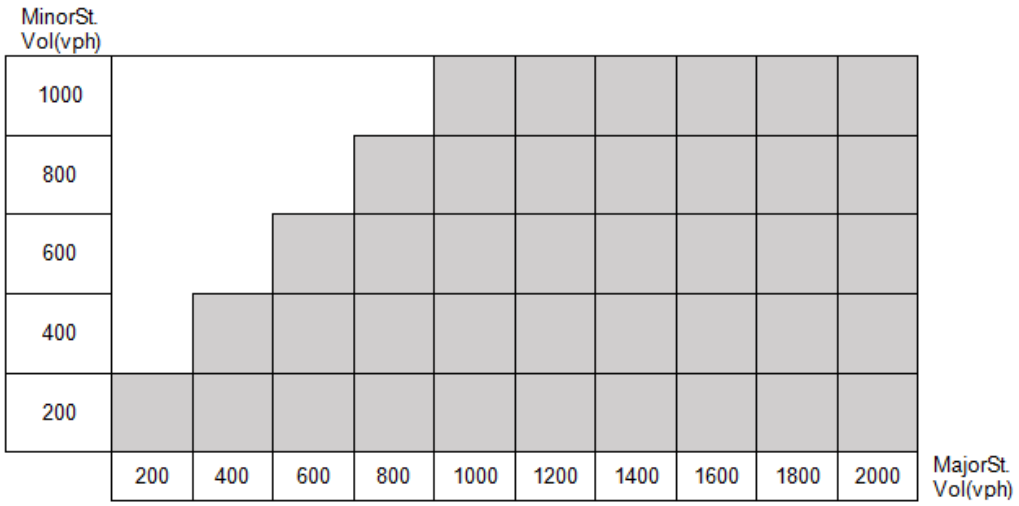

Figure 3 Traffic signal warrant volume scale

3.3. Measures of Effectiveness (MOEs)

The MOEs selected in this report were CO2 emissions and total vehicle delay. The total vehicle delay is defined as the difference between actual travel time and free-flow travel time as in equation (1):

$$Total\ Delay = \sum_{t=1}^{T}\sum_{i=1}^{N}\left(TT_{actual}^{i} - TT_{freeflow}^{i}\right) \quad (1)$$

in which T represents total simulation period in the unit of second, N represents total number of vehicles during simulation period, TT_{actual}^{i} represents actual travel time of vehicle i and $TT_{freeflow}^{i}$ represents free-flow travel time with desired speed of vehicle i.

The CO2 emissions were estimated using Virginia Tech's Microscopic energy and emissions model (VT-Micro) (Ahn et al., 2002). The VT-Micro model is a dual-regime regression model which requires vehicles' trajectory information as an input. Its formula is demonstrated in equation (2):

$$MOE_e = \begin{cases} \exp\left(\sum_{i=0}^{3}\sum_{j=0}^{3}\left(L_{i,j}^{e} \times u^{i} \times a^{j}\right)\right) for\ a \geq 0 \\ \exp\left(\sum_{i=0}^{3}\sum_{j=0}^{3}\left(M_{i,j}^{e} \times u^{i} \times a^{j}\right)\right)\ for\ a < 0 \end{cases} \quad (2)$$

in which MOEe is the instantaneous emission rate (mg/s), Lei,j and Mei,j are the model regression coefficients for MOE "e" at speed power "i" and acceleration power "j" when accelerations are positive and negative, respectively, u is the instantaneous vehicle speed (km/h), and a is the instantaneous vehicle acceleration (m/s2). In this report, a set of parameters of the VT-Micro model which were calibrated under the urban intersection environment (Lee, et al., 2013) was adopted.

3.4. Minimum Sample Size Requirement

By the nature of simulation models, the output is subject to the randomness. The minimum sample size requirement of each MOE was attained with repetition of simulation runs to ensure statistically significant comparison results. Virginia Department of Transportation (VDOT, 2013) provides a methodology to examine the minimum required number of simulation runs as shown in equation (3):

$$N = Z^2 \frac{S_S^2}{E^2} \quad (3)$$

in which N is the minimum sample size, Z is the number of standard deviations away from the mean corresponding to the required confidence level (Z = 1.96 at the confidence level of 95%), Ss is the sample standard deviation, and E is the tolerable error in terms of the sample mean. In this report, the number of initial simulation runs was chosen as 10 times, and the minimum sample sizes of the selected MOEs were calculated at confidence level of 95th percentile. Additional simulation runs were performed when minimum sample size was more than 10.

3.5. Development of Environmentally Sustainable Traffic Signal Warrants

The environmentally sustainable signal warrant was developed by identifying which intersection control type yielded the least CO2 emissions while satisfying the delay thresholds for each of different traffic volume scenario. It is important to note that statistical tests (e.g., ANOVA test and t-test) were thoroughly conducted to examine the significance of difference in CO2 emissions among the control types considered. By doing so, two environmentally sustainable traffic signal warrants were developed: Type I traffic signal warrant considering the three intersection control types including 2WSC, 4WSC and traffic signal; and Type II traffic signal warrant additionally including a roundabout.

In order to ensure that delay remained at acceptable levels even though environmental criteria were prioritized, the two minimum thresholds related to delay measurements were adopted. The first threshold restrained the maximum delay within the controlled approach to be less than the criteria of the level of service (LOS) E from the HCM guidelines (TRB, 2010). The LOS E is an indication that the traffic is nearly operated at capacity and likely to break down and the drivers' level of comfort becomes poor (Papacostas and Prevedourous, 2001). According to the HCM guidelines (TRB, 2010), the delay criteria of LOS E at a stop-controlled intersection (i.e., 2WSC or 4WSC) is 50 sec/veh, and that of a signalized intersection is 80 sec/veh. Different criterion was applied on different intersection control type. The threshold of average delay on the minor street is expressed in equation (4)

$$Average\ Delay_{minor}(sec/veh) \leq \alpha \quad (4)$$

where α is 50 sec/veh for the unsignalized control case and 80 sec/veh for the signalized control. The average delay in equation (4) was estimated as in equation (5):

$$Average\ Delay_{minor}(sec/veh) = \frac{\sum_{t=1}^{T}\sum_{i=1}^{N}(TT_{actual}^{i} - TT_{freeflow}^{i})}{N} \quad (5)$$

Another threshold of delay was developed to ensure that the warranted traffic control type was overall beneficial. The increase in delay may be evitable when prioritizing emissions. However,

the increase rate in delays were kept less than the reduction rates of CO2 emissions to guarantee the overall gains to the system. Technically, in each traffic volume scenario, percentage change rate of delay was compared against to that of CO2 emissions for all control types. Only the control types generating higher emissions savings rates over the delay increase rates were kept as potential candidates, as shown in equation (6).

$$R^k_{delay} \leq R^k_{CO2} \tag{6}$$

in which k is scenario index, R^k_{delay} (%) represents the percentage change rate in delay for scenario k and R^k_{CO2} (%) represents the percentage change rate in CO2 emissions for scenario k. R^k_{delay} and R^k_{CO2} are defined as in equations (7) and (8):

$$R^k_{delay}(\%) = \frac{Delay^k_{Env} - Delay^k_{Base}}{Delay^k_{Base}} \times 100 \tag{7}$$

$$R^k_{CO2}(\%) = \frac{CO2^k_{Env} - CO2^k_{Base}}{CO2^k_{Base}} \times 100 \tag{8}$$

in which k is scenario index, $Delay_{Env}$ and $CO2_{Env}$ represent delay and CO2 emissions under the environmentally sustainable traffic signal warrant, $Delay_{Base}$ and $CO2_{Base}$ represent delay and CO2 emissions under the baseline of MUTCD traffic signal warrant.

3.6. Assessment of Environmentally Sustainable Traffic Signal Warrant

The monetized values of CO2 emissions and delay associated with the implementation of the proposed traffic signal warrant were estimated. For the purpose of this assessment, the following facts and assumptions were utilized. According to the FHWA statistics (US DOT, 2010), there are approximately 300,000 intersections in the US. To estimate the national annual total benefits, it was assumed that intersection facilities are evenly distributed among different traffic volumes scenarios. Based on the 2011 CAFÉ regulations (NHTSA, 2015), the global social benefit of unit CO2 emissions reduction was estimated as $33 per ton in 2007 dollars with an annual interest rate of 2.4 percent (NHTSA, 2015). The changes in the delay performance were monetized based on the value of commuting time which was estimated as $9.96/hour when the average wage rate was assumed as $21.20/hour (Koppelman and Bhat, 2006). The monetized benefits from CO2 emissions reduction and delay reductions were estimated as shown in equations (9) and (10):

$$Q_{CO2} = (\text{Total } CO_2 \text{ reductions}) \times \frac{0.0011 \text{ ton}}{1 \text{ kg}} \times \$33 \times (1 + 0.024)^{(2015-2007)\text{yr}} \tag{9}$$

$$Q_{delay} = (\text{Total delay reduction}) \times \frac{\$21.20}{1 \text{ hr}} \times 0.47 \tag{10}$$

in which QCO2 represents the monetized benefit or cost from the changes in CO2 emissions (in dollars) and Qdelay represents the monetized benefit or cost from changes in delay (in dollars). The total benefit (Qtotal) was calculated by adding up the estimations of monetized benefits and costs of CO2 emissions and delay as shown in equation (11):

$$Q_{total} = Q_{CO2} + Q_{delay} \tag{11}$$

3.7. Simulation Model Development

A set of simulation models that was used to collect data was developed using a microscopic traffic simulation software, VISSIM. This section describes the specifications of the developed simulation models, such as geometry configurations, intersection control principles, traffic signal phases and timing plans, model calibration efforts and the simulation settings.

3.7.1 Geometry Configuration of Simulation Testbed

The number of lanes and inclusion of a left-turn bay of each approach were determined by following the HCM guidelines (TRB, 2010). Figure 4 shows intersection geometry configurations utilized in this report. As shown in Figure 4, different geometry configurations were used for different traffic volume scenarios and intersection control types, instead of applying an identical intersection geometry to all control types. This design aligns with the scenario the research was conducted based on which is planning level. At planning level, the intersection geometries should always ensure that all control types operate at their best performance. Details on the geometry design for each intersection control type is provided in the following sections.

In the case of the stop-controlled intersection model, the intersection lane configuration was determined based on the traffic volume combinations of the major street and the minor street using Table 1 of the HCM guidelines (TRB, 2010). The exclusive left-turn lane was provided when the left-turn volume was greater than 150 veh/hr so the impact of major-street left turns on delay becomes noticeable (Roess et al., 2011). Exclusive right-turn lane was not considered, since right-turn vehicles from a major road do not impose a critical impact on the operation of stop-controlled intersections as they mostly do not conflict with vehicles from other directions (Roess et al., 2011).

As to the signalized intersection model, the intersection lane configuration was determined with the strategy to have the maximum total critical-lane volumes to remain acceptable level in reference to Table 2 of the HCM (TRB, 2010). The provision of a left-turn lane for each approach was determined based on the equation (12) or equation (13) of the HCM guidelines (TRB, 2010):

$$v_{LT} \geq 200 \text{ veh/hr} \tag{12}$$

$$xprod = v_{LT} * \left({}^{v_0}/_{N_0}\right) \geq 50{,}000 \tag{13}$$

where v_{LT} is left-turn flow rate (veh/hr), v_0 is opposing through movement flow rate (veh/hr), and N_0 is the number of lanes for opposing through movement. The exclusive right-turn lanes were not provided for the traffic signal control cases as well, since the right-turn volumes used in this study were not so significant to impede the intersection operations.

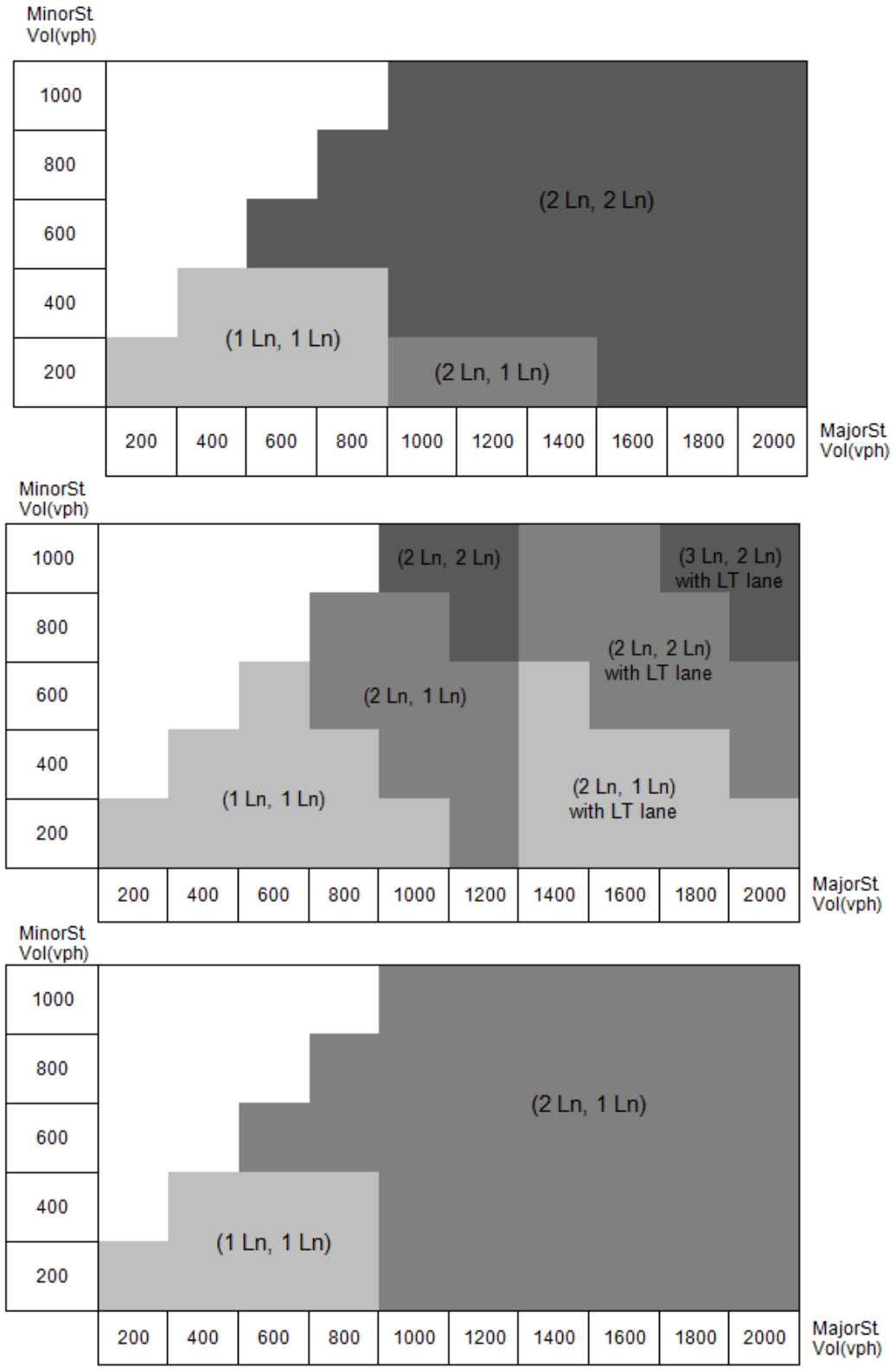

Figure 4 Intersection geometry configuration (Top: stop-controlled intersection; Middle: signal controlled intersection; Bottom: roundabout configuration)

Table 1 Guidelines for Number of Lanes at Stop-Controlled Approaches (TRB, 2010)

Total Volume on Minor Approach (veh/hr)	Total Volume on Major Street (veh/hr)			
	500	1,000	1,500	2,000
100	1 lane	1 lane	1 lane	2 lanes
200	1 lane	1 lane	2 lanes	NA
300	1 lane	2 lanes	2 lanes	NA
400	1 lane	2 lanes	NA	NA
500	2 lanes	NA	NA	NA
600	2 lanes	NA	NA	NA
700	2 lanes	NA	NA	NA
800	2 lanes	NA	NA	NA

Not including multiway STOP-controlled intersections.
NA = STOP control probably not appropriate for these volumes.

Table 2 Maximum Total Critical-Lane Volumes for a Typical Signalized Intersection (TRB, 2010)

Cycle Length (sec)	Number of Phases		
	2	3	4
30	1,015	831	646
40	1,108	969	831
50	1,163	1,052	942
60	1,200	1,108	1,015
70	1,226	1,147	1,068
80	1,246	1,177	1,108
90	1,262	1,200	1,138
100	1,274	1,218	1,163
110	1,284	1,234	1,183
120	1,292	1,246	1,200

In case of the roundabout simulation model, a mini roundabout which is often used in the low-speed urban environments (e.g., average operating speeds of 35 mph or less) was used. It should be noted that no official design guideline for roundabout is currently provided (FHWA, 2000). Thus the geometry configurations of a roundabout for each traffic volume scenario were determined by the simple logic by considering the road capacity and the maximum flow rate. The VISSIM testbed networks were presented in Figure 5 and Figure 6. Figure 5 shows the intersection networks used for stop-control and traffic signal control. Figure 6 shows the mini roundabout networks used in this report. In Figure 5, the red lines represent the locations of stop bars for either stop sign or the traffic signal.

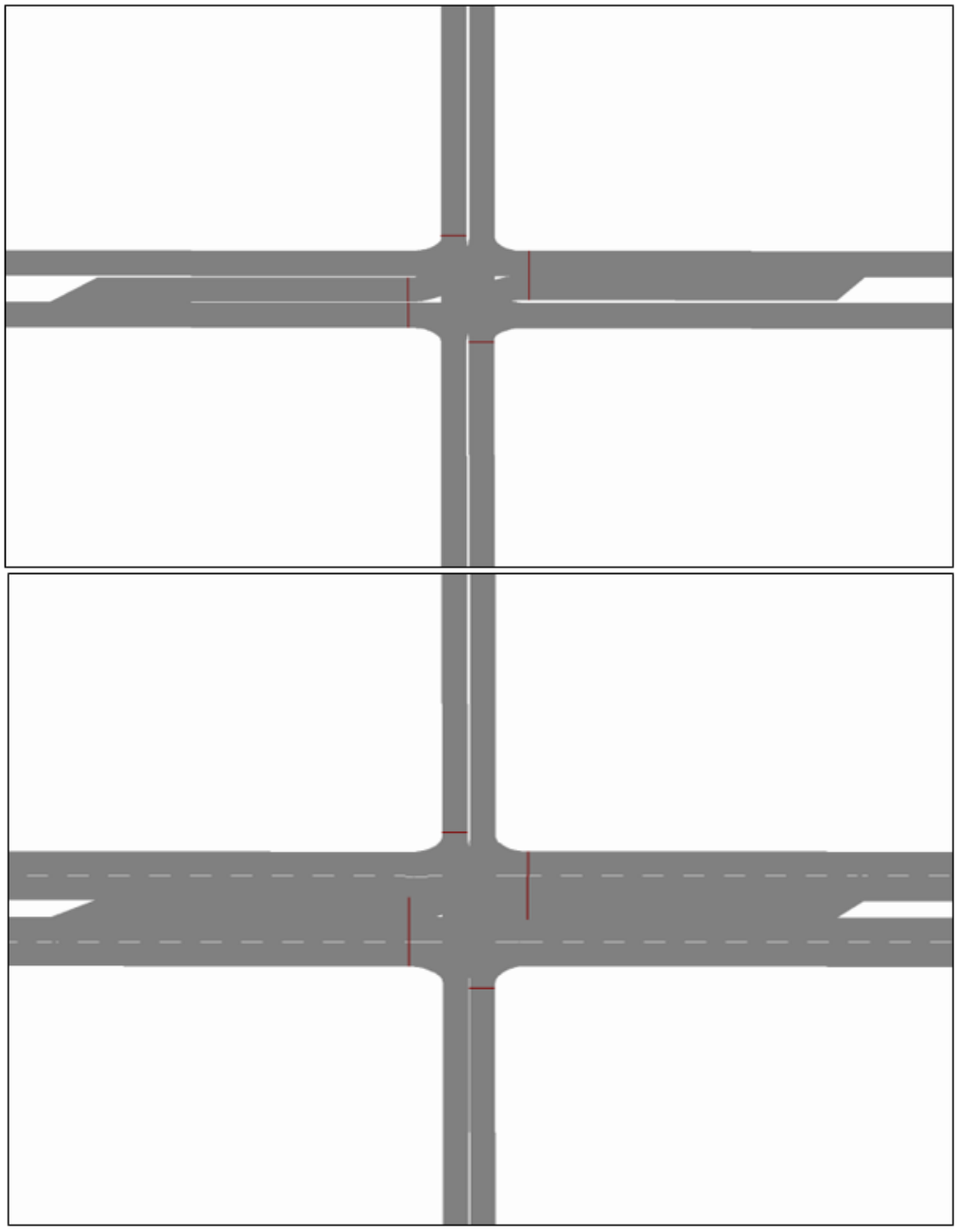

Figure 5 VISSIM network for stop control and traffic signal control

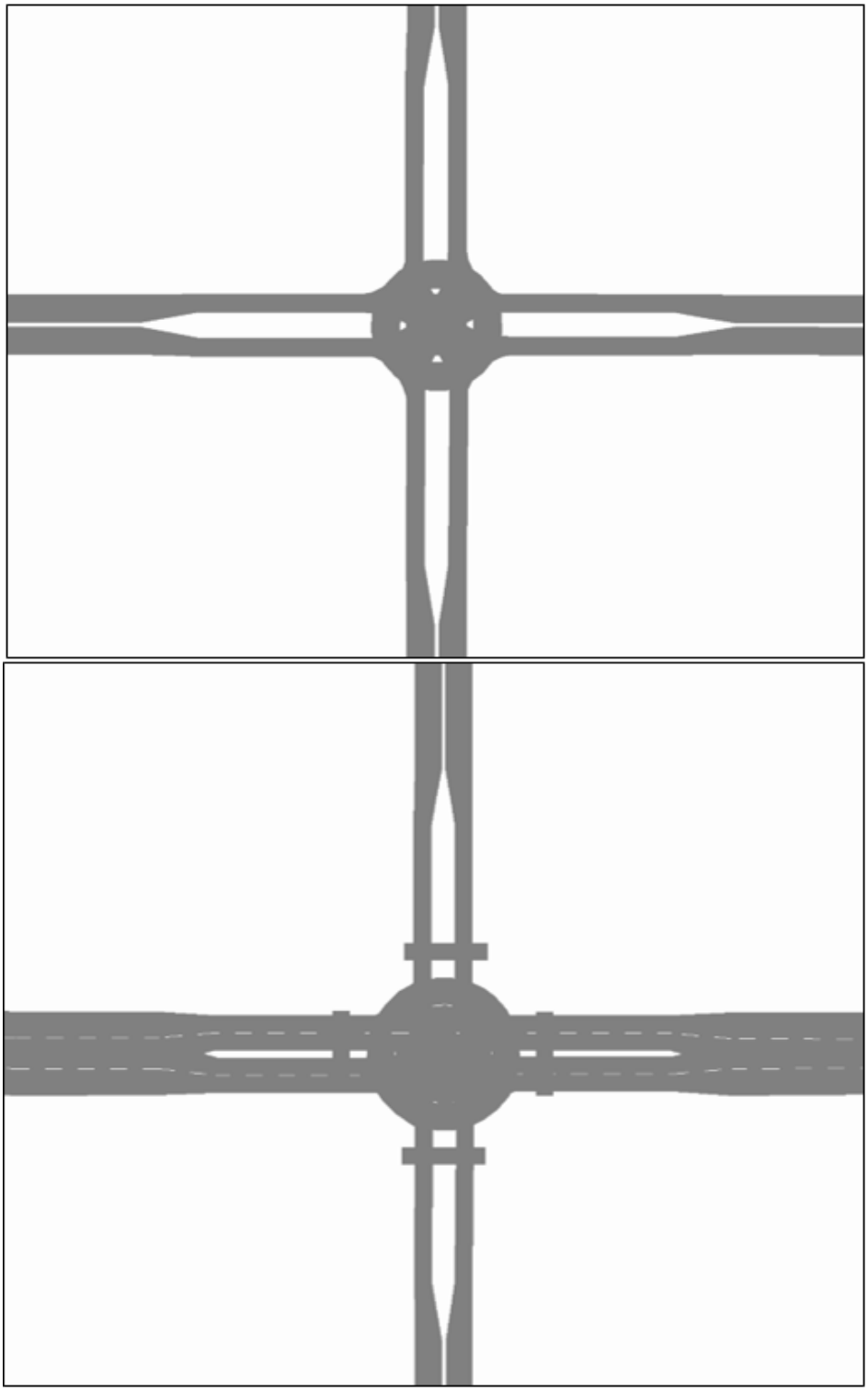

Figure 6 VISSIM network for roundabout

3.7.2 Intersection Control Principles and Plans

As noted, the scope of this report was limited to the four types of intersection control: 2WSC, 4WSC, traffic signal control, and a roundabout. In this section, the principles and scheme of each intersection control type that were incorporated into the simulation models are reviewed.

In the 2WSC intersections, the right-of-way among conflicting streams was assigned in a way that the major streets had higher priority over the minor streets. Also, the through movements and right-turn movements were given higher priority over the left-turn movements. In the 4WSC intersection, the first-come-first-serve rule was applied. The motorist arrives later at the intersection was set to yield to the motorists who arrived before him or her.

As to the traffic signal control, the fully-actuated traffic signal controllers were used. The fully-actuated traffic signal controllers are featured by the detectors installed on all approaches of intersection, which allows rapid responses to the fluctuating traffic demands. The traffic signal phasing and timing plans were calculated using the HCM procedure (TRB, 2010). Various traffic signal phasing and timing plans were applied among different traffic volume scenarios depending on the geometry configurations and traffic volumes. For example, depending on the availability of exclusive left-turn lanes, the phasing scheme was determined as either 2- or 3-phase scheme, and the timing plan was calculated based on the traffic volume of each approach. The 3-phase scheme used in this report is shown in Figure 7. The protected left-turn phase was implemented on the major street approach, which was followed by the leading green of the direction of the heavier left-turn flow and a through phase. Such phasing scheme provides much flexibility by allowing for the left-turn phase to be optional and be skipped in any cycle.

Figure 7 Three-phase signal phasing scheme for fully actuated control

In a roundabout system, the entering vehicles were modeled to yield to the vehicles in the circulating lane until they find acceptable gaps to enter. Once entering the roundabout, stops or lane changes were not allowed until they escaped the circulating lane. For the scenarios that required two lanes for the roundabouts, drivers were modeled to choose their lanes according to their turn movements at the intersection. The vehicles that were intended to execute through movements or right-turns were modeled to enter the roundabout through the right lane, and those who were intended to execute left-turns or U-turns were modeled to enter the roundabout through the left lane.

3.7.3 Calibration of the Simulation Models

The simulation models were calibrated to appropriately replicate driving behaviors in the real world. The saturation flow rate was determined by adopting the calibration measurement of 1,830 veh/hr. By adjusting the parameters of the Wiedemann 99 car following model (i.e., average standstill distance, additive part and multiple part), a saturation flow rate of 1,830 veh/h was achieved as shown in Table 3.

Table 3 Calibration of VISSIM Model

Parameter	Value
Average standstill distance	7.5
Additive part (CC4)	3
Multiple part (CC5)	4
Calibrated headway (sec)	1.96
Calibrated saturation flow rate (veh/hr)	1830

The mini-roundabout models developed by the research group of Lochrane et al. were adopted which were well-calibrated under the urban areas context. Detailed information about the calibration efforts can be found in the previous paper (Lochrane et al., 2013).

3.7.4 Simulation Setup

The simulation-based data collections were performed within the half-mile-long segments for all approaches from the center of the intersection. To ensure the simulation data were collected from a stable network condition, the 300-second warm-up time was executed in advance of the 3600-second evaluation period. The relative flow of right-turn, through and left-turn traffic were assigned as 15%, 70% and 15%, respectively (Wang, 2007).

4. Analysis and Findings

Figure 8 presents the estimated hourly CO2 emissions (kg) of each type of intersection controls. The results were presented as a collection of bar charts under varying traffic volumes cases. Within each cell, the emissions of all four control types for a particular volume condition are demonstrated. Based on this results, Type I and Type II environmentally sustainable signal warrants were developed.

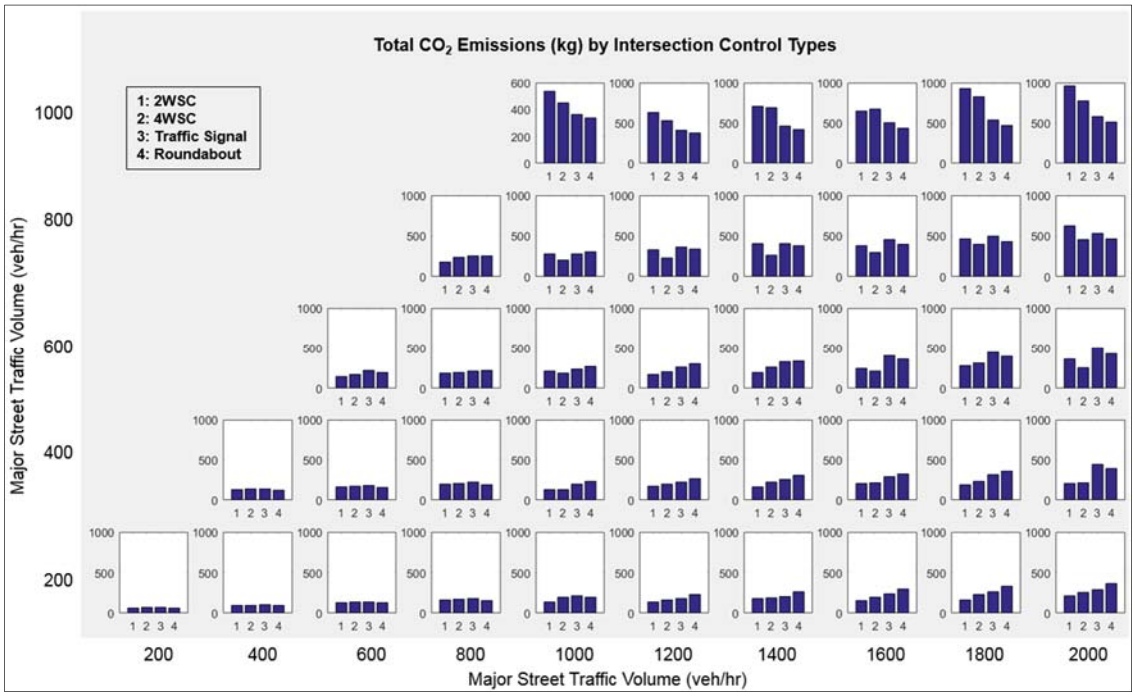

Figure 8 Comparisons of CO_2 emission

Figure 9 shows the Type I environmentally sustainable traffic signal warrant. The noticeable differences between the Type 1 signal warrant and the baseline signal warrant in Figure 2 were found in the cases associated with the intermediate-to-high major traffic volumes (e.g., 1,000-2,000 veh/hr) with the intermediate minor traffic volumes (e.g., 600 veh/hr), where the emission-based warrant did not warrant a traffic signal control while the baseline warrant did. This implied that as long as the minor street volume remained moderate, 2WSC was capable to effectively reduce the unnecessary stops and emissions compared to traffic signal control. In addition, even though the existing baseline warrant did not explicitly distinguish between 2WSC and 4WSC in terms of mobility, Type I warrant showed that 2WSC outperformed 4WSC in terms of CO2 emissions with statistical significance at 95% confidence level. This finding suggests that engineers and practitioners should incline to use 2WSC when both stop control types are showing similar mobility performances. Furthermore, in the scenario of (200, 200), the CO2 emissions showed no significant difference among the three intersection control types.

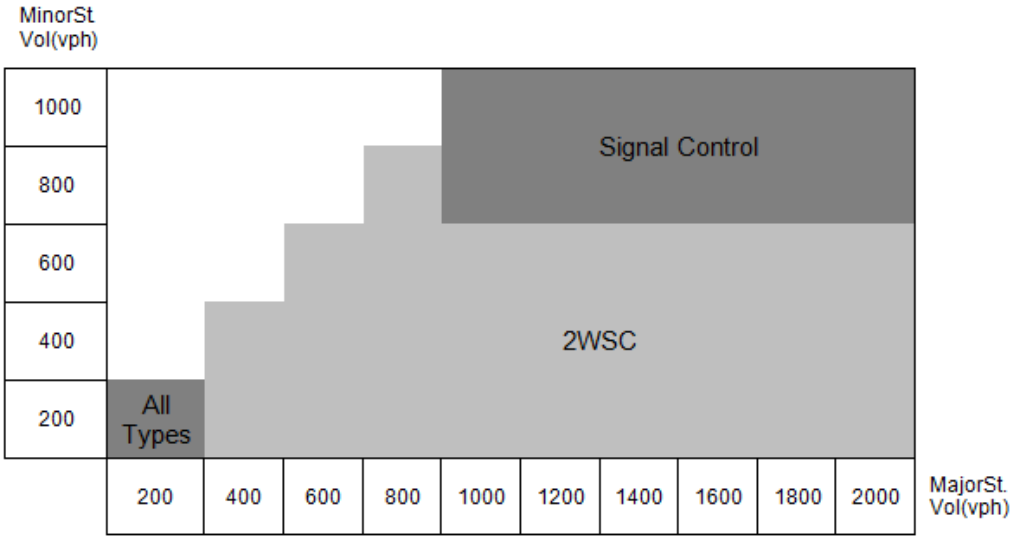

Figure 9 Type I environmentally sustainable traffic signal warrant

Table 4 provided the comparisons analysis between the Type I environmentally sustainable traffic signal warrant and the baseline MUTCD signal warrant. Based on the assumptions and facts presented in the section 2.6, the national annual reductions in CO2 emissions and total delay were 110 T-kg and 3.6 million hours, respectively, as shown in Table 6. Such improvements in traffic delays and emissions were monetized as 41.4 billion dollars per year. According to U.S. Environmental Protection Agency (EPA), the annual CO2 emissions from on-road vehicles is about 1,540 T-kg (US EPA, 2014), thus the implementation of Type I traffic signal warrant would reduce CO2 emissions by 7.2%. The results further prove that delay is not always associated with emission. Take two volume conditions as an example ((800,800) and (1000,800)). In this example, lower delay is associated with higher emission. This is because drivers on the side street (controlled by 2-way stop sign) wait for a longer time compared to higher volume condition (controlled by signal) which drives average delay up. However, for stop sign controlled intersection, both main street and side street experience less speed variation which leads to less fuel consumption and emission.

Table 4 Comparison between MUTCD and Type 1 Warrant (CO_2 Emissions and Total Delay)

Traffic Volumes (veh/hr)		Existing MUTCD Warrant			CO2 based Signal Warrant			Change Rate (%)	
Major St.	Minor St.	Control Type	CO2 Emissions (kg)	Delay (hr)	Control Type	CO2 Emissions (kg)	Delay (hr)	CO2 Emissions	Delay
200	200	Stop Control	66.6	0.5	All types	66.6	0.5	0	0
400	200	Stop Control	97.8	0.6	2WSC	97.8	0.6	0	0
400	400	Stop Control	133.6	1.3	2WSC	133.6	1.3	0	0
600	200	Stop Control	129.3	0.7	2WSC	129.3	0.7	0	0
600	400	Stop Control	165.5	1.5	2WSC	165.5	1.5	0	0
600	600	Stop Control	150.4	1.8	2WSC	150.4	1.8	0	0
800	200	Stop Control	160.5	0.7	2WSC	160.5	0.7	0	0
800	400	Stop Control	197.4	1.7	2WSC	197.4	1.7	0	0
800	600	Signal	216.2	4.1	2WSC	193.0	2.7	-11	-35
800	800	Signal	255.9	5.0	2WSC	176.6	6.1	-31	24
1000	200	Stop Control	138.7	0.9	2WSC	138.7	0.9	0	0
1000	400	Stop Control	131.8	1.1	2WSC	131.8	1.1	0	0
1000	600	Signal	242.9	4.6	2WSC	213.8	2.4	-12	-48
1000	800	Signal	284.5	5.9	Signal	284.5	5.9	0	0
1000	1000	Signal	364.4	6.9	Signal	364.4	6.9	0	0
1200	200	Stop Control	139.8	0.6	2WSC	139.8	0.6	0	0
1200	400	Stop Control	175.9	1.4	2WSC	175.9	1.4	0	0
1200	600	Signal	268.8	5.3	2WSC	176.5	3.9	-34	-27
1200	800	Signal	363.1	7.1	Signal	363.1	7.1	0	0
1200	1000	Signal	407.2	8.7	Signal	407.2	8.7	0	0
1400	200	Stop Control	180.0	0.8	2WSC	180.0	0.8	0	0
1400	400	Stop Control	162.0	1.9	2WSC	162.0	1.9	0	0
1400	600	Signal	329.7	14.7	2WSC	193.8	4.1	-41	-72
1400	800	Signal	411.0	11.2	Signal	411.0	11.2	0	0
1400	1000	Signal	458.5	13.4	Signal	458.5	13.4	0	0
1600	200	Stop Control	157.8	0.8	2WSC	157.8	0.8	0	0
1600	400	Stop Control	207.0	1.8	2WSC	207.0	1.8	0	0
1600	600	Signal	408.5	11.0	2WSC	250.2	6.6	-39	-40
1600	800	Signal	454.6	13.2	Signal	454.6	13.2	0	0
1600	1000	Signal	504.8	15.8	Signal	504.8	15.8	0	0
1800	200	Stop Control	165.1	0.8	2WSC	165.1	0.8	0	0
1800	400	Stop Control	193.1	2.1	2WSC	193.1	2.1	0	0
1800	600	Signal	453.0	13.1	2WSC	278.2	7.8	-39	-40
1800	800	Signal	496.9	15.0	Signal	496.9	15.0	0	0
1800	1000	Signal	538.6	17.1	Signal	538.6	17.1	0	0
2000	200	Stop Control	210.7	0.9	2WSC	210.7	0.9	0	0
2000	400	Stop Control	209.6	2.8	2WSC	209.6	2.8	0	0
2000	600	Signal	507.6	15.5	2WSC	362.0	11.8	-29	-24
2000	800	Signal	531.1	16.2	Signal	531.1	16.2	0	0
2000	1000	Signal	582.6	19.1	Signal	582.6	19.1	0	0
Total			11,252.4	247.7	-	10,414.0	219.8	-235.2	-261.9

Figure 10 shows the Type II environmentally sustainable traffic signal warrant which includes roundabout in addition to the 2WSC, 4WSC and traffic signal control. As shown in Figure 10, the roundabout control was suggested when traffic volumes from both major street and minor street were in the similar levels. In contrast, the roundabout control was observed less eco-friendly than 2WSC when traffic volumes between the major and minor streets were unbalanced (e.g., high volumes at the major street and the low volumes at the minor streets). The reason for the increase in the CO2 emissions lies on the smoother and faster traffic flow within the circulating lane of the roundabout. When the traffic volume from the major street was high, it

took longer for the entering vehicles to find a gap within the circulating traffic. Thus, higher idling time spent for the waiting vehicles resulted in higher total CO2 emissions. For the cases of the similar traffic volumes from major and minor streets, the constant interventions of the vehicles entering from both streets helped reduce the average speed of circulating traffic flow and allowed the entering vehicles to easily find gaps to enter. In addition, the roundabout control reduced mandatory stops at intersections and allowed smoother driving with less speed variations that resulted in CO2 emissions reductions.

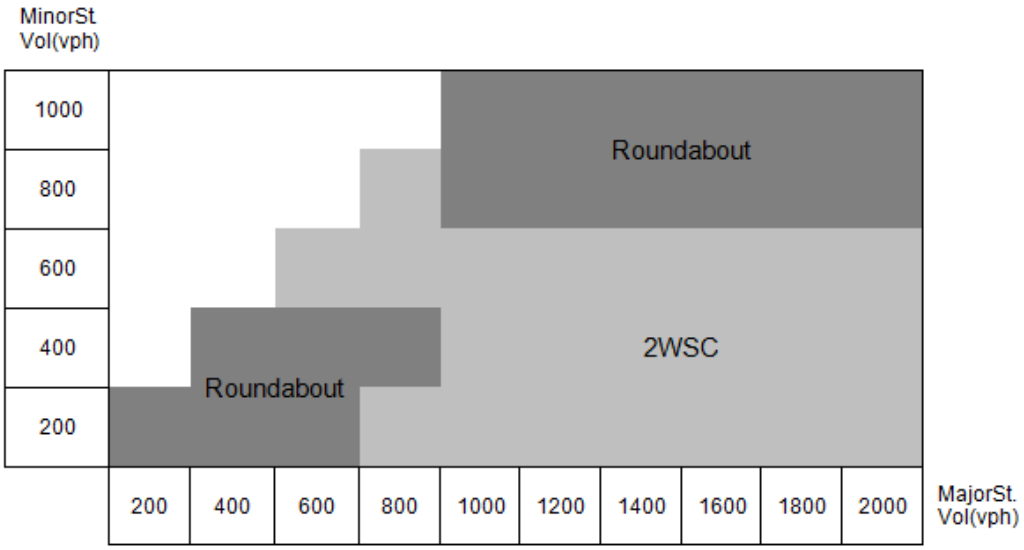

Figure 10 Type II environmentally sustainable traffic signal warrant.

Table 5 provides the comparison analysis between the Type II environmentally sustainable traffic signal warrant and the baseline traffic signal warrant. As shown in Table 6, the estimated annual national reductions in both CO2 emissions and the delay were 211.7 T-kg and 20.6 million hours, respectively. Such improvements in traffic delays and emissions were monetized as 214.7 billion dollars per year. Given the annual CO2 emissions from on-road vehicles is 1,540 T-kg (US EPA, 2014) in the US, the implementation of Type II traffic signal warrant resulted in about 13.8% of reductions in CO2 emissions.

Overall, the results showed that both Type I and Type II warrants improved both emissions and mobility over the current existing practice when they were implemented. This observation was consistent with the several previous studies (Ardekani and Williams, 1996; Saka, 1993; Quan et al., 2011). Both studies demonstrated that the current practice of MUTCD traffic signal control do not optimize mobility for some traffic volume cases, and it is inclined toward a traffic signal control.

Table 5 Comparison between MUTCD and Type 2 Warrant (CO_2 Emissions and Total Delay)

Traffic Volumes (veh/hr)		Existing MUTCD Warrant			CO2 based Signal Warrant			Change Rate (%)	
Major St.	Minor St.	Control Type	CO2 Emissions (kg)	Delay (hr)	Control Type	CO2 Emissions (kg)	Delay (hr)	CO2 Emissions	Delay
200	200	Stop Control	66.6	0.5	Roundabout	63.7	0.1	-4	-76
400	200	Stop Control	97.8	0.6	Roundabout	93.6	0.3	-4	-56
400	400	Stop Control	133.6	1.3	Roundabout	126.0	0.5	-6	-63
600	200	Stop Control	129.3	0.7	Roundabout	126.6	0.6	-2	-16
600	400	Stop Control	165.5	1.5	Roundabout	159.6	0.9	-4	-40
600	600	Stop Control	150.4	1.8	2WSC	150.4	1.8	0	0
800	200	Stop Control	160.5	0.7	2WSC	160.5	0.7	0	0
800	400	Stop Control	197.4	1.7	Roundabout	193.1	1.6	-2	-8
800	600	Signal	216.2	4.1	2WSC	193.0	2.7	-11	-35
800	800	Signal	255.9	5.0	2WSC	176.6	6.1	-31	24
1000	200	Stop Control	138.7	0.9	2WSC	138.7	0.9	0	0
1000	400	Stop Control	131.8	1.1	2WSC	131.8	1.1	0	0
1000	600	Signal	242.9	4.6	2WSC	213.8	2.4	-12	-48
1000	800	Signal	284.5	5.9	Roundabout	304.3	1.1	7	-81
1000	1000	Signal	364.4	6.9	Roundabout	339.8	1.8	-7	-74
1200	200	Stop Control	139.8	0.6	2WSC	139.8	0.6	0	0
1200	400	Stop Control	175.9	1.4	2WSC	175.9	1.4	0	0
1200	600	Signal	268.8	5.3	2WSC	176.5	3.9	-34	-27
1200	800	Signal	363.1	7.1	Roundabout	338.1	2.2	-7	-69
1200	1000	Signal	407.2	8.7	Roundabout	373.1	3.1	-8	-64
1400	200	Stop Control	180.0	0.8	2WSC	180.0	0.8	0	0
1400	400	Stop Control	162.0	1.9	2WSC	162.0	1.9	0	0
1400	600	Signal	329.7	14.7	2WSC	193.8	4.1	-41	-72
1400	800	Signal	411.0	11.2	Roundabout	378.2	2.9	-8	-74
1400	1000	Signal	458.5	13.4	Roundabout	415.5	4.3	-9	-68
1600	200	Stop Control	157.8	0.8	2WSC	157.8	0.8	0	0
1600	400	Stop Control	207.0	1.8	2WSC	207.0	1.8	0	0
1600	600	Signal	408.5	11.0	2WSC	250.2	6.6	-39	-40
1600	800	Signal	454.6	13.2	Roundabout	398.3	2.7	-12	-79
1600	1000	Signal	504.8	15.8	Roundabout	436.0	4.4	-14	-72
1800	200	Stop Control	165.1	0.8	2WSC	165.1	0.8	0	0
1800	400	Stop Control	193.1	2.1	2WSC	193.1	2.1	0	0
1800	600	Signal	453.0	13.1	2WSC	278.2	7.8	-39	-40
1800	800	Signal	496.9	15.0	Roundabout	434.3	3.6	-13	-76
1800	1000	Signal	538.6	17.1	Roundabout	473.0	5.5	-12	-68
2000	200	Stop Control	210.7	0.9	2WSC	210.7	0.9	0	0
2000	400	Stop Control	209.6	2.8	2WSC	209.6	2.8	0	0
2000	600	Signal	507.6	15.5	2WSC	362.0	11.8	-29	-24
2000	800	Signal	531.1	16.2	Roundabout	470.1	3.9	-11	-76
2000	1000	Signal	582.6	19.1	Roundabout	511.1	6.8	-12	-64
Total			11,252.4	247.7	-	9860.8	110.2	-364.3	-1386.9

Table 6 Estimation of National Annual Reduction and Monetization Analysis

Measure	Type 1 Traffic Signal Warrant		Type 2 Traffic Signal Warrant	
	National Annual Reduction	Monetized Value	National Annual Reduction	Monetized Value
CO2 emissions	110,159,226,792 kg	$ 4,843,827,434	211,780,176,192 kg	$ 9,312,217,026
Delay	3,673,438,898 hrs	$ 36,587,451,428	20,623,854,938 hrs	$ 205,413,595,186
Total		$ 41,431,278,862		$ 214,725,812,213

5. Conclusions

With the concerns over the GHG emissions associated with the surface transportation, the environmentally sustainable traffic signal warrant is essential to provide guidelines in making decisions about control types at intersections. In this report, a proof of concept research was conducted to demonstrate difference in traffic signal warrant when CO2 emissions criterion was adopted.

Two types of environmentally sustainable traffic signal warrants were developed: Type I warrant where 2WSC, 4WSC and traffic signal control were included, whereas Type II warrant additionally considered roundabout. The results confirmed that the proposed emissions-oriented traffic signal warrants were significantly different from the current mobility-oriented traffic signal warrant and were superior in terms of emissions with the statistical significance. The evaluations of the two types of proposed warrants revealed the following key findings:

- The environmentally sustainable traffic signal warrants were significantly different from the current MUTCD traffic signal warrant. This implied that better mobility did not always equate the less emissions. The statistically significant discrepancies were observed in cases of intermediate-to-high major street volume (1,000 − 2,000 veh/hr) for major streets with intermediate minor-street volumes (600 veh/hr) for minor streets. In those cases, 2-way stop control was eco-friendlier than traffic signal control, as opposed to the fact that the mobility-based traffic signal warrant recommended the traffic signal control.
- Type I warrant reduced both CO2 emissions and delay by 110 T-kg and 3.6 million hours per calendar year, respectively. This was equal to the monetary savings of $ 41.4 billion per year in the US.
- Type II warrant reduced both CO2 emissions and delay by 211.7 T-kg and 20.6 million hours per calendar year, respectively. This was equal to a total monetary savings of $ 214.7 billion per year in the US.
- Roundabout was a promising eco-friendly intersection control. Roundabout performed the best when traffic flows were balanced between major and minor streets.
- 2WSC was eco-friendlier than 4WSC. Contrary to the current MUTCD warrant where the two types of stop controls were not differentiated, 2WSC significantly outperformed 4WSC in terms of emissions. This implied that, even when the mobility-oriented warrant was adopted, choosing 2WSC was advised over 4WSC.

6. Recommendations

The guideline warrant provided in this report is derived under generalized conditions. Therefore, practitioner should use with caution when apply this warrant to their local intersections. It is recommended that a calibration of the warrant should be conducted before implementation using local traffic data. In addition, the proposed warrants are developed based on simulation data. It has been pointed out that simulation based trajectory data may not always be consistent with the real world condition (Hallmark et al., 1999; Hao et al., 2016; Zhao et al., 2013). The accuracy of the proposed warrant can be further improved with calibration using local field data.

Finally, the proposed emission-based traffic signal warrants can be improved by considering additional factors that can affect CO2 emissions. For example, driving behaviors by different regions, market penetration rates of hybrid/electric vehicles associated with distinctive emissions mechanisms, and the unique driving patterns of vehicles equipped with emerging driving assistance technologies. In addition, the proposed signal warrants are only applicable to the planning level applications when intersection geometry configuration changes according to control type. Additional guidelines of traffic signal warrant could be developed for post-construction phase when intersection geometry is a fixed given fact.

Reference List

American Association of State Highway Officials (AASHO). 1937. Manual on Uniform Traffic Control Devices for Streets and Highways (MUTCD). National Conference on Street and Highway Safety. Washington D.C.

Ahn, Kyungho, H. Rakha, A. Trani. And M. Van Aerde, 2002. Estimating Vehicle Fuel Consumption and Emissions based on Instantaneous Speed and Acceleration Levels, Journal of Transportation Engineering, Vol 128, Issue 2.

Ardekani, A., and P. E. Wiliams. 1996. Impacts of Traffic Signal Installation at Marginally Warranted Intersections. Texas Department of Transportation, Center for Transportation Studies Civil Engineering Department of University of Texas at Arlington.

Bing, X., Y. Jiang, C. Zhang, Y. Zhang, and J. Lu. 2014. Effects of Intersection Lane Configuration on Traffic Emissions. Advances in Transportation Studies. Vol. 32, pp 23-36.

Bretherton, W. M., and M. Elhaj. 1994. A New Signal Warrant for Practicing Traffic Engineers - Turning Conflicts. 64th ITE Annual Meeting. pp. 37-42. Washington D.C.

Federal Highway Administration (FHWA). 2000. Roundabouts: An informational guide (FHWA-RD-00-068). U.S. Department of Transportation. Washington D.C.

Federal Highway Administration (FHWA). 2009. Manual on Uniform Traffic Control Devices (MUTCD). U.S. Department of Transportation. Washington D.C.

Guo, R. and Y. Zhang. 2014. Exploration of Correlation between Environmental Factors and Mobility at Signalized Intersections. Transportation Research Part D: Transport and Environment. Vol. 32. pp. 24-34.

Hallmark, S., & Guensler, R. (1999). Comparison of speed-acceleration profiles from field data with NETSIM output for modal air quality analysis of signalized intersections. Transportation Research Record: Journal of the Transportation Research Board, (1664), 40-46.

Hao, P., G. Wu, K. Boriboonsomsin, and M. Barth. 2016. Modal Activity-Based Vehicle Energy/Emissions Estimation Using Sparse Mobile Sensor Data. 95th Annual Meeting of Transportation Research Board. Washington, D.C.

Hu, Jia, B. Park, and A. Parkany. 2014. Transit Signal Priority with Connected Vehicle Technology. Transportation Research Record: Transportation Research Board. Vol. 2418. pp. 20-29.

Hu, Jia, B. Park, and Young-Jae Lee. 2015. Coordinated Transit Signal Priority Supporting Transit Progression Under Connected Vehicle Technology. Transportation Research Part C: Emerging Technologies. Vol. 55, pp. 393-408.

van Katwijk, R. T., and S. Gabriel. 2015. Optimizing a Vehicle's Approach towards an Adaptively Controlled Intersection. The Institution of Engineering and Technology (IET) Intelligent Transport Systems. Vol. 9, No. 5, pp 479-487.

Khalighi, F., and E. Christofa. Emission-Based Signal Timing Optimization for Isolated Intersections. 2015. Transportation Research Record: Journal of the Transportation Research Board. pp. 26

Koppelman, F. S., and C. Bhat. 2006. A Self Instructing Course in Mode Choice Modeling: Multinomial and Nested Logit Models. U.S. Department of Transportation Federal Transit Administration. Washington D.C.

Lee, J., B. Park, K. Malakorn, and J. So. 2013. Sustainability Assessments of Cooperative Vehicle Intersection Control at an Urban Corridor. Transportation Research, Part C. Vol. 32, pp. 193-206.
Lee, W., Y. Lai, and P. Chen. 2015. A Study on Energy Saving and Emission Reduction on Signal Countdown Extension by Vehicular Ad Hoc Networks. IEEE Transactions on Vehicular Technology. Vol. 64, No. 3, pp 890-900.
Lochrane, T. W. P, N. Kronprasert, J. Bared, D. Dailey, and W. Zhang. 2013. Traffic Capacity Models for Mini-Roundabouts in the United States: Calibration of Driver Performance in Simulation. Transportation Research Board (TRB) Annual Meeting. Washington D.C.
Marek, J. F., M. Kyte, T. Zongzhong, K. Lall, and K. Voigt. 1997. Determining Intersection Traffic Control using the 1994 Highway Capacity Manual. Institute of Transportation Engineers (ITE) Journal. Vol. 67, Issue 12. pp. 22-26.
National Highway Traffic Safety Administration (NHTSA). CAFÉ regulations. http://www.nhtsa.gov/ (accessed June 25, 2015).
National Oceanic and Atmospheric Administration (NOAA). 2012. Climate Change Indicators in the United States. http://www.esrl.noaa.gov/gmd/aggi/ (accessed April 10, 2016)
Neudorff, L. G. 1985. Gap based criteria for signal warrants. Institute of Transportation Engineers(ITE) Journal. pp 15-18. Washington D.C.
Papacostas, C. S., and P. D. Prevedouros. 2001. Transportation Engineering and Planning, 3rd edition. Upper Saddle River, NJ: Pearson Education, pp. 148-149.
Park, Byungkyu Brian, and Anil Kamarajugadda. 2007. Development and Evaluation of a Stochastic Traffic Signal Optimization Method. International Journal of Sustainable Transportation. Vol. 1, Issue 3, pp. 193-207.
Park, Byungkyu Brian, Ilsoo Yun, and Kyoungho Ahn, 2009. Stochastic Optimization for Sustainable Traffic Signal Control. International Journal of Sustainable Transportation (IJST). Vol. 3, Issue 4, pp. 263-284.
Quan, Y., J. Tian-xiao, D. Xiao-hui, and R. Jian. 2011. Control Type Styles Option Research of Intersection Based on LOS. 2011 Intelligent Conference on Intelligent Computation Technology and Automation (ICICTA). pp. 380-383.
Roess, R. P., E. S. Prassas, and W. R. McShane. 2011. Traffic Engineering, 4th Edition. Pearson Higher Education, pp. 437-441.
Saka, A. A. 1993. Microscopic Simulation Modeling of Minimum Thresholds Warranting Intersection Signalization. Transportation Research Record: Transportation Research Board. Washington D.C., Issue 1421. pp. 30-35.
Sampson, J.D. 1999. Queue-Based Traffic Signal Warrants. Institute of Transportation Engineers(ITE) Journal. Vol. 61. No. 7. pp. 30-36. Washington D.C.
Transportation Research Board (TRB). 2010. Highway Capacity Manual (HCM) Special Report 209. National Research Council. Washington, D.C.
U.S. Department of Transportation (US DOT). 2010. http://safety.fhwa.dot.gov/intersection/signalized/presentations/sign_int_pps051508/short / (accessed August 25, 2015)
U.S. Department of Transportation. Transportation's Role in Climate Change. http://climate.dot.gov/about/transportations-role/overview.html (accessed June 25, 2015).
U.S. Environmental Protection Agency (EPA). 2014. Inventory of U.S. Greenhouse Gas Emissions and Sinks: 1990 – 2013. U.S. Environmental Protection Agency (EPA), Washington D.C.

Virginia Department of Transportation (VDOT) Traffic Engineering Division. 2013. Traffic Operations Analysis Tool Guidebook, Version 1.1.

Wang, H., W. Wang, and J. Chen. 2007. Capacity and Delay Performance of Unsignalized Intersection, Huazhong University of Science and Technology (Nature Science Edition), Vol. 35, No. 1, pp. 114-117.

World Energy Council. World Energy Scenarios 2007: Transport Technologies and Policy Scenarios. https://www.worldenergy.org/publications/2007/transport-technologies-and-policy-scenarios/ (accessed June 25, 2015).

Zhao, Y., & Sadek, A. W. (2013). Evaluating the accuracy of approaches to integrating microscopic traffic simulators with emissions models for project-level emissions analysis. In Transportation Research Board 92nd Annual Meeting (No. 13-3228).

Sub-report Task #2

Optimizing Isolated Traffic Signal Timing Considering Energy and Environmental Impacts

Prepared by:

Alvaro J. Calle Laguna
Graduate Research Assistant
Virginia Tech Transportation Institute

Hesham A. Rakha, PhD., P.Eng,
Pritchard Professor of Engineering
Virginia Tech

Jianhe Du, Ph.D., P.E
Senior Research Associate
Virginia Tech Transportation Institute

Acknowledgments

This research effort was jointly sponsored by the MATS University Transportation Center, the TranLIVE University Center and the Virginia Department of Transportation (VDOT).

Disclaimer

Table of Contents

List of Figures

List of Tables

1. Problem

The traditional goal of optimizing traffic signal cycle length usually focuses on minimizing vehicle delay and increasing throughput at the intersection. The classic method is designed by the British researcher, Webster, who developed the optimum cycle length formulation that approximates the necessary signal timings to minimize vehicle delay (Webster, 1958), as seen in Equation (1). This formulation has been used in traffic analysis for years and is still one of the prevailing methodologies to determine the optimum cycle length.

$$C_{opt} = \frac{1.5L+5}{1-Y} \quad (1)$$

Here, Copt is the cycle length that minimizes vehicle delay (s); L is the total lost time per cycle (s); and Y is the sum of the critical group flow ratios based on the phasing scheme.

With the development of the transportation system, traffic demand has increased rapidly. According to the National Transportation Statistics, the total number of vehicles in the United States reached 250 million in 2012 (USDOT and BTS, 2015). These vehicles consume a large portion of the oil (nearly 70% of U.S oil consumption) and have a large impact on the environment. According to a report by the United States Environmental Protection Agency (EPA), the transportation sector in the United States accounts for approximately 28% of the country's Greenhouse Gas (GHG) emissions, making it the second largest source of emissions next to electricity (EPA, 2014).

To alleviate the pollution problem generated by vehicles, numerous research efforts have been conducted focusing on air pollution generated by the transportation system. These efforts included the impact of vehicle acceleration/deceleration levels, vehicle characteristics, and route choice effects on vehicle emissions (Ahn et al., 2009, Ahn and Rakha, 2008, Ahn et al., 2004a, Ahn et al., 2002a, Ahn et al., 2002b, Rakha et al., 2004a, Rakha et al., 2012). Eisele et al. (Eisele et al., 2014) developed a method to determine the carbon dioxide emissions and fuel consumption caused by congestion and found that 56 billion pounds of additional CO2 were produced because of the lower speeds under congested conditions.

As a key element in the urban transportation network, signal controlled intersections will inevitably create speed variations and stops for some of the vehicles. Frey et al. (Frey et al., 2001) confirmed that the speed variations and stops cause variability in on-road emissions, in an effort that conducted experiments to evaluate pollution prevention strategies for on-road vehicles. Chen and Yu furthered this research by analyzing the relationship between instantaneous emissions/fuel consumption rates and instantaneous speed/acceleration using the VISSIM microsimulation software (Chen and Yu, 2007). Rakha and Ding noted that vehicle fuel consumption rates are sensitive to vehicle stops, but in some rare cases can be more sensitive to, or mostly affected by, cruise-speed levels if the stops entail very mild accelerations. However, a vehicle stop, representing a vehicle's acceleration and deceleration level, is affected by to vehicle emission rates (Rakha and Ding, 2003). At signalized intersections, the traffic signals force vehicles to slow down, stop, and accelerate. Significant amounts of emissions are generated due to the variations in vehicle speeds. Consequently, one effective solution to decrease the emissions generated by vehicles is to optimize their trajectory passing through an intersection.

To accomplish this goal, one can carefully design the signal timings at intersections such that the percentage of vehicles that can drive through intersections with only necessarily minimum acceleration/deceleration and stops. Indeed, traffic signal optimization has been a research topic of numerous previous studies. In previous research that aimed at optimizing traffic signal timing, different objective functions are adopted. Some tried to minimize delays, some focused on minimizing the number of vehicle stops and delay, and others tried to maximize the throughput minus queue length (Stevanovic et al., 2009, Li and Gan, 1999, Stevanovic et al., 2011, Hajbabaie and Benekohal, 2013, Abu-Lebdeh and Benekohal, 2000, Dion et al., 2004). However, limited research has focused on optimizing signal timing specifically for the purpose of minimizing vehicle emissions, though previous research studied emissions related to intersections. Papson et al. used MOVES to study the pollution at intersections and confirmed in their study that emissions are much less sensitive to congestion than control delay. They concluded that by modifying control strategies at intersections, vehicle emissions could be significantly reduced (Papson et al., 2012). Hallmark et al. (Hallmark et al., 2011) used a Portable Emission Measurement System (PEMS) to study emissions along two parallel corridors that had similar traffic demands and concluded that under congested conditions, roundabouts can result in higher emissions. Signal controlled intersection and stop sign controlled intersections both performed better in terms of pollution control. Pulter et al. (Pulter et al., 2011) compared the results of their agent-based control mechanism at intersections with a static signal control and concluded that their model can save up to 26% of fuel consumption. Li et al. (Li et al., 2004) created an index to evaluate the performance of signal timing in terms of traffic quality and emissions and illustrated one example intersection in Nanjing, China. Lv and Zhang (Lv and Zhang, 2012) used VISSIM and MOVES jointly to quantify the effects of traffic signal coordination on emissions and found that increased cycle length will generate longer delay but not significantly more stops and emissions. The study demonstrated that an increased platoon ratio will help with the emission reduction. Madireddy et al. concluded that by using a coordinated signal control scheme, a reduction of 10% in emissions was achievable (Madireddy et al., 2011). Ma et al. (Ma et al., 2014) integrated VISSIM and SUMO to optimize traffic signals. They found that there are apparent trade-offs between the goal of mobility and sustainability. Li et al. (Li et al., 2011) studied the emissions at isolated intersections and found that the goal of decreasing delays at intersections and reducing emissions is not simply equivalent. Delays at intersections will increase if the number of vehicle stops are reduced, which will help to decrease the pollution at intersections. Liao, one of the few researchers conducting research on optimization of signal timing plans for the purpose of decreasing emissions and fuel consumption levels (Liao, 2013), considered fuel-based signal optimization based on a model composed of a description of the fuel consumption and defined stochastic effects of vehicle movements which consume excess fuel. She compared her model with the results using Webster's model as well as TRANSYT 7F and Synchro and found that her approach reduced fuel consumption levels by up to 40%.

The research discussed above indicated that: 1) Emissions of vehicles might be reduced with improved traffic control; 2) It is feasible to decrease the fuel consumption and emission levels through optimizing traffic signal timing plans at intersections; 3) The optimum signal timing for minimizing delays is not necessarily identical with the timing plans that aim at minimizing pollutions. Modifying signal timing in terms of pollution control is not only possible but also effective since no major construction of change of the infrastructure is needed. With the

advanced microscopic traffic simulation software and a better understanding of vehicle dynamics, it is now possible to develop a formulation that seeks to move vehicles more fuel efficiently by minimizing emissions and fuel consumption levels at signalized intersections.

2. Approach

The goal of this research is to develop an analytic formulation to approximate an optimum cycle length that minimizes the delay, energy consumption and hydrocarbon (HC), carbon monoxide (CO), oxides of nitrogen (NOx), and carbon dioxide (CO_2) at an isolated intersection. At the same time, the research compares the traffic signal timing settings that minimize delays and the optimum traffic timing recommendations made by Webster.

In terms of the paper organization, initially the research background is presented. Subsequently, the methodology used in the study is described. The results from the simulation are then analyzed, where the INTEGRATION results are presented. The optimum cycle length is then investigated and regression models are fit to develop an analytical formulation to calculate the optimum cycle length for various demand levels and lost times. The final section presents the conclusions of the study.

3. Methodology

The majority of the research discussed in the literature review section integrated two simulation software, namely: a microscopic traffic simulation software and an emission software (Lv and Zhang, 2012, Ma et al., 2014, Madireddy et al., 2011). They usually used vehicle trajectories generated by the simulation software as inputs to the emission software. Alternatively, this study uses the INTEGRATION (Van Aerde and Rakha, 2013b, Van Aerde and Rakha, 2013a), a microscopic traffic simulation software that incorporates the VT-Micro fuel consumption and emission model to estimate and output the fuel consumption and emission estimates directly without the need to post process the data. The INTEGRATION software is a microscopic traffic assignment and simulation software that was developed in the late 1980s and continues to be developed (Van Aerde and Yagar, 1988, Aerde and Rakha, 2007b, Aerde and Rakha, 2007a) It was conceived as an integrated simulation and traffic assignment model and performs traffic simulations by tracking the movement of individual vehicles every 1/10th of a second. This allows detailed analysis of lane-changing movements and shock wave propagations. It also permits considerable flexibility in representing spatial and temporal variations in traffic conditions. In addition to estimating stops and delays (Dion et al., 2004, Rakha et al., 2001a), the model can also estimate the fuel consumed by individual vehicles and the emissions emitted (Ahn et al., 2004b, Rakha et al., 2004b). Finally, the model also estimates the expected number of vehicle crashes using a time-based crash prediction model (A. Avgoustis et al., 2004). The INTEGRATION software uses the Rakha-Pasumarthy-Adjerid (RPA) car-following model to replicate vehicular longitudinal motion. The RPA model is composed of a steady-state first-order model (fundamental diagram), collision avoidance constraints, and vehicle acceleration constraints. The vehicle acceleration and collision avoidance constraints reverts the model from a first-order to a second-order traffic stream model. This model requires four parameters for calibration to local driver behavior. The INTEGRATION software incorporates a variable power model that computes the vehicle's tractive effort, aerodynamic, rolling, and grade-resistance

forces (Rakha et al., 2001b, Rakha and Lucic, 2002). The INTEGRATION model has not only been validated against standard traffic flow theory (Rakha et al., 2001a, Dion et al., 2004, Rakha and Crowther, 2003, Rakha and Crowther, 2002), but also has been utilized for the evaluation of large-scale real-life applications (Rakha, 1990, Rakha et al., 1998, Rakha et al., 2005). The INTEGRATION lane-changing logic was described and validated against field data in an earlier publication (Rakha and Zhang, 2004). Furthermore, Zhang and Rakha (Rakha and Zhang, 2006) demonstrated the validity of the INTEGRATION software for estimating the capacity of weaving sections by comparing to field observed weaving section capacities.

The following assumptions and scenarios were made in conducting the traffic simulations in INTEGRATION:

- All vehicle movements were assumed to be straight through only to avoid the need to consider permissive movements;
- Approach speeds were set at 56 km/h (35 mph) because this is typical of arterial road facilities;
- The base saturation flow rates for all approaches were set at 1800 veh/h/lane, given that this is typical of arterial road facilities;
- The jam density for all approaches was set at 167 veh/km/lane, given that this is typical considering the vehicle length of vehicles;
- The length of the approach links were assumed to be 1,000 meters so that queues did not spillback beyond the entrance points;
- The lost time was controlled by varying the interphase times (yellow and all-red).
- The traffic demand was generated to be totally random (i.e. the inter-vehicle headways followed a negative exponential distribution). For this study, the composition of the vehicles is assumed to be 100% PC;
- Variability in driver car-following behavior was modeled considering a speed variability coefficient of variation of 10 percent based on empirical observations (Farzaneh and Rakha, 2006b, Farzaneh and Rakha, 2006a).

In conducting the analysis, a series of traffic simulations were created to model a wide range of cycle lengths, traffic demand levels, and lost times. Table 1 demonstrates the range of parameters that were explored in the study resulting in a total of 1,224 simulation runs that were executed (17×9×8).

Table 1. Simulation Experimental Design

Parameters	Values
Cycle Length (s)	20, 30, 40, 50, 60, 70, 80, 90, 100, 110, 120, 130, 140, 150, 160, 170, 180
Total Lost Time (s)	6, 7, 8, 9, 10, 11, 12, 13, 14
Demand (veh/h)	360, 540, 720, 900, 1080, 1260, 1440, 1620

In order to determine how much green time should be allocated to each phase, the green time was distributed in proportion to the critical phase y-ratios for the critical lane groups (Mannering and Washburn, 2013). A 20-second cycle length was selected as the lower limit to model minimum green timings appropriate for pedestrian crossings. A 180-second cycle was selected as the maximum limit to model the maximum timings accepted by drivers. The results of each simulation run were then used to determine the optimum cycle length for all measures of

effectiveness (delay, fuel consumption and vehicle emissions). The following summarizes the procedure adopted to conduct the analysis:

1. Create the input files and parameters.
    a. Load the traffic demands in Table 2 for 1800 seconds and set the simulation time to 3600 seconds to ensure that all vehicles clear the network by the conclusion of the simulation.
    b. Vary the cycle length from 20 to 180 seconds in increments of 10 seconds.
    c. Vary the lost time per phase from 3 to 7 seconds at increments of 0.5 seconds.
2. Export the results of each simulation.
3. Create the following plots for each demand, with a series for each total lost time:
    a. Fuel Consumption (liters) vs. Cycle Length (seconds)
    b. HC (grams) vs. Cycle Length (seconds)
    c. CO (grams) vs. Cycle Length (seconds)
    d. NOx (grams) vs. Cycle Length (seconds)
    e. CO_2 (grams) vs. Cycle Length (seconds)
4. Identify the cycle length associated with the minimum delay, fuel consumed, HC, CO, NO_x, and CO_2 values of each demand level. Identify the optimum cycle length for each total lost time.
5. Perform a linear regression analysis to re-calibrate the Webster parameters and develop a new optimum cycle length formulation. Details of the regression analysis will be described in a later section in the paper.

4. Analysis and Findings

4.1. Simulation Results

This section presents the results of the INTEGRATION simulations and the development of the optimum cycle length equation associated with minimizing delay, fuel consumption, and emission levels. The variation of cycle lengths with an increase in vehicle demand was presented for the fuel consumed and tailpipe emissions results of each simulation. Figure 1 through Figure 5 demonstrate the INTEGRATION simulation results. Table 3 and Table 4 list the corresponding numeric output of the simulations. One noteworthy observation from the results is that the Webster optimum cycle lengths is not in accordance with the optimum cycle lengths for minimizing tailpipe emissions. Typically, the Webster optimum cycle lengths are shorter than the optimum cycle lengths identified by simulation when the volume is low. The discrepancy decreases when the demand increases. This difference will be further explored in the next section.

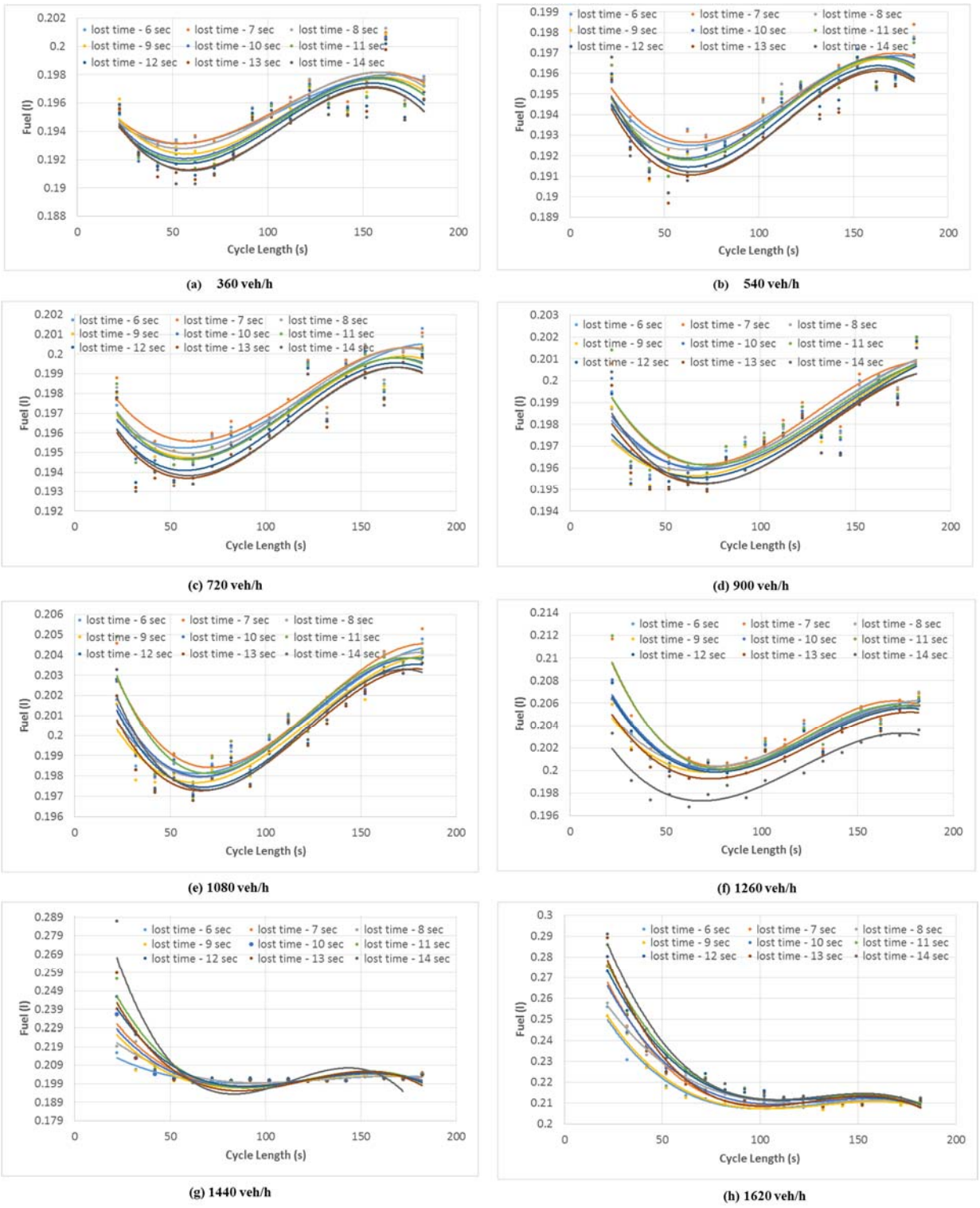

Figure 1. INTEGRATION Fuel Consumption Results

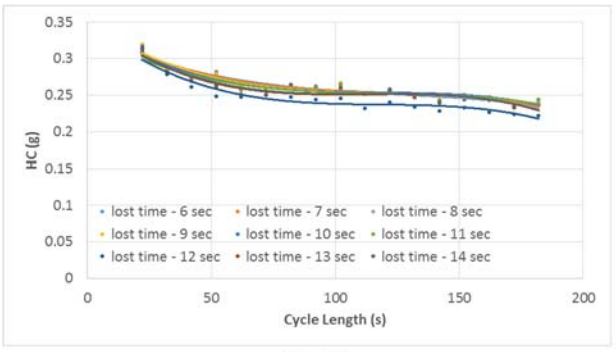

(a) 360 veh/h

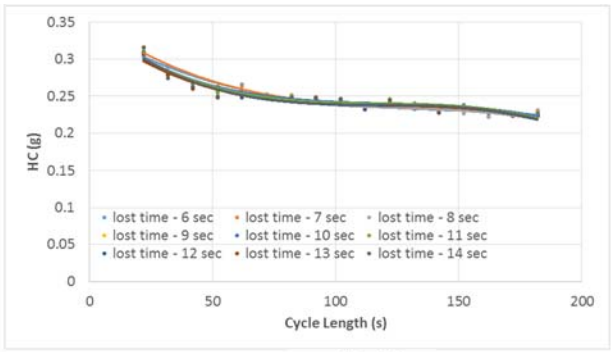

(b) 540 veh/h

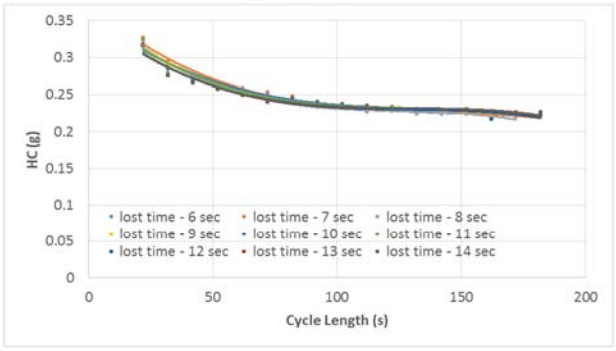

(c) 720 veh/h

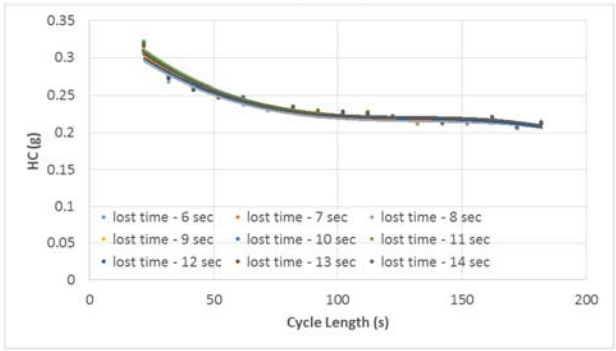

(d) 900 veh/h

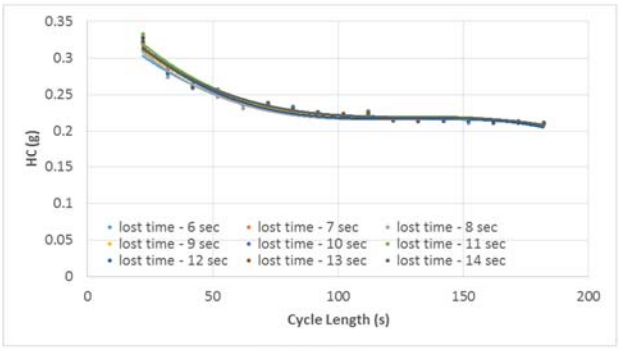

(e) 1080 veh/h

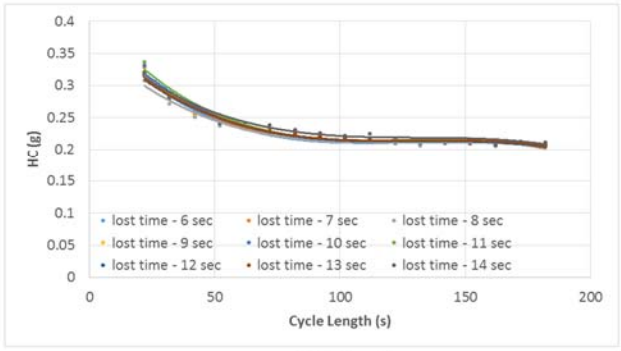

(f) 1260 veh/h

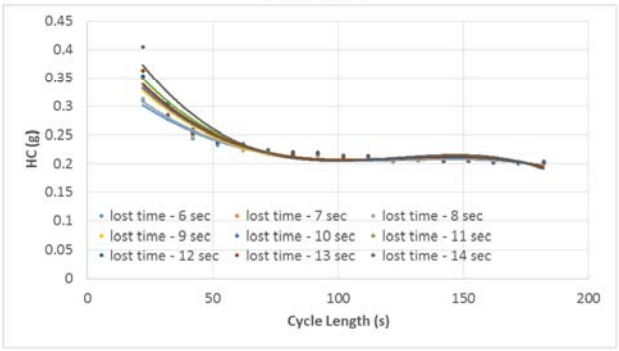

(g) 1440 veh/h

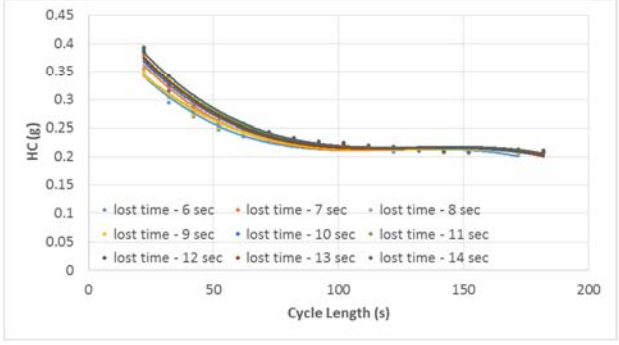

(h) 1620 veh/h

Figure 2. INTEGRATION Hydrocarbon Results

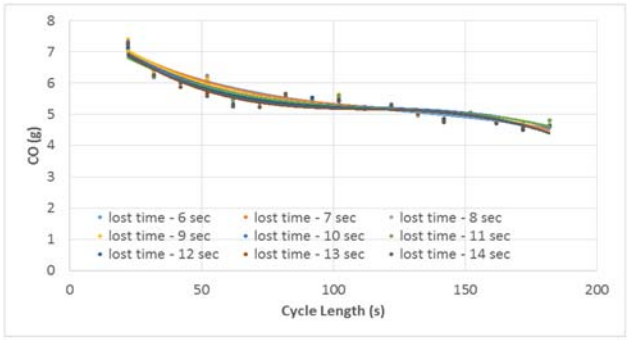

(a) 360 veh/h

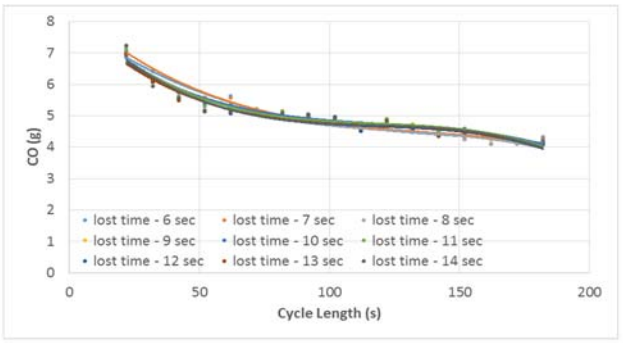

(b) 540 veh/h

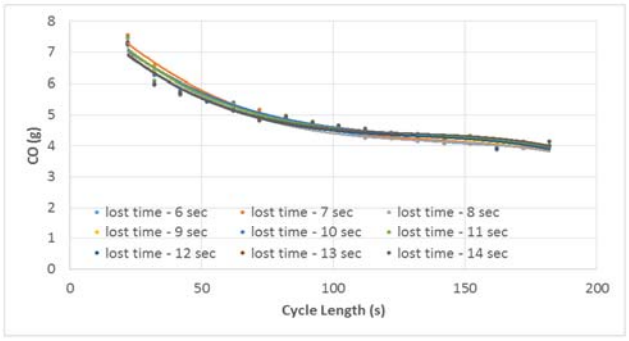

(c) 720 veh/h

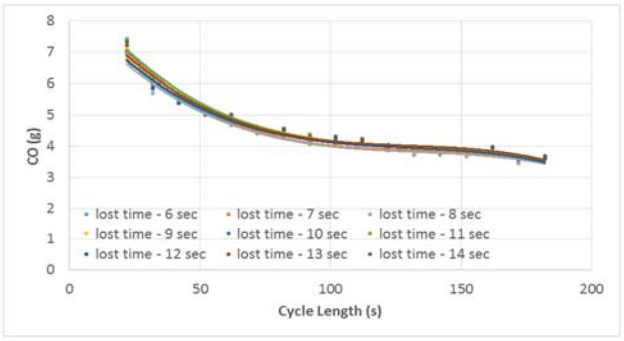

(d) 900 veh/h

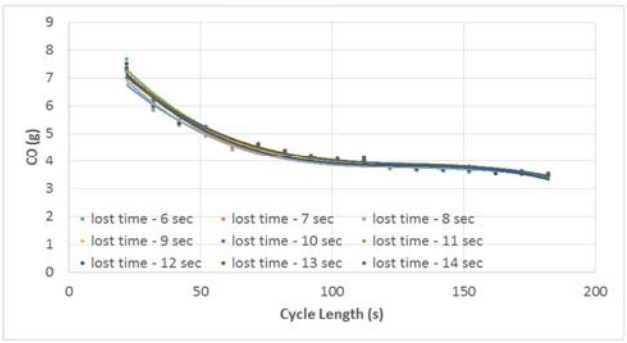

(e) 1080 veh/h

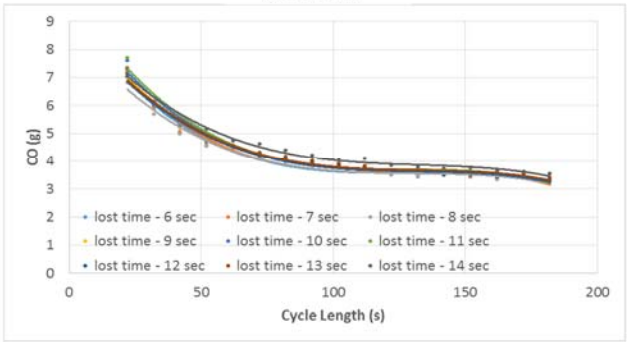

(f) 1260 veh/h

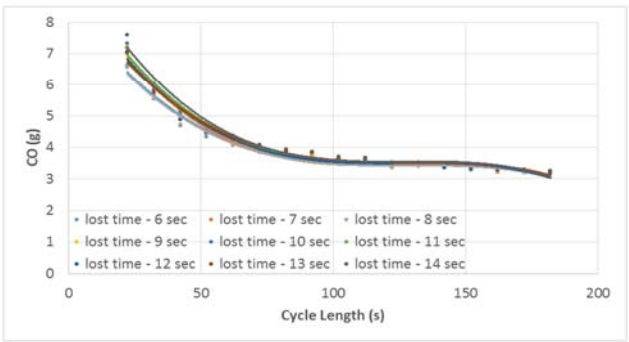

(g) 1440 veh/h

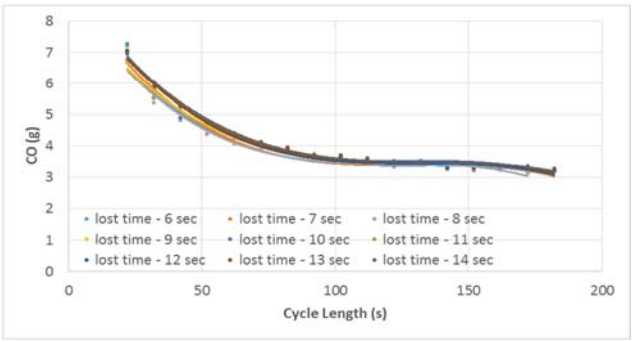

(h) 1620 veh/h

Figure 3. INTEGRATION Carbon Monoxide Results

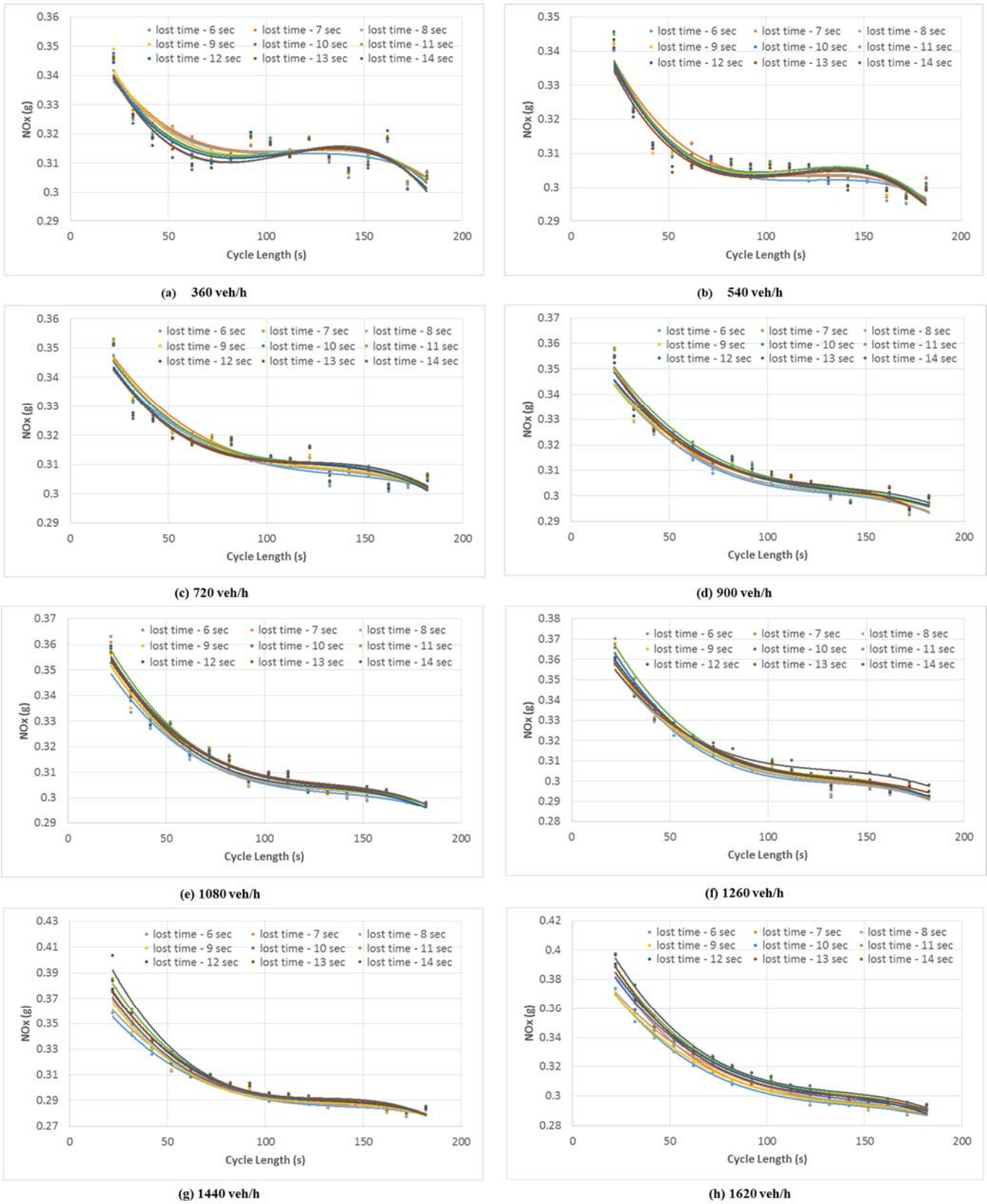

Figure 4. INTEGRATION Nitrogen Oxides Results

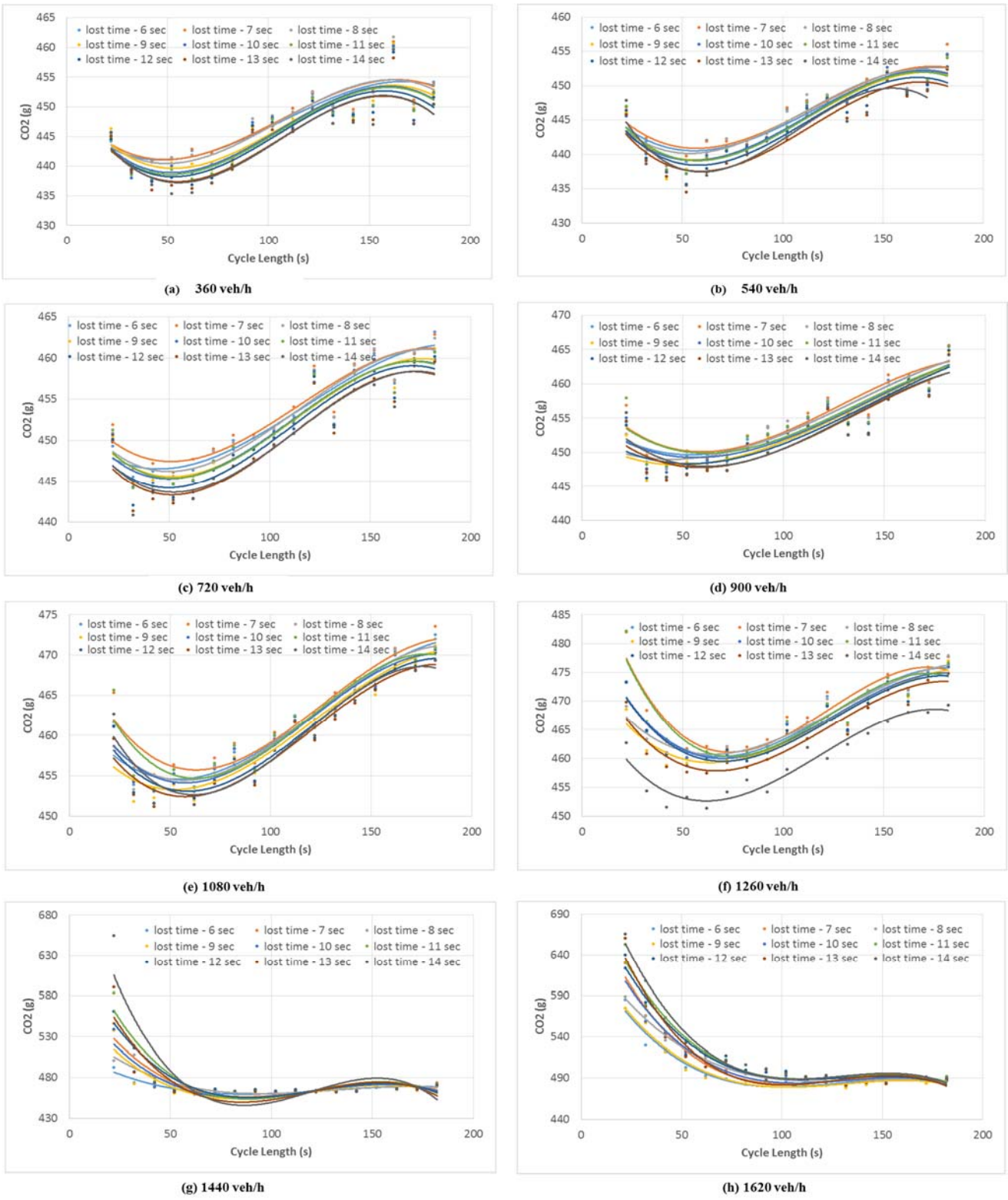

Figure 5. INTEGRATION Carbon Dioxide Results

Table 2. V/S Flow Ratios

Demand	EB	WB	NB	SB
1	0.1	0.1	0.1	0.1
2	0.2	0.2	0.1	0.1
3	0.2	0.2	0.2	0.2
4	0.3	0.3	0.2	0.2
5	0.3	0.3	0.3	0.3
6	0.4	0.4	0.3	0.3
7	0.6	0.6	0.2	0.2
8	0.7	0.7	0.2	0.2

Table 3. Optimum Cycle Length (s) for Different Measures of Effectiveness (MOEs) (L = 6 to 10 s)

	Demand (veh/h)	Y (Σ critical v/s)	Webster-Cobbe	Delay	Fuel	CO_2	CO	HC	NOx
L = 6 s	360	0.2	18	22	32	32	172	172	172
	540	0.3	20	22	42	42	162	162	172
	720	0.4	23	22	52	32	162	162	162
	900	0.5	28	22	62	42	172	172	172
	1080	0.6	35	32	62	42	182	182	182
	1260	0.7	47	32	82	52	182	182	182
	1440	0.8	70	52	102	72	172	172	172
	1620	0.9	140	82	132	132	172	172	172
L = 7 s	360	0.2	19	22	42	32	172	172	172
	540	0.3	22	22	42	42	172	172	172
	720	0.4	26	22	52	52	162	162	162
	900	0.5	31	22	62	42	172	172	172
	1080	0.6	39	32	62	62	182	182	182
	1260	0.7	52	42	82	52	182	182	182
	1440	0.8	78	52	122	122	172	172	172
	1620	0.9	155	132	132	132	172	172	172
L = 8 s	360	0.2	21	22	42	42	172	172	172
	540	0.3	24	22	42	42	172	172	172
	720	0.4	28	22	62	32	162	162	162
	900	0.5	34	22	62	32	172	172	172
	1080	0.6	43	32	62	62	182	182	182
	1260	0.7	57	32	62	62	182	162	182
	1440	0.8	85	62	132	62	182	172	172
	1620	0.9	170	132	132	132	172	172	172
L = 9 s	360	0.2	23	22	42	42	172	172	172
	540	0.3	26	22	42	42	182	172	172
	720	0.4	31	22	52	52	162	162	162
	900	0.5	37	22	42	32	172	172	172
	1080	0.6	46	32	62	32	182	182	182
	1260	0.7	62	32	82	42	182	182	182
	1440	0.8	93	52	72	62	182	172	172
	1620	0.9	185	132	132	132	172	172	172
L = 10 s	360	0.2	25	22	42	42	172	172	172
	540	0.3	29	22	52	52	182	172	172
	720	0.4	33	22	62	32	182	162	162
	900	0.5	40	32	52	42	172	172	172
	1080	0.6	50	32	62	62	182	182	182
	1260	0.7	67	32	82	52	182	182	182
	1440	0.8	100	62	62	62	182	182	172
	1620	0.9	200	132	132	132	172	172	172

4.2. Optimum Cycle Length Formulation

The optimum cycle lengths identified in the simulation for each scenario were used to calibrate the Webster model. As can be seen in Figure 1 through Figure 5, along with Table 3 and Table 4, the optimum cycle length that minimizes the HC, CO, and NOx emissions are very similar to the maximum cycle length. Consequently, cycle lengths should be maximized as much as possible if the objective is to minimize HC, CO and NOx emissions. To identify the optimum cycle length to minimize vehicle delays, fuel consumption and CO2 emission levels three sets of model parameters are calibrated, respectively.

Two model formulations are considered. The first regression model (format I) sought to develop a formulation that would be comparable with the Webster formulation and the 2010 HCM recommendation. Equation (1) is re-written in a more general form, as shown in Equation (2) and then re-cast in Equation (3).

$$C_{opt} = \frac{\propto L + \beta}{1-Y} \quad (2)$$

$$C_{opt}(1-Y) = \alpha L + \beta \quad (3)$$

Here Copt is the optimum cycle length in seconds; $\propto$ & β are the model coefficients; L is the total lost time per cycle in seconds; and Y is the sum of flow ratios for all critical lane groups. Rearranging Equation (2), Equation (3) is cast where the lost time (L) is the independent variable and the Copt×(1-Y) is the dependent variable. A linear regression analysis was conducted on the simulated data using the formulation of Equation (3). Table 5 presents the estimated model coefficients, the associated T-values, and the coefficient of determination (R2) for each model. As can be seen from Table 5 the coefficient of determination for all three models is extremely low, indicating a weak model prediction power. Equations (4) through (6) present the developed models that minimize vehicle delay, fuel consumption and CO2 emissions.

$$C_{opt,delay} = \frac{0.46L+9.5}{1-Y} \quad (4)$$

$$C_{opt,fuel} = \frac{20}{1-Y} \quad (5)$$

$$C_{opt,CO2} = \frac{17}{1-Y} \quad (6)$$

Table 4. Regression Results for Model I

MOE	R^2	Estimated α	T-Value for α (Pr>|t|)	Estimated β	T-Value for β (Pr>|t|)
Delay	0.1407	0.46	3.39 (<0.05)	9.5	6.80 (<0.05)
Fuel	0.0487	0.76	1.89 (0.0624)	20	4.87 (<0.05)
CO_2	0.0236	0.53	1.3 (0.1977)	17	4.07 (<0.05)

In an attempt to enhance the model, another model was developed by reformatting and casting the model, as shown in Equation (7) (format II). In this model, there are two explanatory variables, namely: L/(1-Y) and 1/(1-Y). In addition, an intercept term γ is introduced in the equation. The γ parameter can be viewed as a minimum optimum cycle length. Table 6 lists the

estimated model coefficients, the associated T-value, and the coefficient of determination for each model. As can be seen from Table 6 the model explanatory power increases significantly with coefficients of determination in excess of 0.5. Specifically, the optimum delay model has a coefficient of determination of 0.95 with an intercept term that is very small (3.8 s), demonstrating that the minimum cycle length is rather small. The optimum coefficients are 0.33 and 8.56, respectively, which are comparable to the Webster coefficients of 1.5 and 5.0, respectively.

Table 5. Regression Results for Model II

MOE	R^2	Estimated α	T-Value α (Pr>|t|)	Estimated β	T-Value β (Pr>|t|)	Estimated γ	T-Value γ (Pr>|t|)
Delay	0.95	0.33	4.33 (<0.05)	8.56	10.38 (<0.05)	3.8	2.76 (<0.05)
Fuel	0.54	0.82	3.27 (<0.05)	0.49	0.18 (0.8586)	40	8.83 (<0.05)
CO_2	0.85	0.27	1.97 (0.05)	8.45	5.65 (<0.05)	24	9.66 (<0.05)

The intercept term in the proposed model is a significant addition because it represents a minimum cycle length that is not included in the Webster optimum cycle length formulation. In order to compare the results from Webster formulation (Equation (1)) with the results from the proposed model (Equation (8)), one of the independent variables (1-Y)-1 was plotted against the optimum cycle length, as illustrated in Figure 6. The figure shows the proposed model versus the Webster model overlaid on the simulation results. As can be seen, when the demand is low, the two models produce comparable optimum cycle length estimates. However, the difference between the recommended optimum cycle lengths in the two methods increases as the traffic demand increases. The results are compatible with a previous study by Chen et al., who sought to improve Webster formulation using Synchro 5. They compared the optimum cycle length from the Webster formation with the optimum cycle length generated by Synchro 5 under situations when the traffic demand at an intersection is high and concluded that cycle lengths generated by Webster formulation were approximately 40 seconds longer (Cheng et al., 2003). In our case, this difference can be as large as 150 seconds as the degree of saturation approaches 1.0.

In the case of the fuel consumption and CO2 emission optimum cycle lengths, the intercept is much higher, 40s and 24s, respectively. The results demonstrate that the model coefficients are significantly different depending on the measure of effectiveness that is being minimized (delay, fuel consumption or CO2 emissions).

$$C_{opt} = \frac{\alpha \mathrm{L}}{1-\mathrm{Y}} + \frac{\beta}{1-\mathrm{Y}} + \gamma \tag{7}$$

$$C_{opt,delay} = \frac{0.33L+8.56}{1-Y} + 3.8 \tag{8}$$

$$C_{opt,fuel} = \frac{0.82\mathrm{L}}{1-\mathrm{Y}} + 40 \tag{9}$$

$$C_{opt,CO2} = \frac{0.27L+8.45}{1-Y} + 24 \tag{10}$$

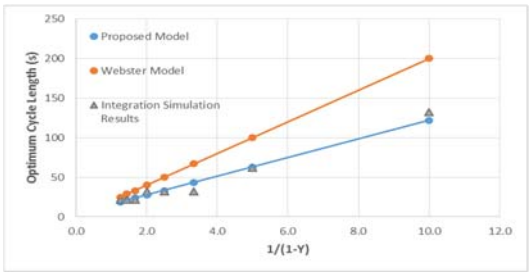

Total Lost Time – 6 sec

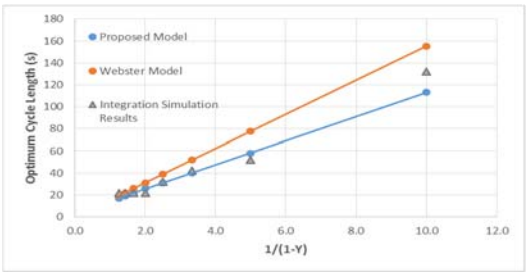

Total Lost Time – 7 sec

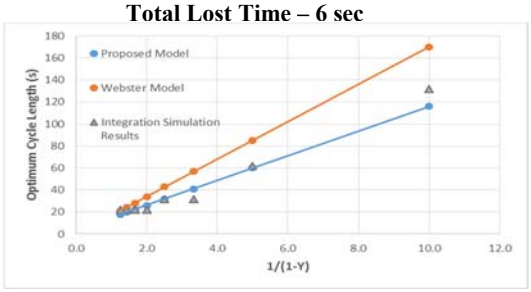

Total Lost Time – 8 sec

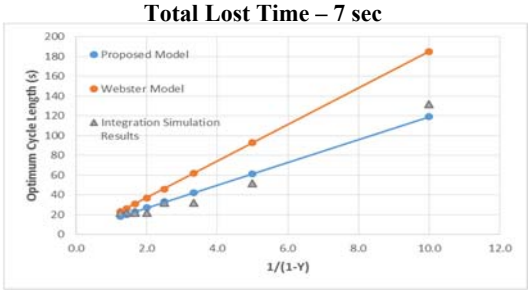

Total Lost Time – 9 sec

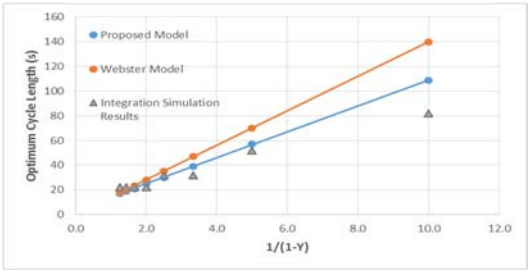

Total Lost Time – 10 sec

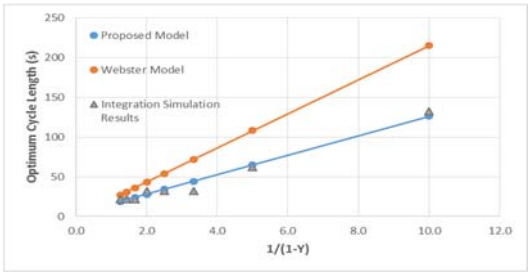

Total Lost Time – 11 sec

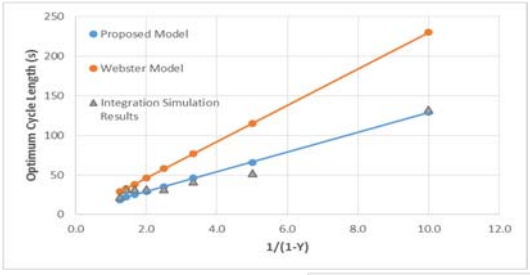

Total Lost Time – 12 sec

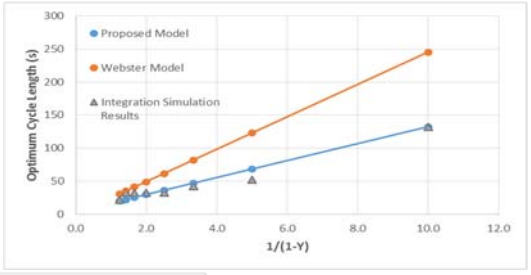

Total Lost Time – 13 sec

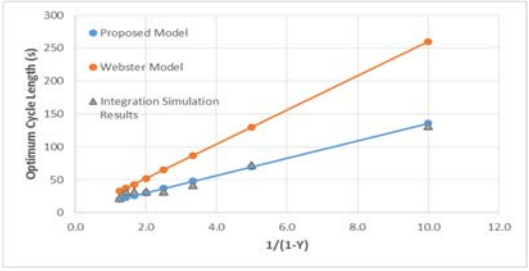

Total Lost Time – 14 sec

Figure 6. Optimum Cycle Length vs. 1/(1-Y)

5. Conclusions

The paper developed analytical models to compute the optimum cycle length that minimizes the intersection delay, fuel consumption levels and GHG emissions using data generated using the INTEGRATION microscopic traffic simulation software considering different demand levels, cycle lengths, and lost times. Optimum cycle lengths were identified for each scenario for the purpose of minimizing vehicle delay, fuel consumption levels, and emissions.

For minimizing HC, CO, and NOx emissions, longer cycle lengths are consistently favored regardless of the demand levels and lost times. To identify the optimum cycle lengths to minimize vehicle delays, the fuel consumption levels, and CO_2 emissions two sets of regression models were fit to the data. The first set of models entailed recalibrating the Webster optimum cycle length formulation. Although the results from this model were comparable with the Webster formulation, the regression results produced poor prediction power. Consequently, a second set of models were proposed considering two explanatory variables, $L(1-Y)^{-1}$ and $(1-Y)^{-1}$, and an intercept term, γ, in the formulation. The results demonstrated that the second set of models provided a very strong explanatory power. This proposed model showed that:

1. Calibration of the Webster formulation to the INTEGRATION delay estimates produced similar model parameters:
    a. The minimum cycle length term is modest (3.8 seconds);
    b. The model parameters, 0.33 and 8.56, are comparable with the parameters used in the Webster formulation, 1.50 and 5.00.
2. At lower demand levels, the modified proposed model generates a similar optimum cycle length to the Webster formulation. However, as the demand increases, the discrepancy increases significantly with the proposed model recommending shorter cycle lengths when compared with the Webster method.
3. The cycle lengths for minimizing fuel consumption and CO_2 emissions are longer than the optimum cycle length to minimize vehicle delays.
4. A minimum cycle length threshold is required for the computation of the optimum fuel consumption and CO_2 cycle lengths.

The results from this study demonstrate that the optimum cycle length for delay is significantly different from that for minimizing vehicle fuel consumption and emission levels. The design of the traffic signal needs to be customized for different design purposes. If the goal is to minimize fuel consumption and CO2 emission levels, a minimum cycle length threshold is required. If the goal is to minimize vehicle delay, the optimum cycle length calculated using the Webster method will typically overestimate the optimum cycle length.

6. Recommendations

This investigation was limited to using a two-phase signalized intersection and only eight vehicle demand levels. Further studies should be conducted on three, four, and multiphase simulations, along with different vehicle volumes, to determine if a more general formulation exits.

Reference List

A. Avgoustis, Aerde, M. V. & Rakha, H., (2004). "Framework for estimating network-wide safety Impacts of intelligent transportation systems." Intelligent Transportation Systems Safety and Security Conference, Miami.

Abu-Lebdeh, G. & Benekohal, R. F., (2000). "Genetic Algorithms for Traffic Signal Control and Queue Management of Oversaturated Two-Way Arterials." Transportation Research Record, 1727, 61-67.

Aerde, M. V. & Rakha, H., (2007a). "INTEGRATION © Release 2.40 for Windows: User's Guide – Volume I: Fundamental Model Features." Blacksburg: M. Van Aerde & Assoc., Ltd.

Aerde, M. V. & Rakha, H., (2007b). "INTEGRATION © Release 2.40 for Windows: User's Guide – Volume II: Advanced Model Features." Blacksburg: M. Van Aerde & Assoc., Ltd.

Ahn, K., Kronprasert, N. & Rakha, H. A., (2009). "Energy and Environmental Assessment of High-Speed Roundabouts." Transportation Research Record, 2123, 54-65.

Ahn, K. & Rakha, H., (2008). "The Effects of Route Choice Decisions on Vehicle Energy Consumption and Emissions." Transportation Research Part D: Transport and Environment, 13, 151-167.

Ahn, K., Rakha, H. & Trani, A., (2004a). "Microframework for modeling of high-emitting vehicles." Transportation Research Record: Journal of the Transportation Research Board, 1880, 39-49.

Ahn, K., Rakha, H. & Trani, A., (2004b). "Microframework for modeling of high-emitting vehicles." Transportation Research Record, 39-49.

Ahn, K., Rakha, H., Trani, A. & Aerde, M. V., (2002a). "Estimating vehicle fuel consumption and emissions based on instantaneous speed and acceleration levels." Journal of Transportation Engineering, 128, 182-190.

Ahn, K., Rakha, H., Trani, A. & Van Aerde, M., (2002b). "Estimating vehicle fuel consumption and emissions based on instantaneous speed and acceleration levels." Journal of Transportation Engineering, Doi 10.1061/(Asce)0733-947x(2002)128:2(182), 128, 182-190.

Cheng, D., Messer, C. J., Tian, Z. & Liu, J., (2003). "Modification of Webster's Minimum Delay Cycle Length Equation Based on HCM 2000." Annual Meeting of the Transportation Research Boar, Washington D.C.

Dion, F., Rakha, H. & Kang, Y.-S., (2004). "Comparison of delay estimates at under-saturated and over-saturated pre-timed signalized intersections." 38, 99-122.

Eisele, W., Fossett, T., Schrank, D., Farzaneh, M., Meier, P. & Williams, S., (2014). "Greenhouse Gas Emissions and Urban Congestion." Transportation Research Record 2427, 73-82.

Epa, (2014). "U.S. Greenhouse Gas Inventory Report: 1990-2013."

Farzaneh, M. & Rakha, H., (2006a). "Impact of differences in driver-desired speed on steady-state traffic stream behavior." Transportation Research Record: Journal of the Transportation Research Board, 1965, 142-151.

Farzaneh, M. & Rakha, H., (2006b). "Impact of differences in driver desired speed on steady-state traffic stream behavior." Transportation Research Record: Journal of the Transportation Research Board, 1965, 142-151.

Hajbabaie, A. & Benekohal, R., (2013). "Traffic Signal Timing Optimization - choosing the objective Function." Transportation Research Record, 2355, 10-19.
Hallmark, S. L., Wang, B., Mudgal, A. & Isebrands, H., (2011). "On-Road Evaluation of Emission Impacts of Roundabouts." Transportation Research Record, 2265, 226-233.
Li, J.-Q., Wu, G. & Zou, N., (2011). "Investigation of the impacts of signal timing on vehicle emissions at an isolated intersection." Transportation Research Part D: Transport and Environment, http://dx.doi.org/10.1016/j.trd.2011.03.004, 16, 409-414.
Li, M.-T. & Gan, A., (1999). "Signal Timing Optimization for Oversaturated Networks Using TRANSYT-7F." Transportation Research Record, 1683, 118-126.
Li, X., Li, G., Pang, S.-S., Yang, X. & Tian, J., (2004). "Signal timing of intersections using integrated optimization of traffic quality, emissions and fuel consumption: a note." Transportation Research Part D: Transport and Environment, http://dx.doi.org/10.1016/j.trd.2004.05.001, 9, 401-407.
Liao, T.-Y., (2013). "A fuel-based signal optimization model." Transportation Research Part D: Transport and Environment, 23, 1-8.
Lv, J. & Zhang, Y., (2012). "Effect of signal coordination on traffic emission." Transportation Research Part D: Transport and Environment, http://dx.doi.org/10.1016/j.trd.2011.10.005, 17, 149-153.
Ma, X., Jin, J. & Lei, W., (2014). "Multi-criteria analysis of optimal signal plans using microscopic traffic models." Transportation Research Part D: Transport and Environment, http://dx.doi.org/10.1016/j.trd.2014.06.013, 32, 1-14.
Madireddy, M., Coensel, B., Can, A., Degraeuwe, B., Beusen, B., Vlieger, I. & Botteldooren, D., (2011). "Assessment of the Impact of Speed Limit REduction an Traffic Signal Coordination on Vehicle Emissions Using an Integraed Approach." Transportation Research Part D: Transport and Environment, 16, 504-508.
Mannering, F. & Washburn, S. (2013). Principles of Highway Engineering and Traffic Anlysis, New York, Wiley.
Papson, A., Hartley, S. & Kuo, K., (2012). "Analysis of Emissions at Congested and Uncongested Intersections with Motor Vehicle Emission Simulation 2010." Transportation Research Record, 2270, 124-131.
Pulter, N., Schepperle, H. & Böhm, K., (Year) Published. "How Agents Can Help Curbing Fuel Combustion – a Performance Study of Intersection Control for Fuel-Operated Vehicles." Proc. of 10th Int. Conf. on Autonomous Agents and Multiagent Systems – Innovative Applications Track (AAMAS 2011), Tumer, Yolum, Sonenberg and Stone (eds.), 2011 Taipei, Taiwan. 795-802.
Rakha, H. 1990. An Evaluation of the Benefits of User and System Optimised Route Guidance Strategies. M.Sc., Queen's University, Kingston.
Rakha, H., Aerde, M. V., Bloomberg, L. & Huang, X., (1998). "Construction and calibration of a large-scale microsimulation model of the Salt Lake area." Transportation Research Record, 1644, 93-102.
Rakha, H., Ahn, K. & Trani, A., (2004a). "Development of VT-Micro model for estimating hot stabilized light duty vehicle and truck emissions." Transportation Research Part D: Transport and Environment, 9, 49-74.
Rakha, H., Ahn, K. & Trani, A., (2004b). "Development of VT-Micro model for estimating hot stabilized light duty vehicle and truck emissions." Transportation Research, Part D: Transport & Environment, 9, 49-74.

Rakha, H. & Crowther, B., (2002). "Comparison of Greenshields, Pipes, and Van Aerde Car-following and Traffic Stream Models." Transportation Research Record, 1802, 248-262.
Rakha, H. & Crowther, B., (2003). "Comparison and Calibration of FRESIM and INTEGRATION Steady-state Car-following Behavior." Transportation Research Part A: Policy and Practice, 37, 1-27.
Rakha, H., Flintsch, A., Ahn, K., El-Shawarby, I. & Arafeh, M., (2005). "Evaluating Alternative Truck Management Strategies Along Interstate 81." Transportation Research Record: Journal of the Transportation Research Board, 10.3141/1925-09, 1925, 76-86.
Rakha, H., Kang, Y.-S. & Dion, F., (2001a). "Estimating vehicle stops at undersaturated and oversaturated fixed-time signalized intersections." Transportation Research Record, 1776, 128-137.
Rakha, H. & Lucic, I., (2002). "Variable power vehicle dynamics model for estimating maximum truck acceleration levels." Journal of Transportation Engineering, 128, 412-419.
Rakha, H., Lucic, I., Demarchi, S. H., Setti, J. R. & Aerde, M. V., (2001b). "Vehicle dynamics model for predicting maximum truck acceleration levels." Journal of transportation engineering, 127, 418-425.
Rakha, H. & Zhang, Y., (2006). "Analytical procedures for estimating capacity of freeway weaving, merge, and diverge sections." Journal of transportation engineering, 10.1061/(asce)0733-947x(2006)132:8(618), 132, 618-628.
Rakha, H. & Zhang, Y. H., (2004). "INTEGRATION 2.30 framework for modeling lane-changing behavior in weaving sections." Traffic Flow Theory and Highway Capacity and Quality of Services 2004, 140-149.
Rakha, H. A., Ahn, K. & Moran, K., (2012). "INTEGRATION Framework for Modeling Eco-routing Strategies: Logic and Preliminary Results." International Journal of Transportation Science and Technology, 1, 259-274.
Stevanovic, A., Kergaye, C. & Stevanovic, K., (2011). "Evaluating Robustness of Signal Timings for Varying Traffic Flows." Transportation Research Record, 2259.
Stevanovic, A., Stevanovic, J. & Martin, P. T., (2009). "Optimizing Signal Timings from the Field VISGAOST and VISSIM–ASC/3 Software-in-the-Loop Simulation." Transportation Research Record, 2128, 114-120.
Usdot & Bts, (2015). "National Transportation Statistics."
Van Aerde, M. & Rakha, H., (2013a). "INTEGRATION © Release 2.40 for Windows: User's Guide – Volume I: Fundamental Model Features." Blacksburg: M. Van Aerde & Assoc., Ltd.
Van Aerde, M. & Rakha, H., (2013b). "INTEGRATION © Release 2.40 for Windows: User's Guide – Volume II: Advanced Model Features." Blacksburg: M. Van Aerde & Assoc., Ltd.
Van Aerde, M. & Yagar, S., (1988). "Dynamic Integrated Freeway/Traffic Signal Networks: Problems and Proposed Solutions." Transportation Research, 22A(6), 435-443.
Webster, F. V. (1958). Traffic Signal Settings, London, Her Majesty's Stationery Office.

Sub-report Task #3

Characterizing Emergency Vehicle Preemption Operation Using High Resolution Traffic Signal Event Data

Prepared by:

Andrew P. Nichols, PhD, PE
Professor
Marshall University

and

Chih-Sheng Chou, PhD
Research Associate
Rahall Transportation Institute

Acknowledgments

This work was supported by the Mid-Atlantic Transportation Sustainability University Transportation Center (MATS UTC).

Disclaimer

Table of Contents

List of Figures

List of Tables

1. Problem

Emergency vehicle preemption (EVP) is implemented at signalized intersections to maximize safety by providing a dedicated green indication for the approaching vehicle. This ensures that no conflicting vehicles will enter the intersection so that the emergency vehicle (EV) can maintain a high rate of speed, minimizing the time needed to reach its destination. Likewise, EVP can help clear an existing queue that may be blocking the path for an approaching EV. Fire trucks and sometimes ambulances are equipped with preemption emitters that can be detected by preemption detectors when they are within a certain distance of the intersection (1). While there are other preemption mechanisms, including audible detectors that respond to a siren and route-based preemption that rely on GPS to apply preempt through a central system, this paper will focus on optical emitters. An EVP control strategy is programmed in each traffic signal controller, which includes the phase(s) that will be served for each preemption call, at a minimum. To ensure exclusive right-of-way, the EVP phase assignment is typically exclusive to the direction of flow so that EV can make any turn at the intersection, which is accomplished by displaying green for the left-turn and thru phases.

EVs are random traffic events that interact with general vehicles along the roadway, typically causing an interruption in traffic flow, both directly and indirectly. For example, some drivers will yield right-of-way to the EV by slowing down and pulling over. The indirect interruption is caused by the controller leaving its normal coordinated operation to serve the EV. Previous studies have investigated movement conflicts between EVs and other vehicles (2), optimal control strategies for minimizing EV response time, and EV route reliability with travel time estimation (3, 4, 5, 6). Since EVs commonly operate along coordinated arterials, their impacts on signal coordination have been explored. Nelson and Bullock examined various control algorithms and their impact on operations at a diamond intersection using hardware-in-the-loop simulation and reported the impact is a function of EV demand (7). Obenberger and Collura assessed the state-of-practice EVP control strategies, and applied a software-in-the-loop platform to evaluate travel delay and travel time for various transition methods versus different levels of general traffic demand. They emphasized the importance of minimizing the time required for completing an EV service and for the signal operation to return back to coordination plan (8, 9). Yun et al. followed this research direction and used hardware-in-the-loop simulation to compare various EVP parameters based on a performance measure of “average time back to coordination plan”, among others. They relied on a computer screen recording tool to calculate this value, and used simulation output for other performance measures (10). Most studies in this area rely on performance metrics that can be compiled from simulation output. This paper attempts to produce performance metrics from data generated by field controllers.

2. Approach

High resolution traffic signal event data generated by the controller is already being used to monitor the performance of traffic signals through a variety of calculated metrics (11, 12, 13). This data has been generated using the Traffic Signal Performance Monitoring System (TSPMS), the Systematic Monitoring of Arterial Road Traffic and Signal (SMART-Signal) system, and the data logger of the Econolite ASC/3 controller (14) among other controllers. The high resolution data are generated by controllers in 0.1-second intervals, and includes phase changes, preemption triggers, coordination status, vehicle detection and other events characterizing the controller state (15).

This study proposes the use of a Signal Phase Spectrum (SPS) plot to facilitate the analysis of high resolution data for any application. The SPS will be used to calculate performance measures characterizing EVP operation at a single intersection and a network of intersections. In the next section, the process for plotting high resolution data in the SPS is presented. The following section covers the calculation of the performance measures from the high resolution data. An overview of the signal system in Morgantown, WV is provided because this system is used for (a) demonstrating the performance measures in a simulation environment for evaluating transition modes when leaving preemption and (b) demonstrating the use of high resolution data for identifying potential problems in preemption operations and configurations in the field.

3. Methodology

3.1. Signal Phase Spectrum Plot

The Signal Phase Spectrum (SPS) plot is created to visualize the high resolution data and facilitate the analysis of that data. The SPS plot in this paper is developed using high resolution data collected with the data logger of the Econolite ASC/3 controller (15). Four categories of high resolution data were extracted from the logs for this study, summarized in Table 1. Those categories are related to phase status, EV triggers, coordination status, and vehicle detection.

Table 1. High Resolution Codes for Developing EVP Signal Phase Spectrum Plot

Category	Event Code	Parameter	Event Description
Phase Event	1	Phase #	Phase begin green
	8	Phase #	Phase begin yellow
	10	Phase #	Phase begin red
Detector Event	81	Channel #	Detector call OFF
	82	Channel #	Detector call ON
Preemption Event	102	Channel #	Preemption (call) input ON
	104	Channel #	Preemption (call) input OFF
Coordination Event	150	0	Coordination free
		1	In step
		2	Transition Add
		3	Transition Subtract
		4	Transition Dwell
		5	Local Zero
		6	Begin Pickup

This data was plotted to an Excel spreadsheet chronologically to produce the SPS plot shown in Figure 1. The process to generate a SPS plot includes:

1. Plot Phase Events. Records associated with phase events are plotted for each phase chronologically, with cells colored green (code 1), yellow (code 8) or red (code 10).
2. Plot Preemption Events. Records associated with preemption input ON (code 102) and OFF (code 104) were plotted over the phase for which the EVP is assigned. The EVP phase assignments are stored in the controller and cannot be determined from the high resolution data alone. In Figure 1, the preemption records are plotted on phase 1 and 6 (callouts ‘A’ and ‘B’), meaning that this preemption trigger called these two phases.
3. Plot Coordination Events. Once an EVP call is triggered and served at an intersection running a coordination plan, coordination is interrupted and the controller goes into FREE mode (code 150, parameter 0). After the preemption call ends, the controller will transition back to coordinated operation. Depending on the coordination transition mode configured in the controller, a record will be generated corresponding to ADD (code 150-2), SUBTRACT (code 150-3), or DWELL (code 150-4). Once the transition period has ended and the controller is in coordination, a record will be

generated indicating the controller is IN STEP (code 150-1). These states are depicted in the middle portion of Figure 1 as callouts ‘C’, ‘D’, and ‘E’.

4. Plot Detector Events. In some cases, it may be desirable to additionally investigate vehicle arrivals at the intersection, if sufficient and properly placed vehicle detection is installed at the intersection. Code 82 is generated when a detector channel turns ON and code 81 is generated when it turns OFF. The detector channel phase assignments are stored in the controller and cannot be determined from the high resolution data alone. For advanced detection, it is sufficient to only indicate when the detector turns ON (as indicated by callout ‘F” in Figure 1 for phase 2 and phase 6). For stopbar detection, it would be more desirable to indicate the presence by plotting both the ON and OFF records.

Figure 1 depicts a portion of an SPS plot when an EVP trigger occurred (denoted by ‘A’). The controller is serving phases 2 and 6 when the EVP trigger occurs at time 9:01:58.1 AM calling phases 1 and 6. The coordination is interrupted and goes into FREE mode (‘C’). After serving the clearance interval for phase 2, the controller serves phases 1 and 6 until the EVP trigger turns off at time 9:02:18.2 AM (‘B’). At that time, the controller begins transitioning back into coordination by adding time (‘D’). The transition period ends at time 9:03:24.8 AM when the controller is IN STEP (‘E’).

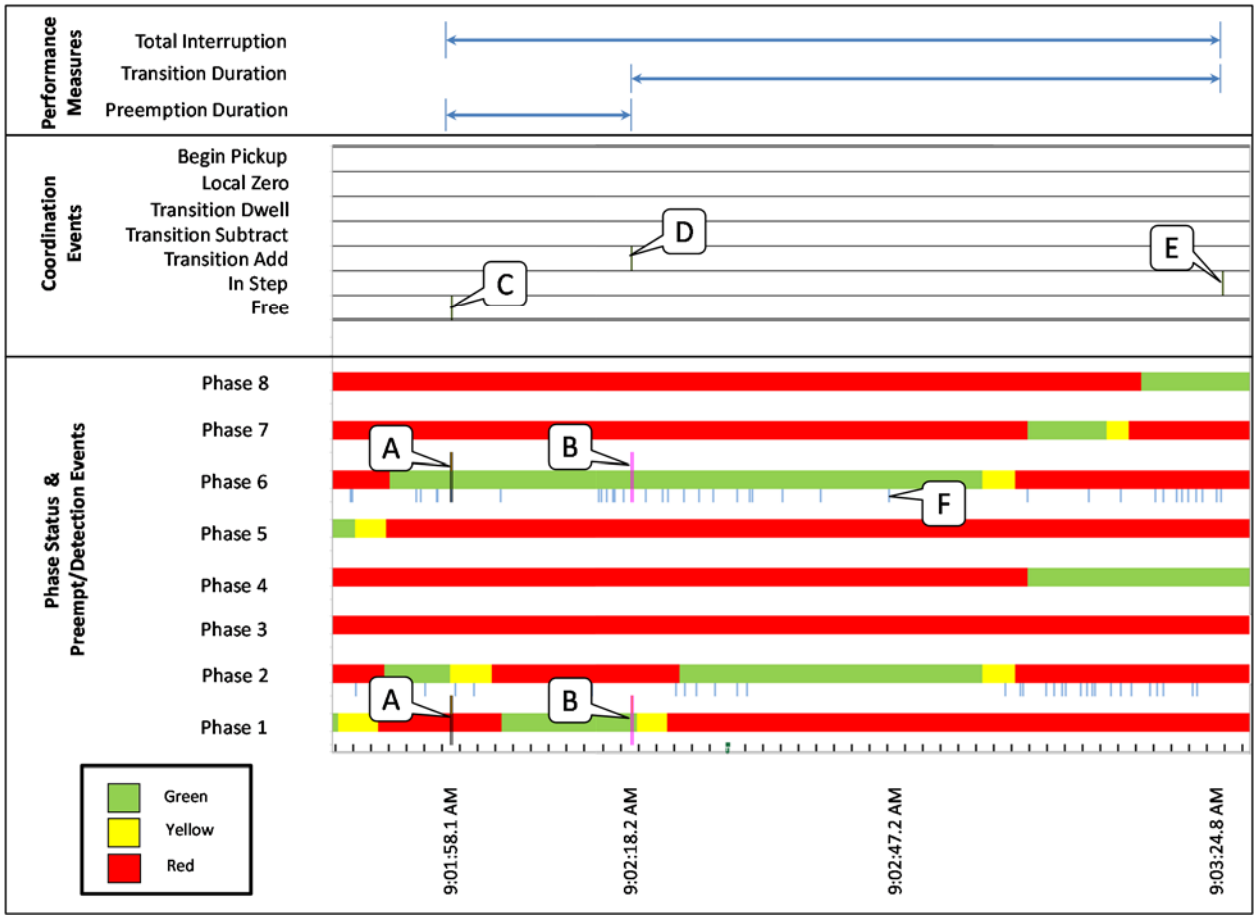

Figure 1. Signal Phase Spectrum (SPS) Plot for EVP Performance Measures

3.2. Emergency Vehicle Performance Measures

Different preemption performance measures can be calculated for individual intersections and networks based on the SPS plot, as presented in this section and applied to a simulation network in the following sections.

To illustrate the calculation of the performance measures, an EVP trigger (i) is generally assigned the characteristics time (t) and space/location (s) based on the high resolution event code (c) as:

EVP trigger = (t_i^c, s_i^c);
where

t_i^c : timestamp corresponding to code (*c*) associated with trigger (*i*);
s_i^c : space attribute corresponding to code (*c*) associated with trigger (*i*);
c : event code *c* = {102, 104, 150-0, 150-1, 150-x};
150-x: the first transition response to a trigger, it can be any one of 150-2 (Transition Add), 150-3 (Transition Subtract) or 150-4 (Transition Dwell); and
i : EVP trigger sample *i* = {1,2,….*I*}.

3.2.1 Individual Intersection Analysis

For a selected intersection, the EVP performance measures are illustrated in the upper portion of Figure 1 and defined below.

- Preemption Duration (PD) of EVP trigger (*i*):
  $EVP\ PD_i = t_i^{104} - t_i^{102}$.
  This period is defined by the time difference between the preemption trigger turning ON and OFF. Longer preemption durations would indicate that it is taking the EV longer to pass through the intersection. Variation of this duration is most likely caused by traffic congestion, which impedes the EV progression.
- Transition Duration (TD) of EVP trigger (*i*):
  $EVP\ TD_i = t_i^{150\_1} - t_i^{150\_x}$.
  This period is defined by the time difference between the controller entering transition mode due to the EVP trigger turning OFF and the controller being IN STEP. A smaller value is preferred when considering the time required for the coordination to be back to normal operation.
- Total Interruption (TI) of EVP trigger (*i*) :
  $EVP\ TI_i = t_i^{150\_1} - t_i^{150\_0} = EVP\ PD_i + EVP\ TD_i$.
  This period is defined between the preemption trigger turning ON to the time when the controller is IN STEP.

3.2.2 Network Analysis

The individual intersection metrics can be applied to multiple intersections in a network. Furthermore, additional network metrics can be derived by estimating the trajectory of each EV through the network, which requires both the time and location attributes of the EVP triggers.

Since the preemption call turns OFF (Code 104) when the EV emitter is no longer in the field of view for the detector, the time of this event is specifically used in this analysis to represent the EV's arrival at the intersection. The location of Code 104 will be more deterministic across EVs and intersections compared to Code 102, since the location of the vehicle relative to the intersection when the preemption input turns ON is affected by many factors (e.g., intersection approach geometry, emitter and detector ranges).

For computing distance between intersections, the actual travel distance is used, which must be obtained from an external source (e.g., online maps, simulation network). In this methodology, the cumulative distance along the network is computed from an assumed starting point at one network boundary based on the known segment distances. The cumulative distance of each intersection is used as the physical location attribute (s) to represent each intersection in the network.

In order to generate the trajectory through the network, triggers that occur across multiple intersections and are likely from the same vehicle need to be assigned a unique vehicle attribute (v). Since there is no way to uniquely identify individual vehicles from the high resolution data, the four-step re-identification process below is applied to assign each trigger (i) to a vehicle.

1. Define the possible EV routes (*r*) through the network, which includes the sequential intersections and corresponding EVP phases, where $r = \{0,1,\ldots.R\}$.
2. Assign an identifier (*v*) for a trigger (*i*) that occurs at a boundary entrance to the network along route (*r*) and set its time (*t*) and location (*s*) as an origin. Set $(t_i^{104}, s_i^{104}) = (t_v^{104}, s_v^{104})_n$ and $n = 0$ (i.e., it is an origin), if it is a trigger associated with the EV entering the network.
3. Set $n = n+1$ (i.e., entering subsequent intersection), and search for a trigger (*j*) (t_j^{104}, s_j^{104}) from the vehicle (*v*) at an adjacent intersection along the possible EV route (*r)* (i.e., $(s_j^{104}) \in r$). If the time difference between *i* and *j* triggers are reasonable based on an assumed travel speed and known distance (e.g., minimum < $\Delta t = [(t_j^{104}) - (t_v^{104})_n]$ < maximum), they will be assigned to the same vehicle (*v*) and the *j* trigger attributes are set $(t_j^{104}, s_j^{104}) = (t_v^{104}, s_v^{104})_{n+1}$.
4. Repeat Step 3 to find triggers at subsequent intersections until reaching the end of route (*r)*, where $n = N$ for vehicle (*v*). Afterward, an EV trip for vehicle (*v*) along route (*r*) can be represented by a collection of triggers:
   $EVP\ Trip_v = \{(t_v^{104}, s_v^{104})_n\} = \{(t_v^{104}, s_v^{104})_0, (t_v^{104}, s_v^{104})_1, (t_v^{104}, s_v^{104})_2, \ldots, (t_v^{104}, s_v^{104})_N\}$.

For the network level, the EVP performance measures can be characterized as defined below.

- Segment Travel Time (*TT*) from intersection *a* to intersection *b* for *EVP (v)*:
  $EVP\ TT_{a,b,v} = [(t_v^{104})_b - (t_v^{104})_a]$, where a, b ∈ $n = \{0,1,\ldots.N\}$.
- Segment Speed (*S*) estimation from intersection *a* to intersection *b* for *EVP (v)*:
  $EVP\ S_{a,b,v} = [(s_v^{104})_b - (s_v^{104})_a] \div [(t_v^{104})_b - (t_v^{104})_a]$, where a, b ∈ $n = \{0,1,\ldots.N\}$.
- EVP Origin-Destination (*OD*) matrix illustrating the intersections in the network that each vehicle (v) preempted.

Set *EVP* $Trip_{(v)}$ O_pD_q = 1 for an EV (v) with Origin from intersection p and Destination at intersection q in a network.
EVP OD matrix = $\left[\sum_{v=1}^{V} EVP\ Trip_{(v)} O_p D_q\right]$, where p = {*1,2,..P*} and q = {*1,2,..Q*}.

4. Analysis and Findings

4.1. Morgantown Traffic Management System

4.1.1 Field Deployment

In 2010, West Virginia DOT implemented a project to improve the traffic flow along the WV-705 corridor in Morgantown, WV. The project upgraded controllers, detection and communication at all 17 intersections along the corridor to provide real-time communication to each controller from the Econolite Centracs Central Management System software. The Centracs system uploads the high resolution data logs from each intersection and archives them in an SQL database for further analysis. The logs from the field deployment will be further investigated in the Field Application section of this paper.

4.1.2 Simulation Deployment

The Centracs system used for the field deployment was replicated for use in a simulation environment in order to evaluate various control strategies off-line. The central system-in-the-loop (CSIL) simulation environment consists of Centracs communicating with VISSIM software, which utilizes a software-in-the-loop (SIL) platform emulating the Econolite ASC/3 controllers. The SIL for each intersection is a duplicate of the controller configuration in the field. This platform has previously been used to evaluate various adaptive signal control strategies for this corridor (13). Traffic volumes in the VISSIM simulation were calibrated with field survey data collected in 2010. It is worth noting that the CSIL simulation must be executed in real time (i.e. one simulation second equal to one real second) in order for the high resolution data to be collected.

4.2. Emergency Vehicle Simulation Configuration

In the field, an EV is typically equipped with an optical emitter to trigger a preemption phase when the vehicle is within a certain distance of the intersection (16). If there are no occlusions and the emitter is working properly, the trigger should be constant until the vehicle passes the preemption detector, which is typically installed adjacent to the signal indications. In order to replicate the preemption mechanism in VISSIM, a detection zone was configured on the intersection approach that starts 850 feet upstream (assumed optical emitter range) and ends at the stopbar. The detection zone is configured to only respond to a certain defined vehicle class (e.g., EV). Each EVP detection zone is mapped to the corresponding preemption channel in the controller. Each preemption channel is associated with an EVP plan, which includes the phase assignments and other parameters.

EVs (defined vehicle class) are introduced into the simulation network at certain time intervals and have predefined routes. It is known that drivers respond to the presence of an EV by slowing down or changing lanes to let them pass. However, it is difficult to replicate this behavior in VISSIM. Therefore, for this study, it is assumed that the EV in the simulation will travel with the flow of all traffic. The desired speed of the EV vehicle class was set to be 35-55 mph, which is higher than the other vehicle classes that are set to 29-36 mph.

4.3. Simulation Application: Performance Measures

High resolution data from either the field or simulation environments can be applied to develop SPS plots and characterize EVP performance measures. This section first presents a case study that is conducted with the CSIL platform. Since many controller parameters can be manipulated in the simulation environment, it provides the ability to compare performance based on different configurations.

4.3.1 Scenarios Evaluated

The CSIL of the Morgantown system is applied herein. Four intersections along the WV-705 Corridor as indicated (i.e., Intersection 113, 115, 116, and 117) in Figure 2 are studied. Three EVP routes crossing these four intersections were defined:

- Route 1: Point A to Point C (Intersection 117→116→115→113),
- Route 2: Point C to Point A (Intersection 113→115→116→117), and
- Route 3: Point B to Point A (Intersection 116→117).

The simulation duration is 14.5 hours (4:30 AM to 7:00 PM). The EV triggers were controlled to occur once per hour from 6:00 AM to 7:00 PM in a sequence of Route 1, Route 2, and Route 3. Thus, one 14.5-hour simulation will have 13 EVs traversing the study corridor. Based on the route layouts, Intersections 116 and 117 will experience 13 EV triggers while 113 and 115 will have nine EV triggers. The corridor utilizes cycle lengths of 120 seconds, 124 seconds, and 158 seconds for the AM, mid-day, and PM periods.

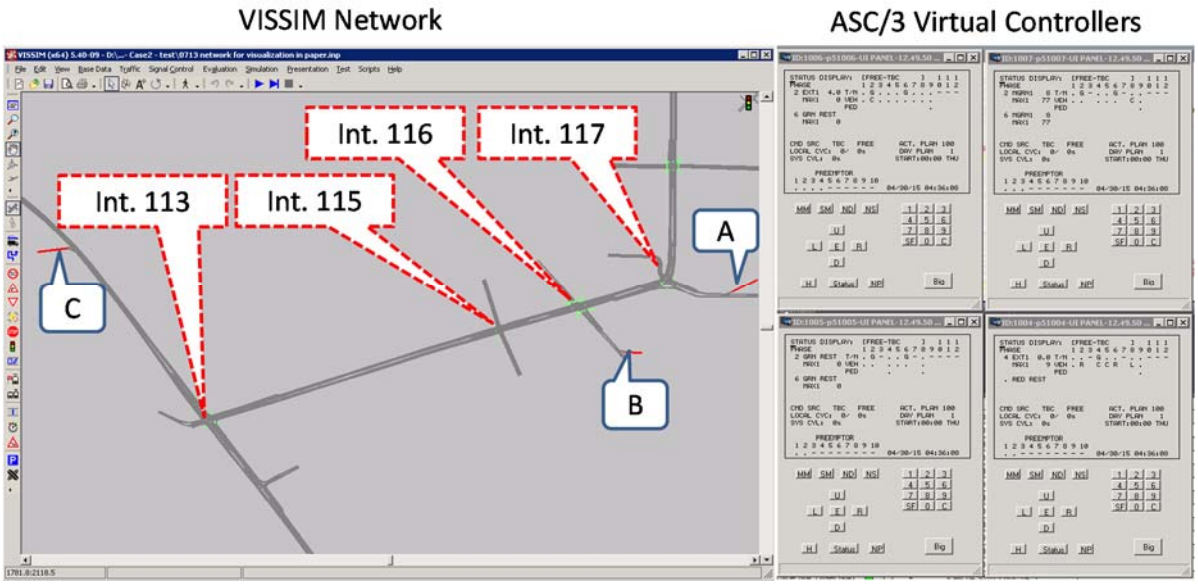

Figure 2. Study Intersections in VISSIM Simulation Environment

In order to illustrate the application of the EVP performance measures, certain controller parameters will be varied between simulation runs. The specific parameter varied in this study is the transition method, which affects how quickly a controller returns to coordination after the EVP is served. In the ASC/3 controller, the transition modes are Smooth, Dwell, and Add Only. Additionally, the maximum amount of time that can be added or subtracted during each cycle

can also be configured for each transition mode, which is capped at 20 seconds/cycle in the ASC/3 controller. After the completion of each simulation, the high resolution data were retrieved from the database and applied to develop a single SPS plot for each intersection. Therefore, four SPS plots are generated from each simulation. A VB macro was programmed to generate the SPS plots and compute the EVP performance measures.

4.3.2 Preemption Duration and Transition Duration

Results from Intersection 116 were analyzed to illustrate the EVP performance measures for an individual intersection. The Preemption Duration (PD) and Transition Duration (TD) are plotted for each EVP trigger from Scenario 1 in Figure 3a. The sum of these two values also constitutes the Total Interruption (TI). For example, the fifth trigger occurred at 10:05 AM, requesting service for phases 2 and 5. At the time when the trigger occurred, those phases were red. The PD for this trigger was 19.8 seconds and the TD was 497.9 seconds, which results in a TI of 517.7 seconds. For all triggers at this intersection under Scenario 1, the PD ranges from 17 seconds to 66 seconds with an average of 28 seconds and the TI ranges from 98 to 698 seconds with an average of 314 seconds.

The individual performance measures associated with each intersection are summarized in Figure 3b for the three transition modes. It is found that PD values are similar across different simulation scenarios at each intersection, which is expected since the duration of the preemption call isn't impacted by the transition mode. Variations in PD are reflective of the congestion level of the intersection, which would impede the vehicle's progress, and the phase being served when the preempt call is received. EVs experienced the longest PD at intersection 116 and the shortest at intersection 117. Intersection 116 is the most congested along this corridor because the cross street has a relatively high demand. Based on the TD results, the Smooth transition produced the shortest transition periods. This is expected since the smooth transition algorithm can either add or subtract time to reach transition in the shortest amount of time (one controller brand refer to this method as "short way"). At intersections 113, 115, and 117, Add Only produced the next shortest transition periods, followed by Dwell with the longest transition periods. At Intersection 116, the Dwell transition duration was shorter than Add Only.

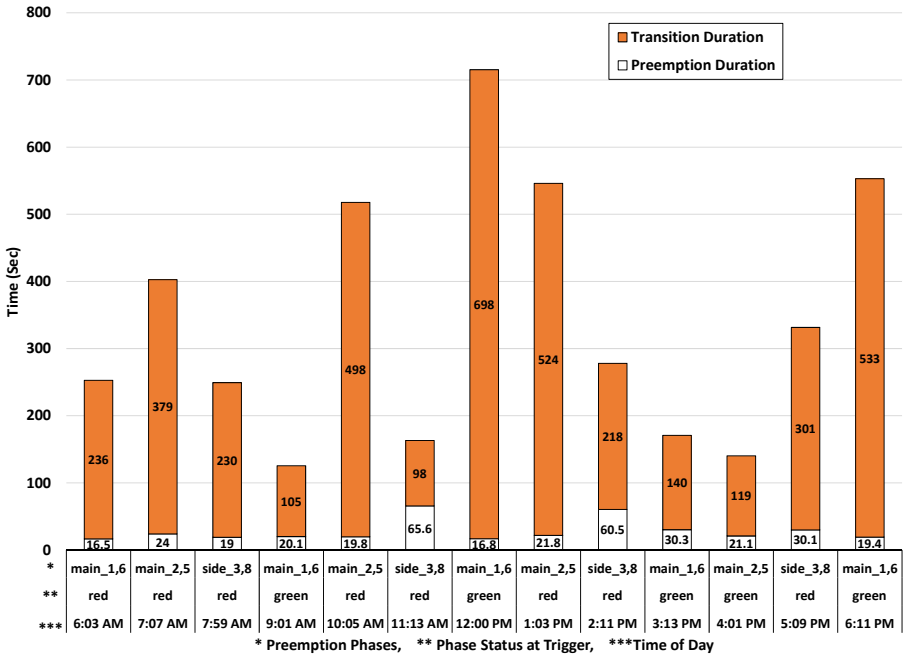

(a) Intersection 116, Smooth Transition Scenario

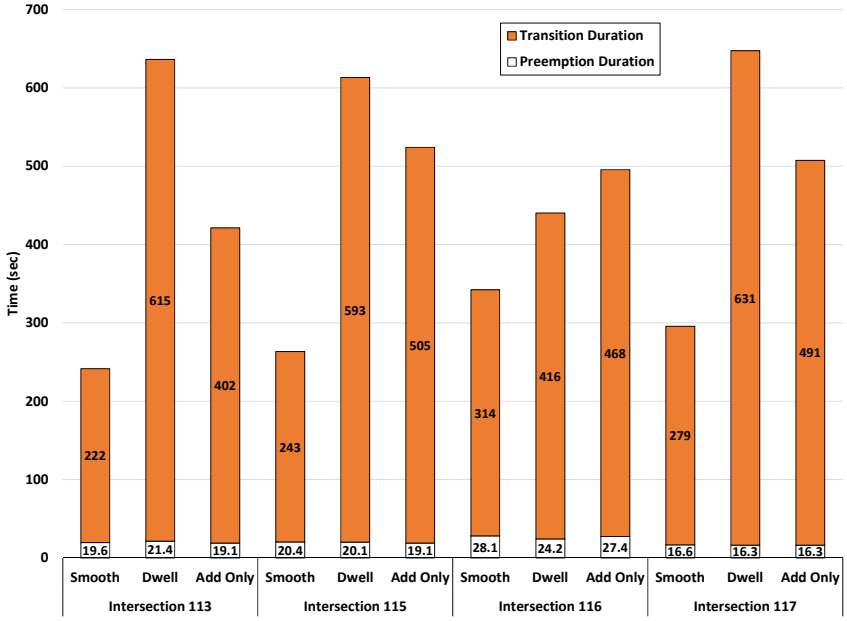

(b) Network Performance, All Transition Scenarios

Figure 3. Preemption Duration and Transition Duration

4.3.3 Travel Time and Speed

Results from multiple intersections can be applied to estimate an EV's travel time and speed in the network. For this purpose, the time and space attributes corresponding to each of the 44 EVP triggers turning OFF were plotted as shown in the upper portion of Figure 4 with results from the

Smooth transition mode. Note that Intersection 113 is located at a cumulative distance of 2000 feet based on the intersection location assignment described earlier, followed by Intersections 115, 116, and 117. Each data point on the plot represents the time the EV passed through the intersection (i.e., trigger turning OFF). These triggers were then assigned to unique EVs using the re-identification process discussed previously, and each EV is illustrated in the Figure by a unique color.

The lower portion of Figure 4 shows a zoomed view of the triggers associated with the 5th EV. These points are connected to represent its trajectory through the network. Based on this view, it is clear that the EV was traveling from Intersection 113 to 117. The time and space difference between consecutive dots is used to estimate the travel time and speed on that segment. The figure has been labeled with the speed based on this calculation. The average travel speed for this vehicle varied from 31 to 34 mph along the three segments. This range is expected based on the desired speed parameter defined for the EV in VISSIM.

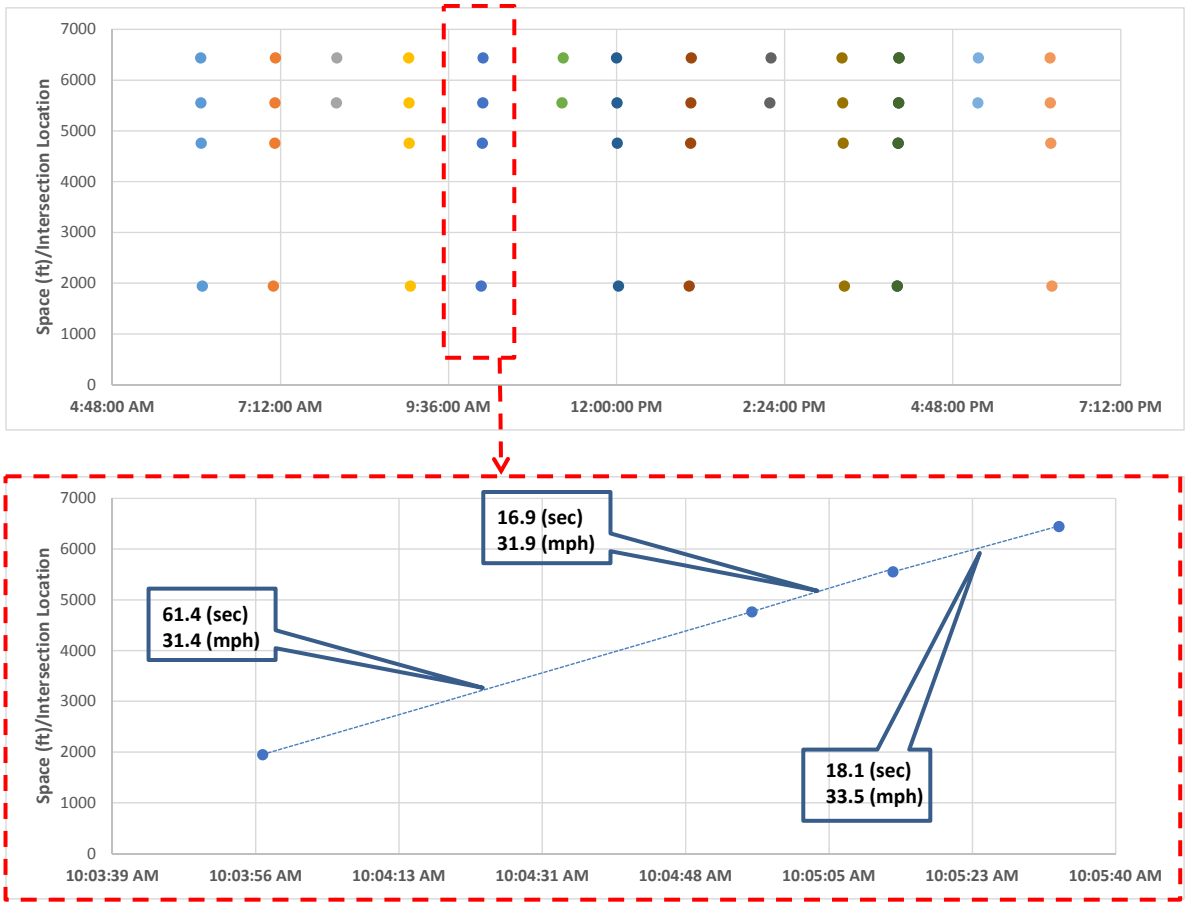

Figure 4. Travel Time and Speed, Smooth Transition Scenario

The results from estimating the segment speed for EVs in all three scenarios are summarized in Figure 5, including the average speed, standard deviation, maximum speed, and minimum speed. The estimation shows minimal variation across the simulation scenarios for each segment. Segment 116-117 experienced the highest travel speeds because all eastbound EVs exit the network turning right at Intersection 117, which has an exclusive right-turn lane with a large

turning radius. The highest standard deviations were associated with Intersection 116, which is expected due to the higher congestion levels and the fact that some of these EVs entered from the side street at this intersection.

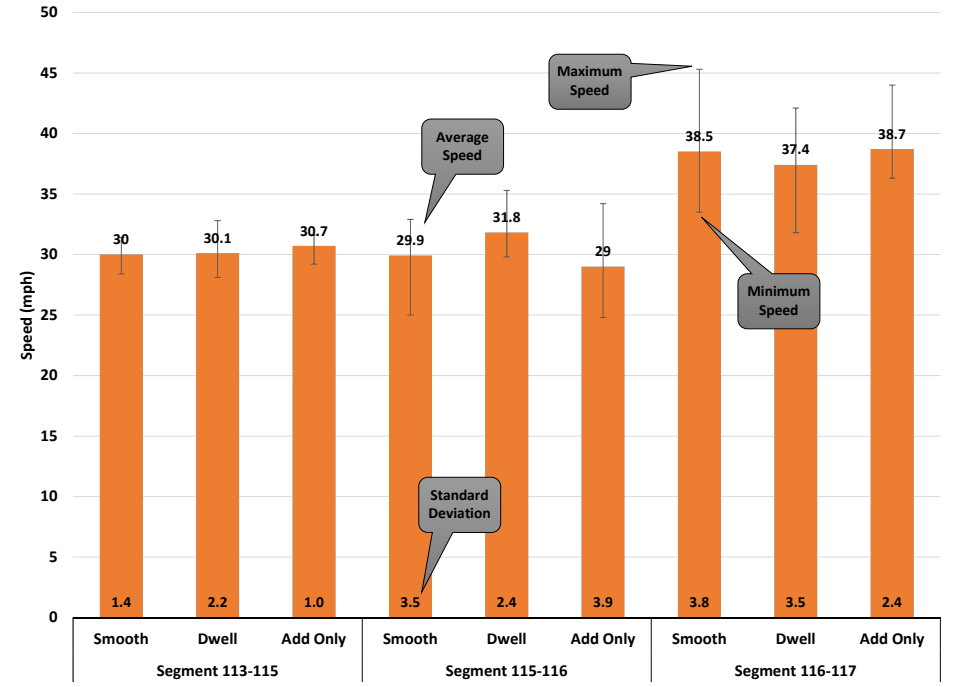

(a) Eastbound

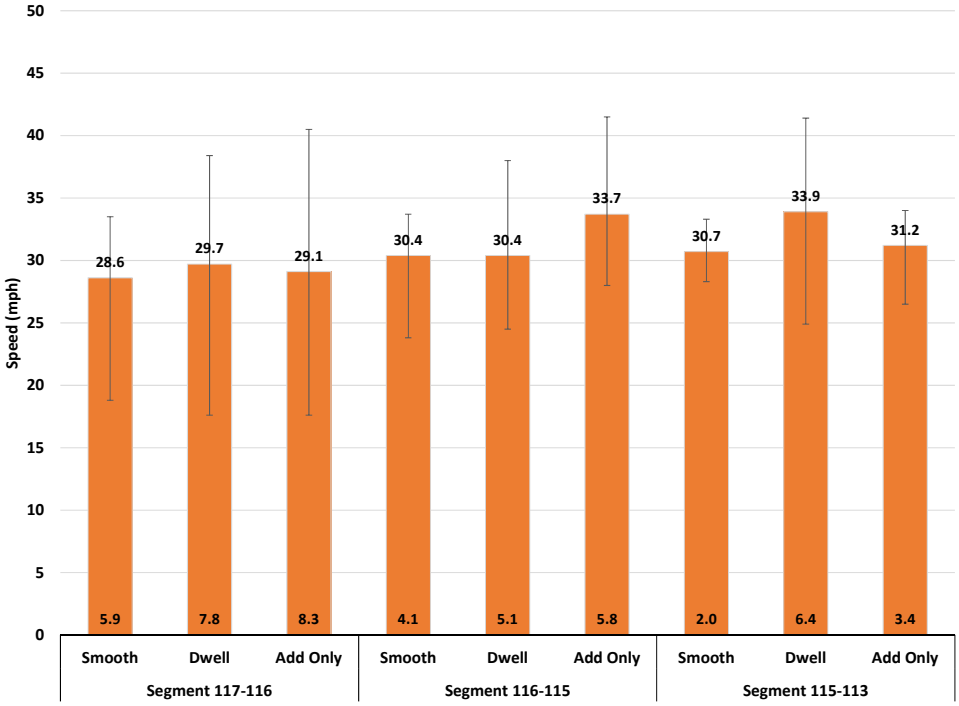

(b) Westbound

Figure 5. Segment Travel Speed Estimations

4.3.4 Origin-Destination Matrix

After profiling each EV trip in the network, an overall O-D matrix can be estimated. For example, the first EV passed through four intersections and its trip is profiled as "117-116-115-113". Therefore, set EVP $Trip_{(1)}$ $O_{117}D_{113} = 1$. Table 2 illustrates the O-D results for all EVs in Scenario 1. Since these routes were predefined in the simulation, the results would be the same for all scenarios. Therefore, this matrix would have more value in a field implementation to help understand the EV patterns and their frequency.

Table 1. EVP Network Performance (Origin-Destination Matrix), Scenario 1

Origin \ Destination	113	115	116	117
113	-	-	-	4
115	-	-	-	-
116	-	-	-	4
117	5	-	-	-

4.4. Field Application: Troubleshooting Preemption Operation

Proper preemption operation is dependent on proper cabinet wiring and controller configuration. Typically, performance is verified when the traffic signal is initially installed, but rarely checked on a routine basis or after maintenance activity unless complaints are received. It is also undesirable to test the preemption operation in the field because it could unnecessarily affect the signal operations, depending on the methods used. Most traffic signal controllers do not provide an easy mechanism for inspecting preemption performance at an intersection. Investigation of the high resolution data related to preemption events can provide some insight into the performance and assist in identifying configuration problems. Thus, selected high resolution data from two field deployments in West Virginia are investigated in this section to demonstrate this concept.

4.4.1 Inspecting EVP Trigger Frequency to Identify Preemption Emitter Problems

The EVP frequency distribution over time can be quickly examined to identify uncharacteristic behavior at an intersection, which might warrant further investigation. Figure 6a illustrates the distribution of Code 102 (i.e., EVP trigger ON) during May-June 2015 from Intersection 115 in Morgantown. Three triggers occurred on May 13: 1:00 AM for EVP plan 2 (phases 2 and 5), 5:00 AM for EVP plan 1 (phases 1 and 6) and 12:00 PM for EVP plan 2. The general pattern indicates there were less than five triggers per day at this intersection, except on May 31, when there were 76 triggers for EVP plan 2 within the 9:00-10:00 AM hour.

From the SPS plot in Figure 6b for the specific timeframe in which the 76 triggers occurred, it is observed that all of the triggers occurred within a 23 second period from 9:20:24 AM to 9:20:47 AM, which suggests it was generated by the same EV on one approach to the intersection (for each Code 102, there is a corresponding Code 104, but only the last Code 104 is shown in the

plot). The triggers are so close together, that it appears as two boxes on phases 2 and 5. The 7-second gap between bursts was long enough that the controller started transitioning out of preemption and then initiate a new preemption sequence. This is indicated by phase 5 serving a yellow and all-red clearance and returning to green (this operation will be discussed in a following section). The burst of calls is most likely attributed to a faulty EV emitter not transmitting a constant signal.

Since phases 2 and 5 at Intersection 115 are the eastbound movement, the EVP frequency distribution at Intersection 116 was inspected to see if the same EV could be identified on the same date and timeframe. Figure 7a shows the distribution for May-June 2015, where there is a high frequency of calls for EVP plan 2 on May 31 within the 9:00-10:00 AM hour. Figure 7b confirms that all of these calls also occurred within a 6-second period, which is consistent with the burst of calls at Intersection 115. This confirms that the cause of this behavior is attributed to a single EV. The eastbound movement at Intersection 116 is also served by phases 2 and 5. However, EVP plan 2 at this intersection corresponds to phases 3 and 8. This inconsistency will be discussed in the next section.

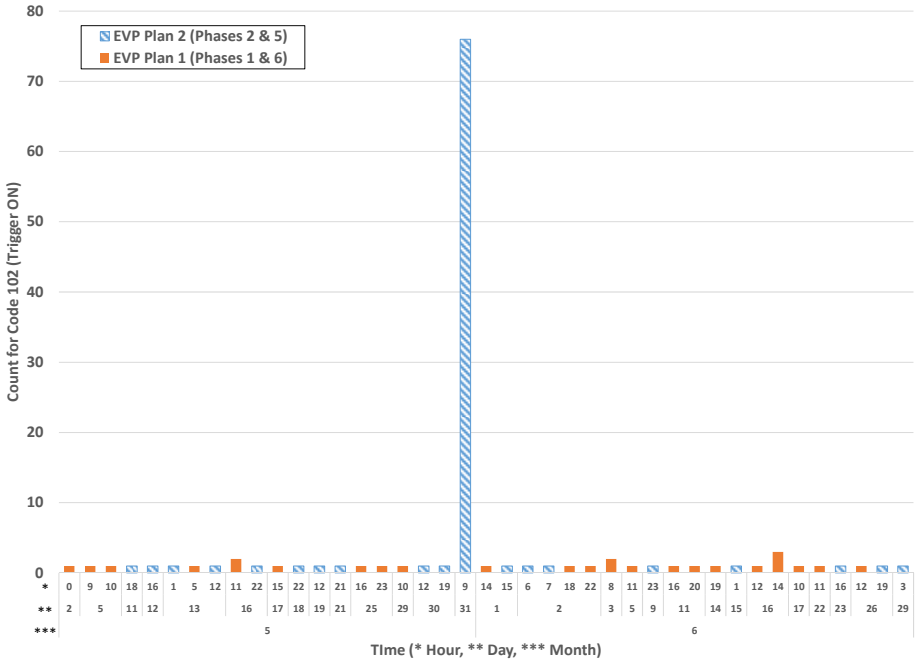

(a) EVP Trigger Frequency Distribution (Code 102 – Trigger ON), May-June 2015

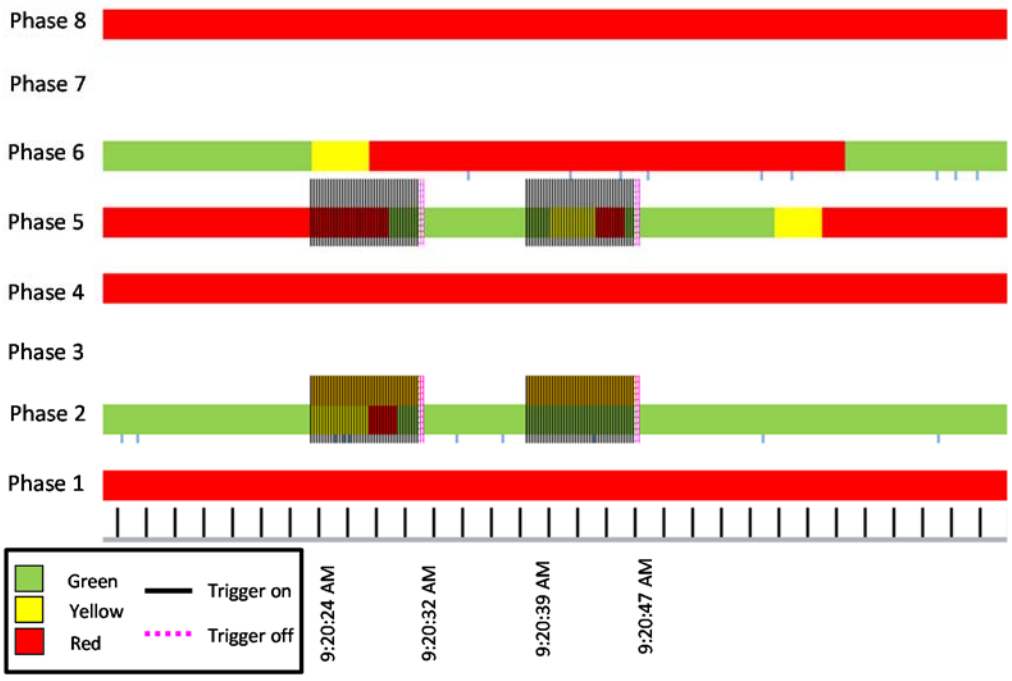

(b) SPS Plot for May 31, 2015, 9:20:12-9:21:06AM

Figure 6. EVP Analysis of Intersection 115 in Morgantown, WV

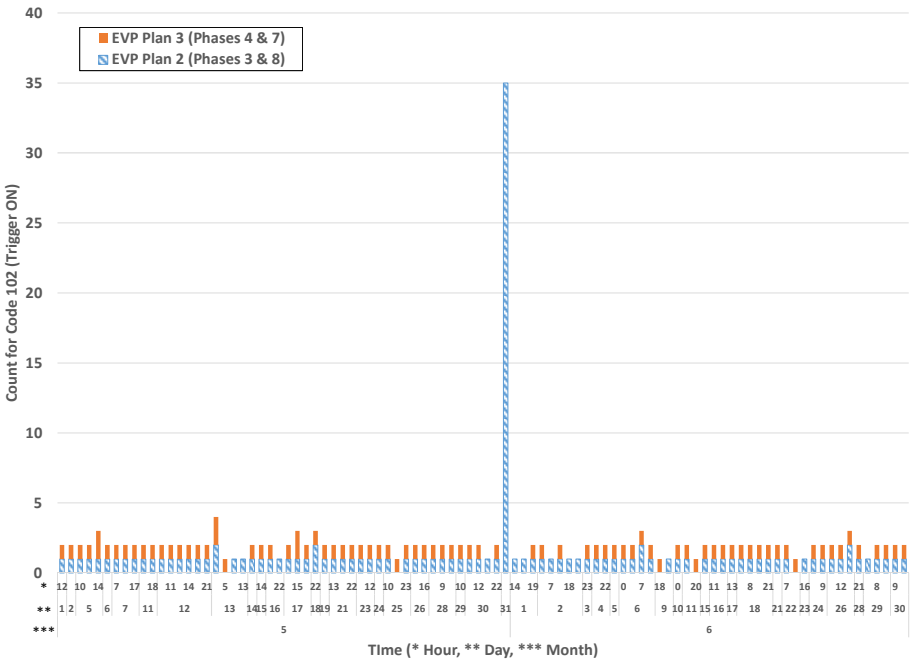

(a) EVP Trigger Frequency Distribution (Code 102 – Trigger ON), May-June 2015

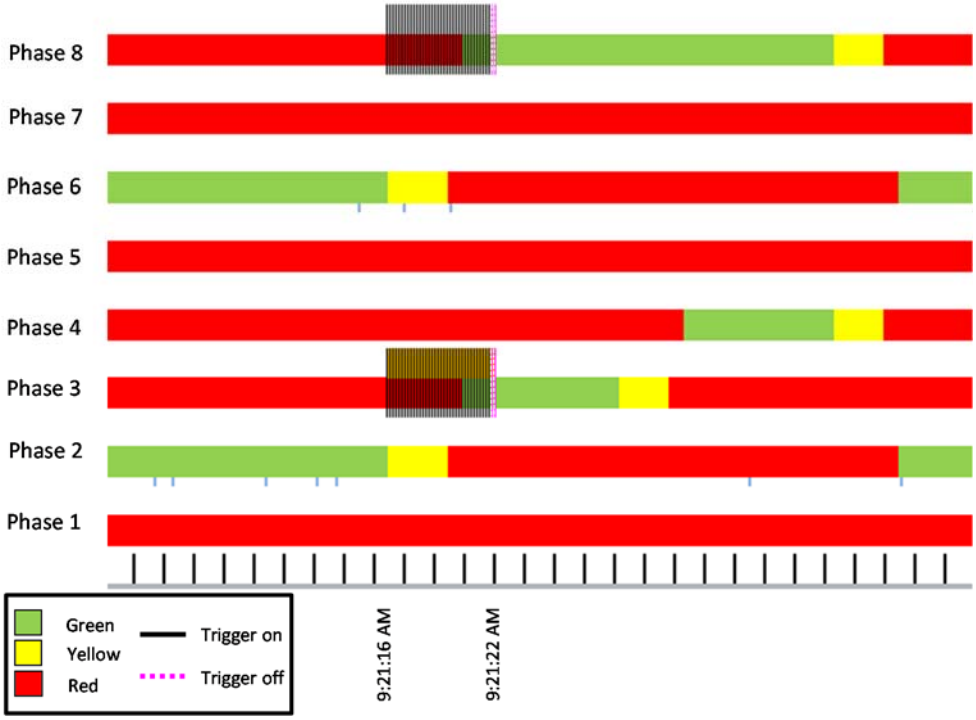

(b) SPS Plot for May 31, 2015, 9:21:08-9:21:58AM

Figure 7. EVP Analysis of Intersection 116 in Morgantown, WV

4.4.2 Inspecting EVP Trigger Frequency to Identify Preemption Detector Problems

Inspection of the EVP trigger frequency at adjacent intersections can facilitate the identification of improperly assigned preemption detectors, which could be a result of improper cabinet wiring or incorrect controller programming. If the preemption detectors are not assigned correctly, this will result in an EV on one approach triggering phases on a different (probably conflicting) approach, which will increase the amount of time for the EV to pass through the intersection. While this type of problem should be identified during initial or routine inspections, it is still possible that this problem could occur in conjunction with cabinet maintenance activity (e.g., a controller being replaced after a lightning strike). An example of this problem was discovered at Intersection 116, as indicated in the previous section. The EV with the faulty emitter was traveling eastbound along the corridor and should have preempted phases 2 and 5 at both Intersections 115 and 116. However, the preemption was triggered for phases 3 and 8 at Intersection 116. Therefore, the detector for the eastbound approach is incorrectly wired to the channel for the northbound approach or the EVP phase assignments in the controller have been configured incorrectly.

The EVP trigger frequency distribution can be reviewed over time to identify detectors that may not be working at all, although the expected frequency of EVs on an approach should be taken into consideration. The frequency for Intersection 116 in Morgantown in Figure 7a reveals that one of the preemption detectors has likely stopped working. This is a four-way intersection with preemption detectors on three of the approaches that call three different plans. However, only EVP plans 2 and 3 are being triggered. Subsequent inspection of the controller configurations revealed that three plans are configured, therefore the detector must not be working.

Figure 8a illustrates the EVP trigger frequency distribution for an intersection in Huntington, WV from May 1-7, 2015, which is also managed using the Centracs system to facilitate high resolution data collection. The x-axis includes the minute in which the trigger occurred, in addition to the day and hour. Based on this plot, it appears that EVP plans 2 and 4 have a high correlation, in that both plans are being triggered within the same minute, even though the frequency of calls throughout the day is relatively low. EVP plan 2 (phase 2) at this intersection is a major one-way movement and EVP plan 4 (phase 4) is the conflicting side street movement. Investigation of the SPS plots (excerpt for May 7 event in Figure 8b) confirmed that the triggers for these two plans overlap. Therefore, it is likely that an EV is somehow triggering both plans. This could be caused by the detector facing in the wrong direction or a nearby building reflecting the signal coming from the emitter. Since the plans are triggered simultaneously, this would rule out a wiring issue.

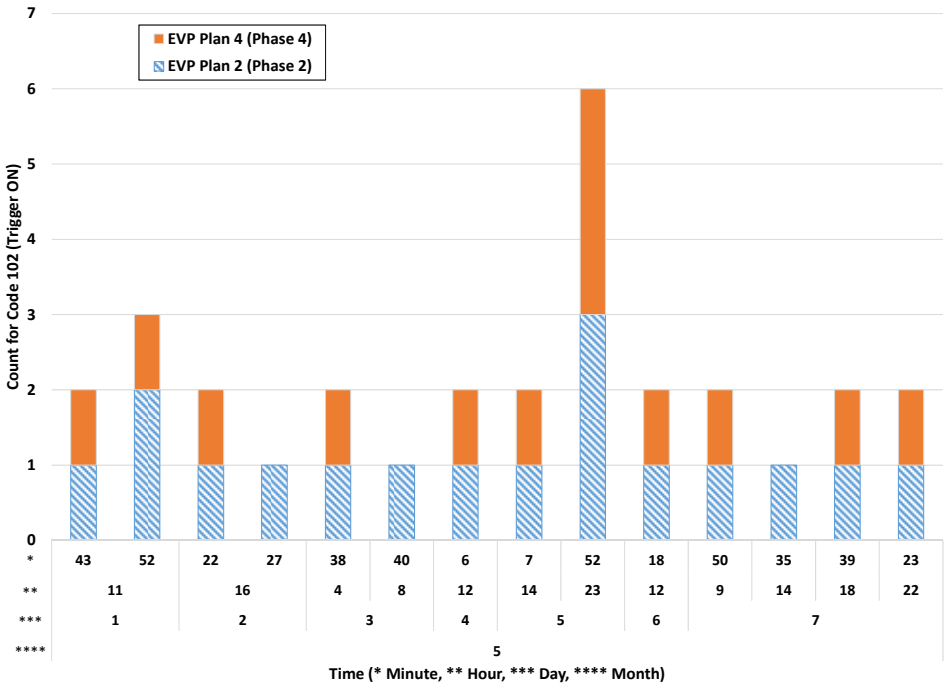

(a) EVP Trigger Frequency Distribution (Code 102 – Trigger ON), May 1-7, 2015

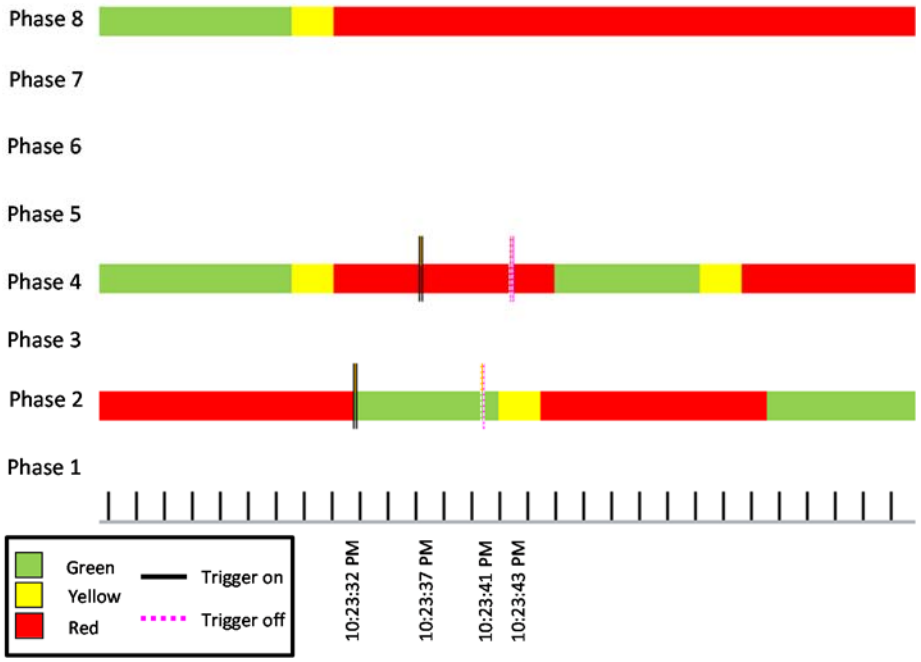

(b) SPS plot for May 7, 2015, 10:23:04-10:24:08 PM

Figure 8. EVP Analysis of Intersection in Huntington, WV

4.4.3 Inspecting SPS Plot for Other Preemption Operation Problems

The SPS plot can be visually inspected to observe the signal operations in response to preemption triggers on a case-by-case basis. This level of inspection can provide insight into unintended operations being caused by incorrect controller programming, which could be considered problems by some. For example, Figure 6b illustrates that even though the phase being called by the EVP trigger is already green, that phase is terminated (serving yellow and all-red clearance) before serving the preempt phase. Phase termination is a setting that can be configured in the controller preemption plan. However, further investigation at this intersection determined that this termination was instead being caused by the backup prevention settings, not the settings in the preemption plan (17). Phases 1 and 5 are protected-permitted left-turn movements and backup prevention is enabled for those phases to avoid the yellow trap scenario.

Another undesirable operation that can be identified with the SPS plot is the programmed preemption phases. On approaches with left-turn arrows, it is common for the preemption plan to activate both the left-turn and through phases. The left-turn phase inclusion can easily be overlooked when programming the controller. In addition to verifying this assignment in the controller, it is also possible to observe this operation in the SPS plot.

5. Conclusions

High resolution data has provided a new mechanism for quantifying the performance of traffic signals, as previous research has documented. This paper proposes the use of a signal phase spectrum plot to facilitate the analysis of high resolution data and visualization of controller events. Specifically, this paper proposed performance measures attributed to emergency vehicle preemption events and illustrated the use of those performance measures to quantify preemption duration and subsequent transition duration based on a simulation network. Network level performance measures related to travel time, speed, and origin-destination estimates were also generated for the simulation network. Furthermore, the high resolution data was used to troubleshoot preemption operations and configurations of field deployments in West Virginia.

6. Recommendations

Future research could leverage the SPS plot to visualize and evaluate other aspects of traffic signal operation, particularly with the inclusion of vehicle detection inputs (both stopbar and advanced detection). This would allow the incorporation of vehicle arrivals to calculate percent arrivals relative to green and capacity utilization, consistent with previous research. The methodology developed to estimate the speed and origin-destination of emergency vehicles is based on the ability to re-identify a unique vehicle in the traffic stream at sequential intersections. This same capability will be possible with connected vehicles, so the methodologies presented in this paper may have other applications beyond connected vehicles.

Reference List

1 Paniati, J., and Amoni, M., "Traffic Signal Preemption for Emergency Vehicles – A Cross-Cutting Study," Federal Highway Administration and National Highway Traffic Safety Administration, Jan. 2006.

2 Louisell, C., Collura, J., Teodorovic, D., and Tignor, S., "Simple Worksheet Method to Evaluate Emergency Vehicle Preemption and Its Impacts on Safety," Transportation Research Record: Journal of the Transportation Research Board, No. 1867, pp. 151-162, Washington, D.C., 2004.

3 Zhang, Z., He, Q., Gou, J., and Li, X., "Performance Measure of Travel Time Reliability of Emergency Vehicles in an Urban Region," Conference Proceeding of 94th TRB Annual Meeting, Washington, D.C., 2015.

4 Qin, X., and Khan, M.A., "Control strategies of traffic signal timing transition for emergency vehicle preemption," Transportation Research Part C: Emerging Technologies, Vol. 25 pp 1-17. 2012.

5 Kamalanathsharma, R.K., and Hancock, K.L., "Congestion-Based Emergency Vehicle Preemption," Research Report No. VT-2009-04, Mid-Atlantic Universities Transportation Center. 2010.

6 Jordan, C.A., and Cetin, M., "Signal Preemption Strategy for Emergency Vehicles Using Vehicle to Infrastructure Communication," Conference Proceeding of 94th TRB Annual Meeting, Washington, D.C., 2015.

7 Nelson, J.E., and Bullock, D., "Impact of Emergency Vehicle Preemption on Signalized Corridor Operation," Transportation Research Record: Journal of the Transportation Research Board, No. 1727, pp. 1-11, Washington, D.C., 2000.

8 Obenberger, J., and Collura, J., "Methodology to Assess Traffic Signal Transition Strategies for Exit Preemption Control," Journal of Transportation Research Record Vol. 2035 pp 158-168. 2007.

9 Obenberger, J., and Collura, J., "Transition Strategies to Exit Preemption Control State-of-the-Practice Assessment," Journal of Transportation Research Record Vol. 1748 pp 72-79. 2007.

10 Yun, I., Park, B.B., Lee C.K., Oh, Y.T., "Comparison of Emergency Vehicle Preemption Methods Using a Hardware-in-the-Loop Simulation," KSCE Journal of Civil Engineering 16(6):1057-1063. 2012.

11 Lavrenz, S., Day, C., Hainen, A., Smith, B., Stevens, A., Li, H., and Bullock, D., "Characterizing Signalized Intersection Performance Using Maximum Vehicle Delay," Conference Proceeding of 94th TRB Annual Meeting, Washington, D.C., 2015.

12 Hainen, A., Li, H., Stevens, A., Day, C., Sturdevant, J., and Bullock, D., "Sequence Optimization at Signalized Diamond Interchanges Using High-Resolution Event-Based Data," Conference Proceeding of 94th TRB Annual Meeting, Washington, D.C., 2015.

13 Day, M.C., Ernst, J., Brennan, T., Chou, C.S., Hainen, A., Remias, S., Nichols, A.P., Griggs, B., and Bullock, D., "Performance Measures for Adaptive Signal Control – Case Study of System-in-the-loop simulation," Journal of Transportation Research Record Vol. 2311 pp 1-15. 2012.

14 Wu, X., and Liu, X.H., "Using High-Resolution Event-Based Data for Traffic Modeling and Control: an Overview," Transportation Research Part C: Emerging Technologies, Vol. 42 pp 28-43. 2014.

15 Sturdevant, J. R., T. Overman, E. Raamot, R. Deer, D. Miller, D. M. Bullock, C. M. Day, T. M. Brennan, H. Li, A. Hainen, and S. M. Remias. Indiana Traffic Signal Hi Resolution Data Logger Enumerations. Publication., Indiana Department of Transportation and Purdue University, West Lafayette, Indiana, 2012. doi: http://data.datacite.org/10.4231/K4RN35SH.
16 Jue, M., and Jarzab, J.T., "Detection Range of Optical Emergency Vehicle Preemption System under Typical System maintenance Conditions," ITE Journal Vol. 83 Issue 6.
17 . Econolite, "ASC/3 Advanced System Controllers Programming Manual," Econolite Control Products, INC, 2009.

Sub-report Task #4

Emissions-Based Performance Assessment of Traffic Control using High Resolution Data

Prepared by:

Dr. Montasir Abbas
Associate Professor
Virginia Tech

Nadezhda Morozova
Graduate Research Assistant
Virginia Tech

Acknowledgments

This work was supported by the Mid-Atlantic Transportation Sustainability University Transportation Center (MATS UTC).

Disclaimer

Table of Contents

List of Figures

List of Tables

1. Problem

A major role of traffic engineers is to devise strategies for vehicles to reach their destinations as quickly as possible while maximizing safety and minimizing the impact on the environment. For passenger cars, busses, trucks, and other types of wheeled vehicles, this task is achieved by developing road networks that are appropriate for the type and volume of the expected traffic. Intersections are an unavoidable component of road networks. Some form of control mechanism is necessary to direct vehicles through intersections without collisions. Currently, control mechanisms for intersections with high traffic volume have taken the form of traffic lights, which tell drivers whether they have right-of way or not. Although necessary for safety, signalized intersections have the unwanted effects of increased noise pollution, increased emissions, and an overall decrease in the rate of traffic flow because drivers who encounter a red light must come to a complete stop and then accelerate back to their previous speed. A well-designed intersection will minimize these detrimental effects to achieve the highest possible level of efficiency. Efficiency of an intersection can be estimated by evaluating traffic delay and calculating emissions.

Traffic controllers installed at such signalized intersections have certain outputs that can be logged and stored. Researchers can then use this data to analyze when specific detectors were triggered. Although detector logs were initially stored in a multitude of different formats, a universal format for representing events of controllers using High Resolution Data (HRD) is now widely in use. Much of the earlier literature has been published on how to best apply HRD to evaluate intersection performance measures, emergency vehicle preemption (EVP), and emission models. However, limited research has been performed to predict vehicle emissions at intersections based on HRD. The work presented herein focusses on using HRDfor estimation of vehicle emissions. As known, emission from vehicles is influenced by timing plan, traffic volume, and characteristics of the traffic. The question that we seek to answer here is how to distinguish between a set of timing plans that produces maximum emissions and a set of timing plans that produces minimum emissions just by looking at the HRD. As a result of this research effort a Traffic Engineer will be equipped with the classifier threshold to identify if any changes to existing timing plans are required.

Furthermore, traffic light delays are a particular problem for emergency vehicles. It is in the interest of public safety to give emergency vehicles (EVs) right of way over all other vehicles at intersections and thus allow them to reach their destination sooner. However, this process of interrupting the regular cycle in order to allocate a green light to an EVs disrupts the normal life of an intersection and might cause extra delays. It is important to minimize these disruptions thus adverse effect on the network. A careful choice of transition strategy from emergency vehicle preemption (EVP) back to the normal cycle operation is necessary to quickly restore traffic light coordination and prevent unnecessary delays.

Any method of improving the efficiency of intersections requires an efficient method to evaluate the performance of intersections. Some traffic controllers use sensors and loops to track signal and traffic event and save this information in the form of high resolution data (HRD). It is very useful for a Traffic Engineer to be able to estimate whether level of emission at the intersection is acceptable just by looking at HRD. One approach is to use a formula or algorithm to process

outputs from HRD, such the number of vehicles that stopped at the intersection, and compare the results to a threshold condition in order to make a decision about whether to change timing plans for traffic lights or not.

The present study discusses efforts to come up with a classifier to distinguish between maximum and minimum emission cases with a model developed in the simulation-optimization software AnyLogic. As a secondary objective, this report compares effect of presence of Emergency Vehicle's (EV) (so, EVP is given to it by traffic lights and right of-way is given by other vehicles) on the road network in terms of emission with base case scenario without EV.The remainder of this report is organized as follows. First the relevant literature is reviewed. Then our proposed model is discussed with the aid of an EV life cycle flowchart and EVP flowchart. The network simulation in AnyLogic and offset variation are also described. A classifier to distinguish between maximum and minimum emission cases along with its threshold and equation is developed and discussed. Cases including and excluding EV were compared in terms of emission values. The work is concluded with applications and ideas for future research.

1.1. Literature Review

1.1.1 Emergency Vehicle Preemption

Preemption of emergency vehicle (EVP) concept was around probably as long as signalized intersections themselves. One of the earliest mentions about EVP was in 1929 in the publication "Street Traffic Signs, Signals, and Markings" of American Engineering Council (Paniati [1]). Since then the topic of EVP was widely explored by researchers in their previous publications.

Part of the previous research concentrated on decision making process of EVP and on cost-benefit ratio of preemption implementation. For example, research of Paniati [1] identified available technology options for preemption and agencies that should be involved in decision making process. Paniati [1] also performed a site study at Fairfax county, VA, Plano, TX and St Paul, MN. These studies discussed the costs of EVP implementation and benefits from this system in place at each particular site.

Some studies made an attempt to address deficiencies of available EVP methodologies. For instance, Louisell [2] proposed a method that decides which intersections or which corridors should use EVP. Safety, delay, distance to origin/destination of EV and intersection index in regional emergency response plan were the suggested criteria for this method.

Other group of researchers focused on developing and deploying different control strategies for EVP. Qin [3] came up with signal sequences-based control strategies: one that transitions from normal traffic operation to EVP mode and another that brings traffic back to normal operation. It was claimed that these strategies work better than existing approaches even when over-saturated traffic conditions are involved. Nelson [4] provided results of a case study performed in a four-intersection corridor in Lafayette, IN. Researchers estimated the impact of EVP on general traffic considering different preemption paths, transition algorithms, and frequency of preemption events. Jordan [5] developed three preemption strategies based on vehicle-to-infrastructure communication and assessed them using EV travel time and overall network delay as guidelines.

These researchers tried to clear the queue at the intersections prior to EV arrival and thus allow the EV to proceed unimpeded. All proposed strategies aimed to estimate, find, or calculate the appropriate start time of preemption. Simulation runs showed that the queue length-based strategy provided the best performance.

Some researchers considered how preemption delays traffic. Chou [6] used preemption duration and transition duration to quantify the effect of EVP on overall traffic flow. Researchers defined preemption duration as time between the states of trigger ON and OFF of a controller. Similarly, they defined transition duration as the time taken by the controller to return to its normal operation (time between states OFF and IN STEP). The research presented in current study expands EVP and utilizes Dwell as the most appropriate for our purposes of transition strategy.

1.1.2 Emissions

It is an important task for Traffic Engineers to use appropriate emission models [7]. Emission models can be classified as macroscopic, microscopic and mesoscopic. Macroscopic models that are commonly used include the Elemental, MOBILE, and EMFAC models [8]. Macroscopic models do not have strict resources requirements. However, their estimations are not precise, so they are typically used for rough project estimates for big road networks. Macroscopic models are outside the scope of this study since they do not suit our research purposes.

Microscopic models are mostly used in microscopic traffic simulation software when second-by-second vehicle characteristics of each vehicle are available. The most wide-spread microscopic models are VT-Micro [9] and CMEM [10]. Both models are acceptable to use in some cases. However, some research shows that CMEM behaves abnormally in some scenarios, possibly due to model complexity [11].

Mesoscopic models require less data than microscopic models and yield more accurate results than macroscopic models [12]. Therefore, they are desirable for situations that call for a balance between high accuracy and low computational cost. The commonly used mesoscopic models are Akcelik [13] model and MEASURE model [14].

Although the system developed in this study is mesoscopic, a microscopic emission model is appropriate because based on output of loop detectors, individual speed of a vehicle and its acceleration can be calculated. Since we have sufficient data to use a microscopic model, the computational cost compared to a mesoscopic model is negligible. VT-Micro is a simple model that is effective for this purpose. Previous work demonstrates that it can provide estimates of vehicle fuel consumption to within 2.5 percent of actual measured field values [15]. Thus we choose to use the VT-Micro model in AnyLogic [16].

1.1.3 High Resolution Data

HRD is provided by the traffic controllers in commonly agreed format and contains traffic info and signal phase info [17]. HRD is stored in traffic controllers 10 times per second. If two loop detectors are installed in one lane, then HRD is a great tool for measuring the characteristics of

vehicle arrival such as speed and acceleration. This significant tool has attracted much attention from researchers recently.

Some research groups wanted to get away from the conventional way of measuring performance of signalized intersection based on calculating average vehicle delay and total approach delay and made an attempt to calculate something more vehicle-specific. For example, group of Lavrenz [18]) used HRD to estimate the upper threshold of delay of the particular vehicle based on time interval between first detection event on an approach and start of green time of this approach.

Other group of researchers utilized HRD for studies on diamond interchanges. For example, (Hainen [19]) made efforts to optimize offsets while keeping the existing sequence of signal phases. In later work, the same researchers also included left turns in different sequences in addition to offset optimization (Hainen [20]).

Some research was done on measuring performance of system-in-the-loop simulations [21] [22] [23]. For example, Day [21] estimated delay as a traditional measure of simulation performance and arrivals on green along with traffic volume to lane capacity ratios as operational measures of simulation performance. Researchers compared a few strategies for intersection network under heavy traffic.
Other groups of researchers tried to visualize HRD and facilitate analysis of this data [24][6]. For example, Chou [6] developed an improved format to present performance measures and coordination events with the use of signal phase spectrum plots.

Although much progress has been made in the related topics of EVP, HRD and emission models, very limited research has been done to determine a classifier to distinguish between optimal and non-optimal vehicle emissions cases based on HRD and considering EVP. The primary objective of the work presented here was to find the combination of traffic flow characteristics that affect emission the most and to come up with an equation for this classifier. A secondary objective was to evaluate if and to what degree the presence of EVs affect network emissions. To this end, a model was developed in AnyLogic simulation software with flowcharts for all four traffic lights of the road network, for EV life cycle, and for EVP. The VT-Micro emission model was implemented in AnyLogic as a tool for finding vehicle emission to analyze it later on. The current work uses HRD obtained from a corridor in WV-705 in Morgantown, WV to estimate vehicle emissions.

2. Approach

2.1. Proposed Model

This section describes the way the real road network was created in simulation and optimization software AnyLogic. The signal phase diagram for all intersections coordinated with each other along with offsets are presented. Turning volumes for all approached within the road network is introduced. The section also gives an overview of proposed EVP mechanism along with EV life cycle. VT-Micro model is presented in the end.

2.1.1 Road Network (Physical Layer)

The road network is the representation of the WV-705 traffic corridor in Morgantown, West Virginia. A Google Earth satellite view of this corridor is presented in Figure 1.

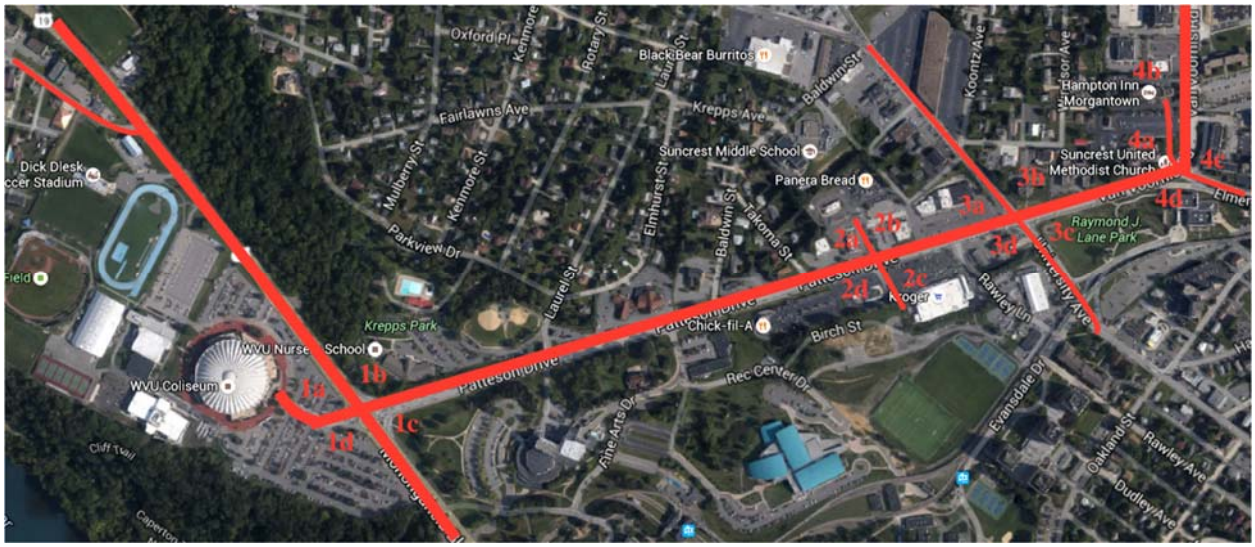

Figure 1 Google maps Earth view of the route WV-705

The flow (the geometry) of the corridor, the distances between intersections, number of intersections, number of lanes in each direction, and the lengths of the turning lanes are accurately modeled to match their real-world dimensions. The distance between intersection 1 and intersection 2 is 2792 ft (851.0 m), between 2 and 3 is 774 ft (236.0 m), between 3 and 4 is 868 ft (264.4 m). All modeled lanes allow traffic to proceed in a single direction even if the corresponding real lane is designed to allow traffic to proceed in two directions. For example, if a real lane allows traffic to go straight or turn right, then the modeled lane only allows traffic to turn right and a separate lane is used for vehicles going straight through the intersection.

The simulation and optimization package AnyLogic was used in this research. Two different layers, one physical and one functional, should be created for every road segment to run a model in AnyLogic. Figure 2 represents a physical layer of the road in terms of lines and arcs. Arcs are always used for turning lanes as well as for making curved road sections. The circle near each traffic light of the intersection represents the overall state of the traffic light. Only one signal color is shown for simplicity. Green circle of the traffic signal represents that green light is given

at least to one of the approaches (either through, left or right). Yellow light turns on after green light, warns drivers that light is about to turn red and stops vehicles on every lane from moving. Red circle of the traffic signal turns on after yellow light and prevents vehicles on every lane from moving.

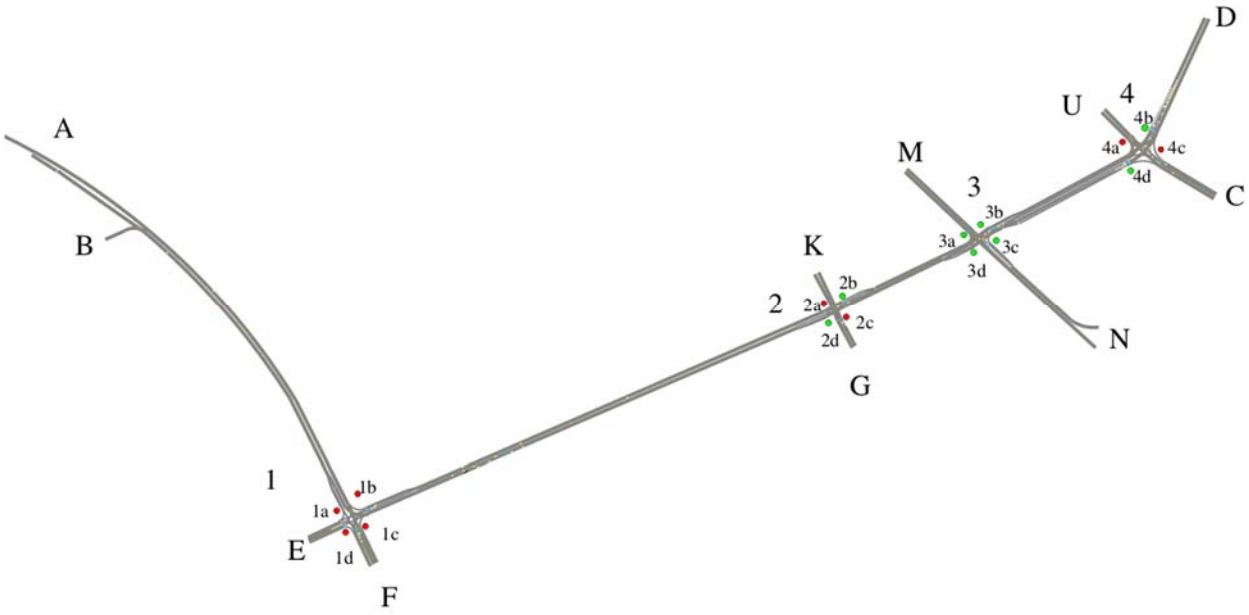

Figure 2 The physical layer of the road in AnyLogic

2.1.2 Logic of the Model (Functional Layer)

Vehicle interactions on a physical layer mostly depend on the logic inside of the functional layer. Thus, the functional layer is used for controlling vehicle movements. The functional layer consists of few blocks, which are arranged in a specific order as shown in Figure 3. CarSource is the block at the beginning of the road that produces vehicles. It also generates infusion of vehicles in the road network. There are eleven CarSources for normal vehicles and one for EV. CarMoveTo blocks are responsible for one of the road segments/road stretches. There are 201 CarMoveTo blocks. CarDispose blocks represent the end of the road where vehicles get extracted/removed from the simulation. There are 11 CarDispose blocks in the model. SelectOutput(5) blocks are responsible for dividing lanes and reassigning the vehicle flow. To facilitate programming, lanes are handled as separate roads at intersections with each road allowing traffic to proceed in a single direction (either through, right, or left).

For example, in Figure 3 the two lane road represented by carMoveTo15 is divided to three 1-lane roads (carMoveTo132, carMoveTo122, carMoveTo112) with the help of SelectOutput(5)8. Hold blocks is needed to stop the first vehicle of the vehicle queue of the particular lane at the red traffic light. A Queue block is placed before a Hold block and is needed to store the second vehicle of the vehicle queue of the particular lane. Queue and Hold blocks are present in each lane to account for lane assignment in each lane separately. Hold blocks for center, right-turn, and left-turn lanes are designated as C, R, L respectively. SelectOutput(5), hold and queue blocks along with lines, arcs, and statecharts participate in the traffic light creation and operation. Connectors on the right from carMoveTo16 and carMoveTo47 connect current route with other

routes. After traffic light queue22+hold3cL car turns left, gets on the road segment carMoveTo47 and merges into another route with the help of the connector.

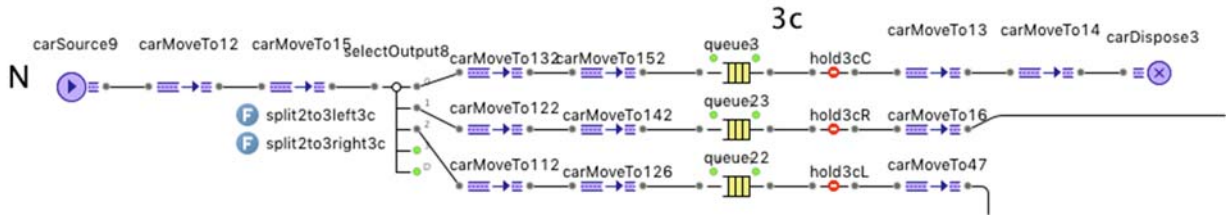

Figure 3 A sample of the functional layer of the roads in AnyLogic

The scheme of the whole road network is too large to include in a single figure. Only part of it is shown in Figure 3. That is why names (lettering) of intersections, approaches and CarSources are important. There are four intersections numbered from 1 to 4. There are four approaches at each intersection like 1a, 1b, 1c and 1d. Letters a, b, c, and d represent southbound, westbound, northbound, and eastbound respectively (Figure 2). CarSources are named alphabetically as A, B, C etc. The lettering of the intersections, approaches, and CarSources are the same on the physical layer of the roads (Figure 2) and on the functional layer of the roads (Figure 2).

2.2. Signalized Intersections (Statechart of the Intersection, Signal Phase Diagram, Offsets)

The Road Traffic Library of the current version of AnyLogic lacks native support to implement signalized intersections (Anylogic [16]). To circumvent this limitation, intersections were built from combinations of existing blocks of AnyLogic including custom classes and functions. Besides combinations of SelectOutput(5)+hold+queue blocks on the functional layer, statecharts are used to manipulate hold blocks and signal timings. There is a separate statechart for each of the four intersections of the model. Figure 4 displays the statechart of one of the traffic lights in the model. In a statechart, the first state in yellow on the left is an initialization state that is responsible for a traffic light to start operating. Signal phases in real life can go parallel (start in the same time) or sequentially (start one after another). Signal phases are represented in AnyLogic as the sequence of different states (events) on the timeline. Each state describes the lane assignments of all four approaches of the particular intersection. Each phase contains two states: one for green signal, one for red signal. There are two modes of traffic light operation: normal and after EVP (to restore cycle to its original timings). Normal mode is displayed in Figure 4 by arrow from one state to another with watch in between. After EVP mode is displayed by arrow from one state to another with the question mark in between.

For example, the statechart of intersection 2 is displayed in Figure 4. Signal phases 1, 2, 3 are presented at the top and phases 5, 6, 7 are presented at the bottom. Since green light of the phases 1 and 5 start in the same time, there is only 1 state that represents both of them. Red light of phases 1 and 5 also starts in the same time, so similarly there is only 1 state for both of them. The same is applied for green and red of states 2 and 6, 3 and 7. For visual purposes a state is allocated on green background if it represents green state of the traffic light and on a red background if it represents a red state. The dimensions of the sections are to scale with respect to their durations. Green light of phases 1 and 5 continues for 7.1 seconds and red light of these phases for 4.9 seconds. Green light of phases 2 and 6 continues for 72.7 seconds and red light of

these phases for 5.3 seconds. Green light of phases 3 and 7 continues for 25.1 seconds and red light of these phases for 4.9 seconds. The red and green bars are sized proportionally based on these durations.

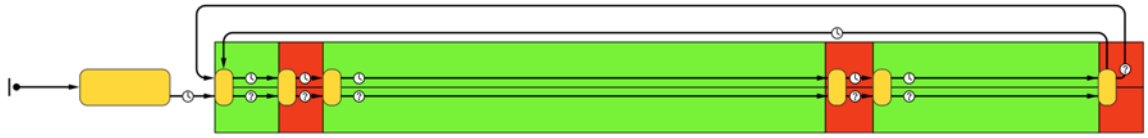

Figure 4 State charts of second intersection

The ring diagram and signal phase diagram display traffic assignment on each lane. The diagrams on Figure 5 and Figure 6 represent real vehicle assignment in traffic corridor WV-705 in Morgantown, WV along with the duration of each phase [6].

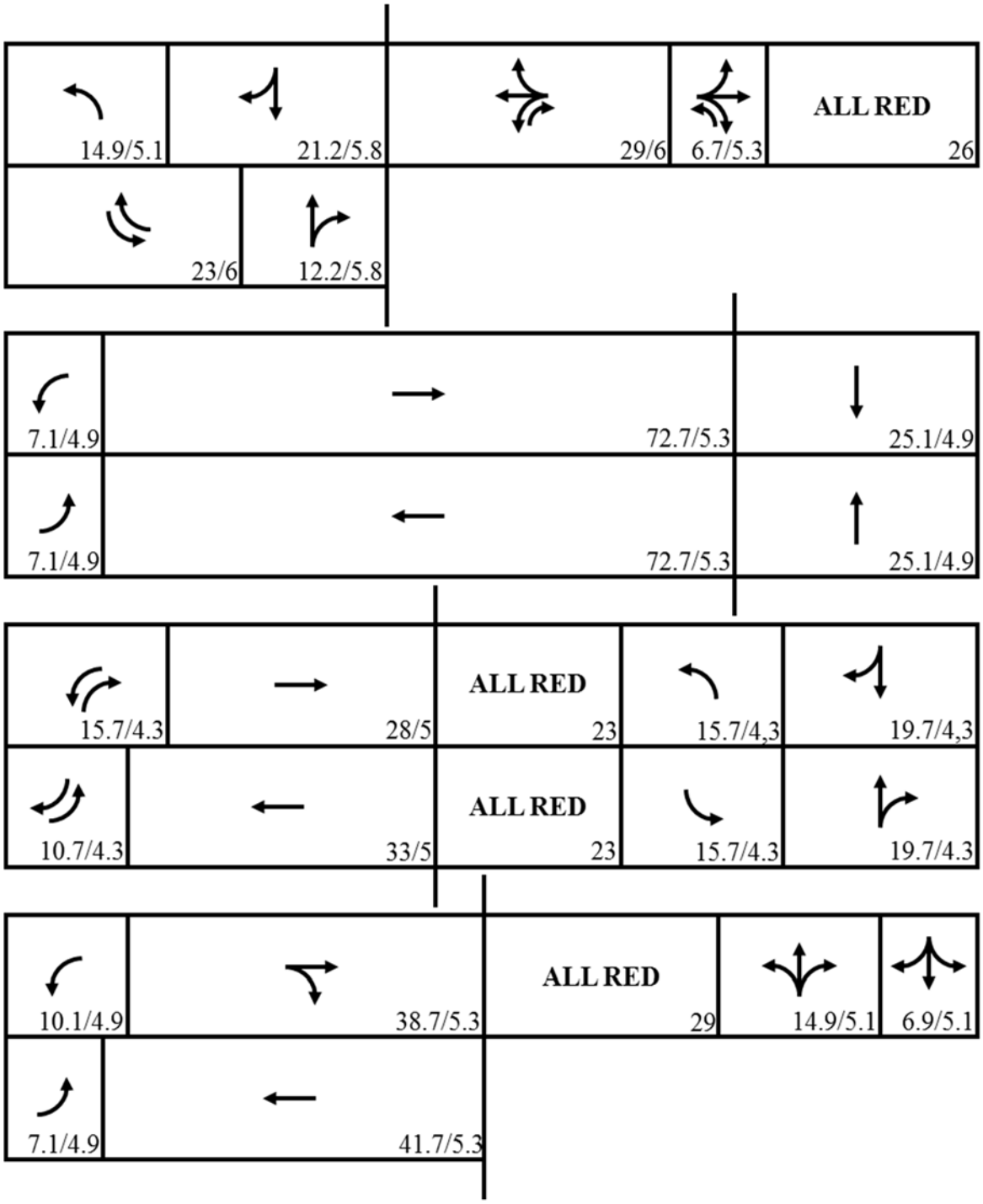

Figure 5 Ring barrier diagram for the four studied intersections

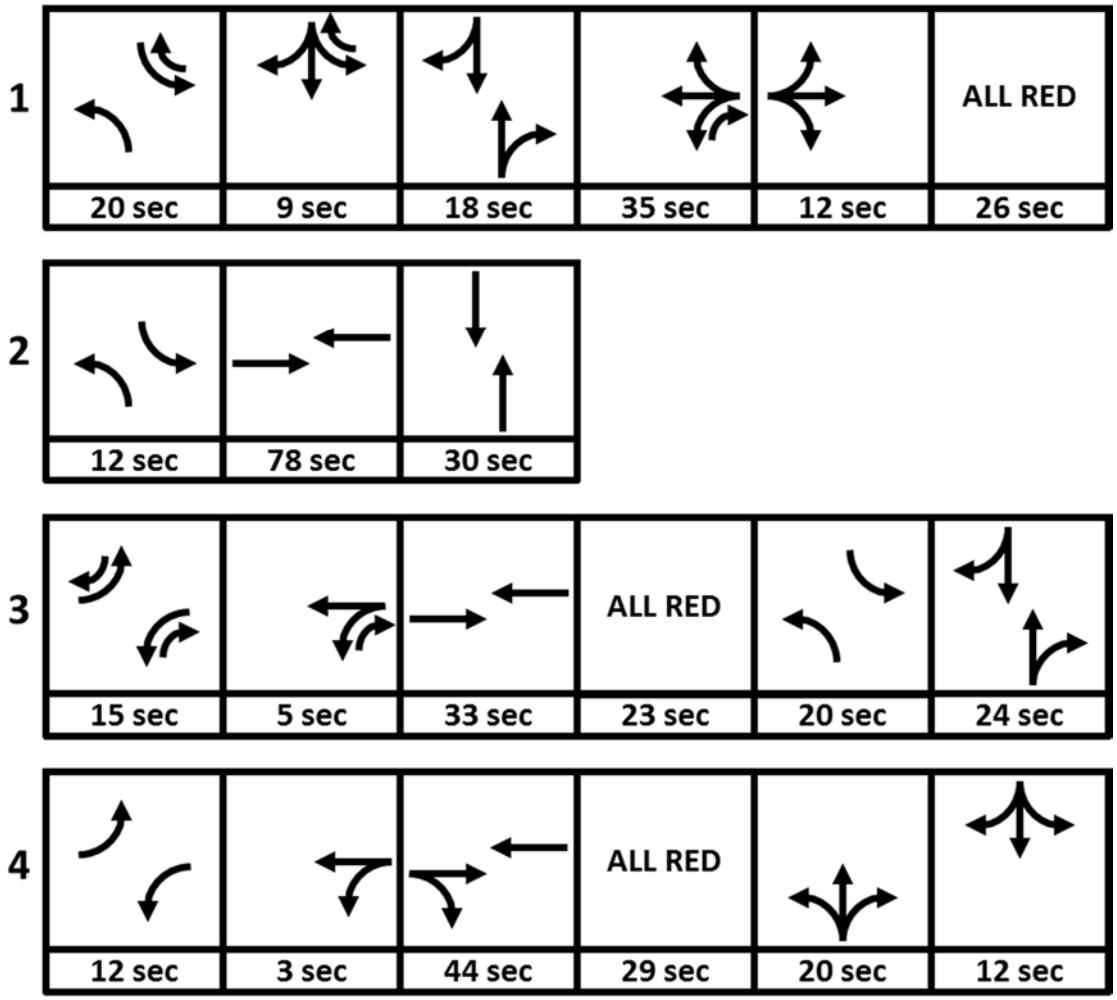

Figure 6 Signal phase diagram for the four studied intersections

The offsets of downstream traffic lights are important for traffic coordination. The offsets in the developed model on Figure 7 represent real offsets in the coordinated traffic corridor WV-705 in Morgantown, WV [6]. Offsets values of 110 seconds, 26 seconds and 28 seconds were provided from a case study on WV-705. These are in agreement with the output values 110, 20, 20 seconds from offset variation with step equal to 20 seconds in the current work.

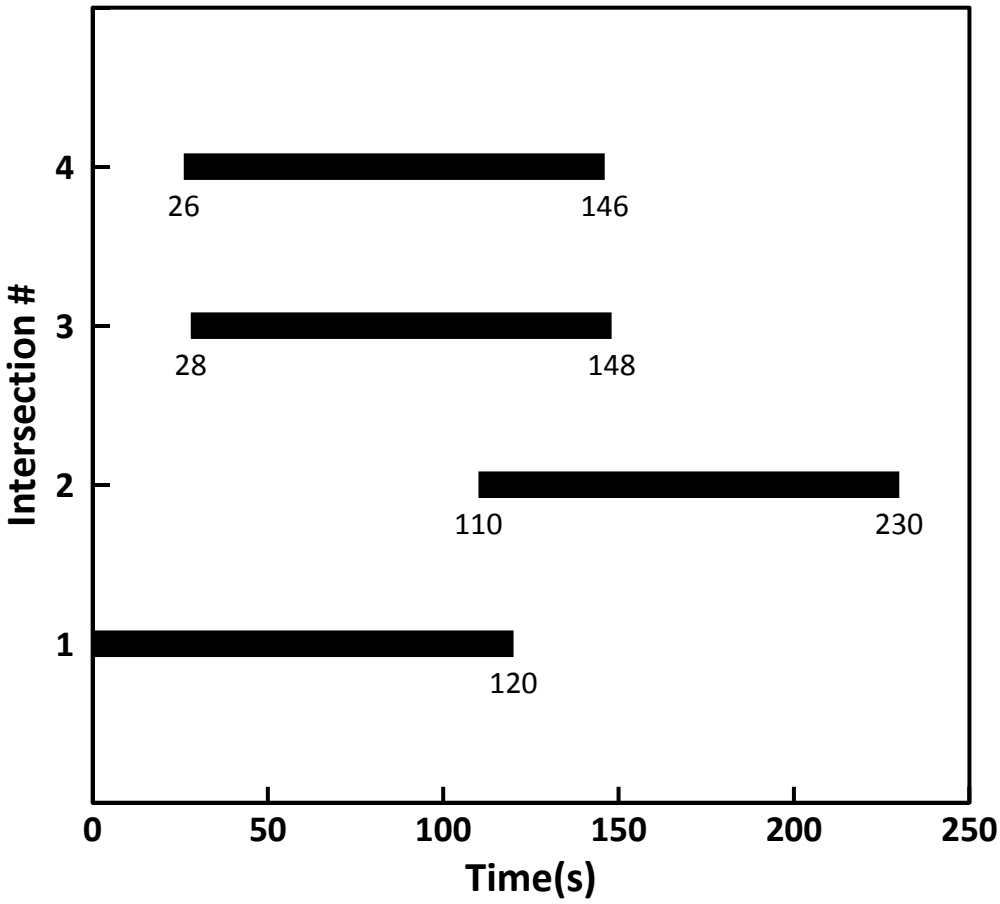

Figure 7 Offsets of the four coordinated intersections

2.3. Turning Volumes

The turning volumes in the developed model on Figure 8 represent real traffic flow going through, left and right in the Morgantown WV-705 corridor [6]. The morning peak-hour data (5:30-9:30 am) are used as an input parameter to represent the maximum load on the road network and to test the robustness of our model. The frequency of u-turns is negligibly small even at peak traffic volume, thus they are omitted from the model.

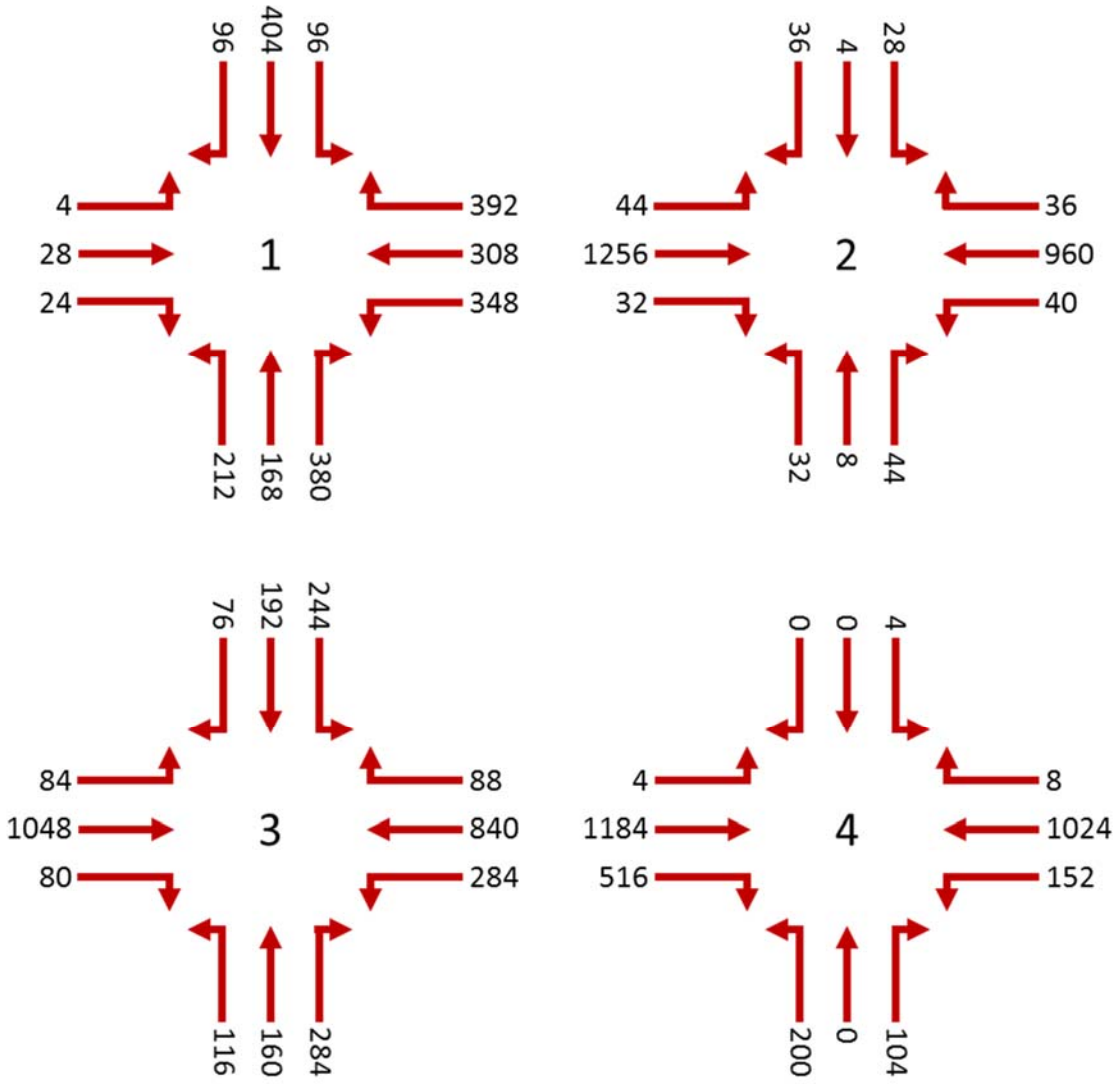

Figure 8 Turning volumes for morning peak-hour 5:30-9:00am

3. Methodology

3.1. EV Life Cycle

When a simulation starts, vehicles are constantly produced by all carSources blocks based on the corresponding rates/minute assigned there. EV in the proposed model runs every 15 minutes on major westbound approach. An EV can potentially effect emission since other cars have to give it right-of-way and stop for a few seconds. Therefore, it makes more sense to put EVs on the approach with more vehicles, the westbound approach in this case. A flowchart is developed to display life cycle of each EV.

The life cycle of an EV starts from production by its own EVcarSource block that is located near carSource D (Figure 9). The next step is to check whether the EV is in the road network or not. If the EV is not in the road network, it means that the EV has already made it through all 4 intersections and has already been disposed by carDispose block at A. If the EV is still in the road network, then we check if the next road segments that the EV is about to enter are included in "intersection set." This check is done as follows: we determine which road segment the front of the car is on (we specify front because the front and back of a car can be on different segments if the car in is transition between them) and consider the upcoming road segments. We iterate through the next segments to check if one of them is included in one of our four intersections. For that we look inside IntersectionCollection in AnyLogic and call the getTrafficLightByLaneName() method of every intersection with «segment name» as a parameter. This method returns the particular traffic light that the EV is approaching. Thus, we can determine whether this next segment belongs to any of the traffic lights and if it does belong, to which one exactly so we can give EVP to the specific intersection. If no traffic light is determined, the simulation goes back to check whether EV is on the road network. If a traffic light was found, we check the distance to this traffic light by calling the getOffset() method. This method returns distance that car already passed along current road segment. The distance to intersection is stored in the variable offsetToIntersection and is calculated by subtracting the distance that the car already passed along the current road segment from the segment length. If the distance to the intersection is bigger than the preemption distance of 200 meters, then it is too early to activate the EVP. In this case, the flowchart checks whether EV is still in the road network. If the distance to the intersection is smaller or equal to the preemption distance, we turn on EVP on the relevant traffic light by calling the method preemptionOn() with the traffic light as a parameter. As a next step, the simulation checks whether the EV entered an intersection. If the EV did not enter an intersection yet, it probably got hold/stuck in the traffic jam, so we turn EVP ON again. If the EV already entered an intersection, the next step of the simulation is to check whether the EV left an intersection. If the EV did not leave an intersection yet, the simulation continues to check every second until the EV leaves this intersection. If the EV already left an intersection, the simulation checks again if the EV is still in the road network.

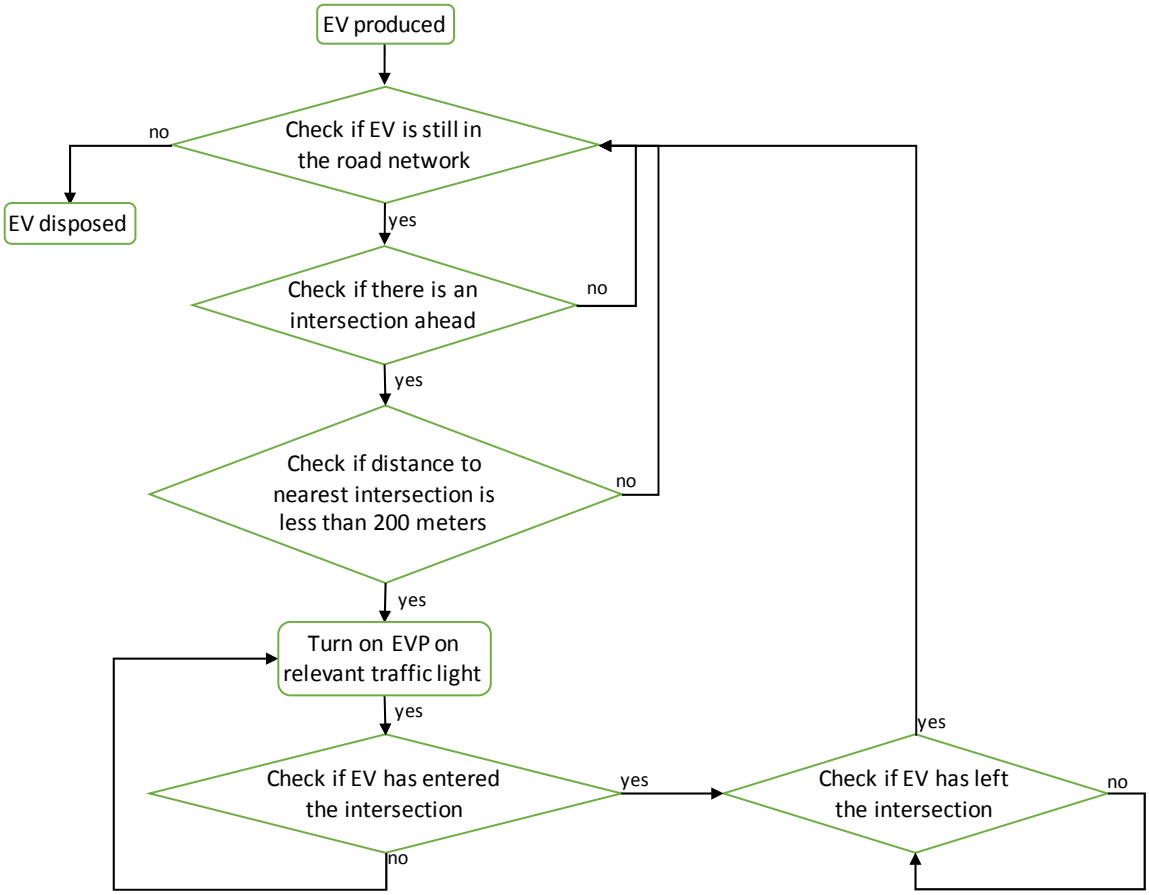

Figure 9 EV life cycle flowchart

3.2. EVP

EVP consists of Flowchart of preemption and dwell transition strategy, Agent-based behavior of EV and normal vehicles, giving Right-of-way to EV by normal cars, Stop of normal vehicles after lane switching for EV.

3.3. Flowchart of Preemption and Dwell Transition Strategy

The topic of EVP is of prime importance because of its implications for the efficiency of emergency responses and the safety of personnel in the EV. Much work has been done on this topic already, but further research is needed to encounter for EV and give it right-of-way by other vehicles and preemption by traffic light. The EVP flowchart on Figure 10 describes how the proposed model transitions between EVP and normal signal operation.

As described in Figure 9, preemption is started when the EV is within 200 meters of the traffic light. In this condition, a green light is given to the current approach of the EV and red lights are given to all other approaches. This allocation of green and red lights continues until the EV leaves the intersection and does not need EVP anymore. One of the main challenges is to restore traffic cycle back to its original timings so all intersections are coordinated again in the same way as before the EVP call disrupted normal operation. The Dwell transition strategy is

implemented in the current research as an efficient way to restoring signal. Transition can go different ways depending on which phase EVP call came in and which phase EVP call ended in. There are five possible situations depicted in Figure 10. These situations can be illustrated in an example using intersection 2 as the intersection that needs EVP. The major phases for intersection 2 are 2 and 6, and the statechart for intersection 2 is depicted in Figure 4.

Situation a (start: main – end: same phase): The EVP call comes in phase 2 and ends in phase 2. After the EVP call ends phase 2 is turned on again for the number of seconds left (i. e. we dwell right away).

Situation b (start: main – end: different phase): The EVP call comes in phase 2 and ends in phase 3. After the EVP call ends, phase 3 is skipped and phase 1 is turned on. After phase 1 ends, phase 2 is turned on and we dwell in that phase (i.e. we add to normal duration of phase 2 the number of unused seconds from phase 3).

Situation c (start: not main– end: same phase): The EVP call comes in in phase 3 and ends in phase 3. After the EVP call ends, phase 3 is skipped and phase 1 is turned on. After phase 1 ends, phase 2 is turned on and we dwell in that phase (i.e. we add to normal duration of phase 2 the number of unused seconds from phase 3).

Situation d (start: not main– end: different phase (main)): EVP call comes in phase 1 and ends in phase 2. After EVP call ends, phase 2 is turned on again for the number of seconds left (i.e., we dwell right away).

Situation e (start: not main– end: different phase (not main)): The EVP call comes in phase 3 and ends in phase 1. After the EVP call ends, phase 1 is skipped, phase 2 is turned on and we dwell in phase 2 (i.e., we add to normal duration of phase 2 the number of unused seconds from phase 1).

The main task regardless of situation is to restore the normal traffic coordination of intersections as soon as possible.

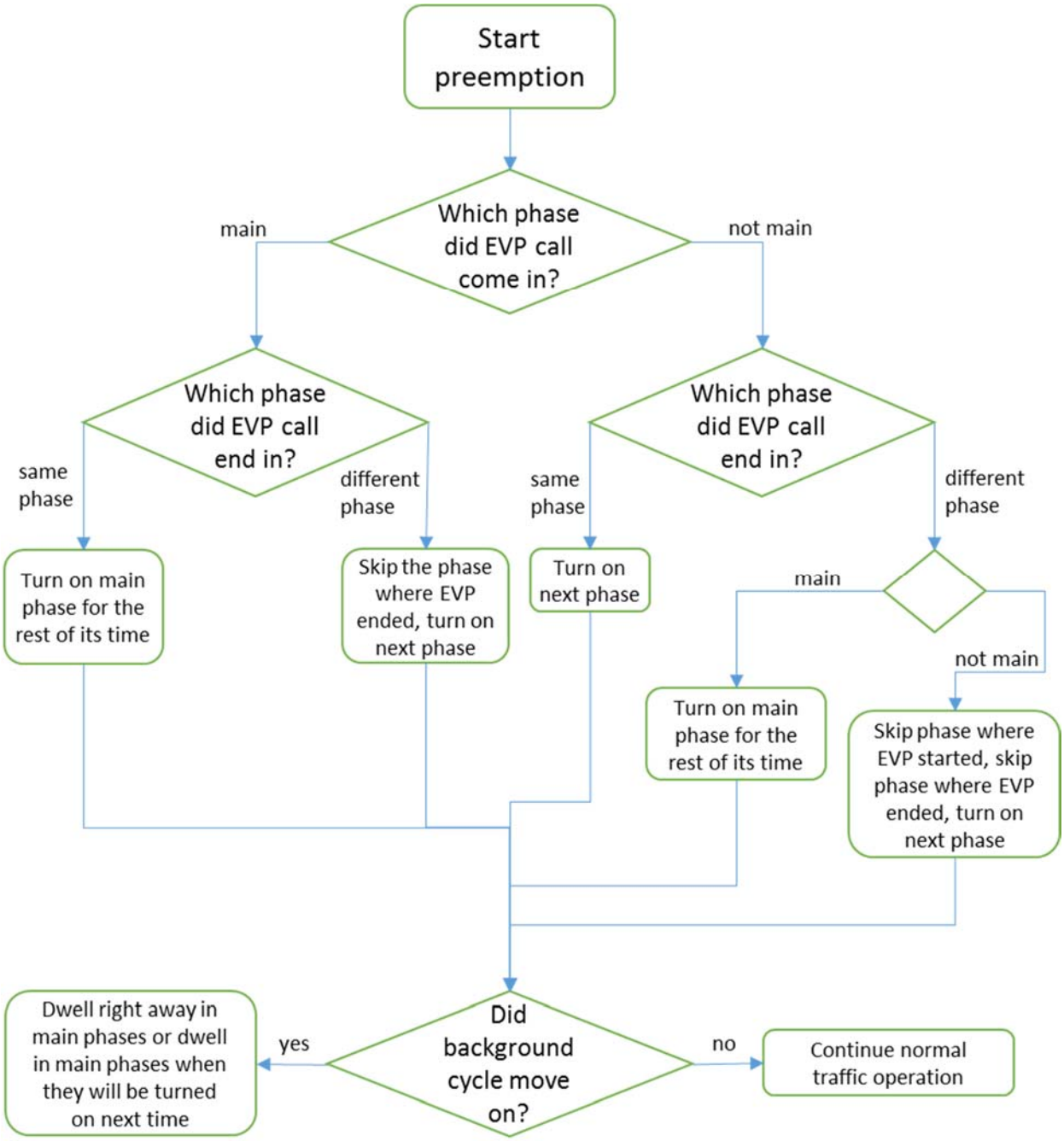

Figure 10 Flowchart of EVP with dwell transition strategy

3.4. Agent-based Behavior

The agent-based modeling is implemented in the current model in AnyLogic. This functionality allows normal vehicles and EV to behave like the agents and to interact with each other via messages.

3.5. Right-of-Way

When an EV appears in the road network, it needs to move as fast as possible. The EV knows the intended destination and is sure to occupy the appropriate lane in advance. The EV is forced to follow the same rules as all other vehicles regarding lane assignment. For example, it cannot turn left from the right most lane because there is no physical connector between right lane and left turn. Once the EV enters the road network, it constantly sends messages to normal vehicles in front and asks them to yield right-of-way by moving to the right lane and stopping. When normal vehicles receive such messages, they try to switch lanes if possible. Rules of lane switching are displayed in Figure 11 and explained below. If switching is not possible right away, vehicles keep trying until they succeed.

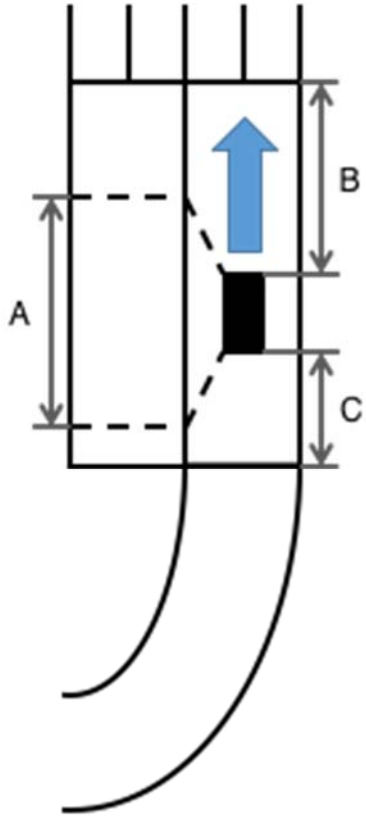

Figure 11 EV lane changing rules

Stop:
After normal vehicles give right-of-way to EV by switching lanes, they stop on the right lane for a few seconds before resuming their normal motion. Stopping time is a parameter that can be configured in settings before the start of the simulation.

Merging:
Sometimes in the process of merging, vehicles attempt to occupy the same space on the road at the same time. For example, one vehicle may cross the intersection going westward while another vehicle is turning left from northbound. In the real life this situation would cause a crash.

In the simulation there is only an exception in the software. There is no embedded functionality to solve these merge conflicts between vehicles in the current version of AnyLogic [16]. To avoid such cases, Lane Merge and Merge Resolver algorithms were implemented. The essence of Merge Resolver algorithm is that the pair of arc or arc and lane combinations where collisions take place are stored in a file. Then vehicles approaching that same potentially dangerous location communicate with each other and decide who will yield the right-of-way. The dynamics of Lane Merge algorithm is depicted on Figure 11. A represents the search length, which includes one car length in front of the car and one car length in the back of the car. B represents the distance remaining until the division of the two lane road to a four lane road. C represents the distance between the intersection and the current position of the vehicle. Figure 11 describes the situation when EV is travelling on the right lane of a two lane road and needs to switch to the left lane of the same two lane road. To accomplish this goal, a few requirements should hold true. First, no cars should be present in road segment. Second, B should be greater than 10 car lengths from the front of the car. Third, C should be greater than 20 meters. The same rules are applied for normal (not EV) vehicles when they are trying to give right-of-way to EV.

3.6. VT-micro Microscopic Emission Model

As mentioned earlier, this work used the VT-micro emission model. The equation of this microscopic emission model is presented below along with the table with coefficients that were provided by the field survey [25]:

$$\begin{aligned} MOE = \exp(& C_{11} + C_{12}V + C_{13}V^2 + C_{14}V^3 + \\ & C_{21}A + C_{22}AV + C_{23}V^2 + C_{24}AV^3 + \\ & C_{31}A^2 + C_{32}A^2V + C_{33}A^2V^2 + C_{34}A^2V^3 + \\ & C_{41}A^3 + C_{42}A^3V + C_{43}A^3V^2 + C_{44}A^3V^3) \end{aligned} \quad (1)$$

Where,
MOE is the calculated measure of effectiveness (fuel, HC, CO, NO_x) per second,
V is Speed (km/h),
A is Acceleration (m/s^2), and
C_{xy} are the coefficients provided in Table 1 (Rakha [25])

Emission of every vehicle for every second is calculated based on the VT-micro model and stored in the log file in the end of a simulation.

Table 1 Coefficients of VT-Micro Emission Model

Coefficients	Fuel	HC	CO	NOx
C_{11}	-7.533E+00	-7.280E-01	8.874E-01	-1.068E+00
C_{12}	3.255E-02	2.738E-02	7.790E-02	5.094E-02
C_{13}	-3.323E-04	-2.468E-04	-9.464E-04	-2.083E-04
C_{14}	1.965E-06	2.575E-06	6.099E-06	7.518E-07
C_{21}	1.484E-01	0.000E+00	1.633E-01	2.791E-01
C_{22}	5.789E-03	1.222E-02	4.660E-03	1.864E-02
C_{23}	-2.713E-05	-1.361E-04	1.232E-04	-1.731E-04
C_{24}	8.032E-08	8.959E-07	-1.024E-06	4.755E-07
C_{31}	1.920E-02	2.814E-02	3.678E-02	1.068E-02
C_{32}	1.101E-04	-7.253E-04	-1.223E-03	3.800E-03
C_{33}	1.358E-06	5.450E-05	7.130E-05	-8.504E-05
C_{34}	-3.945E-08	-3.388E-07	-4.995E-07	3.818E-07
C_{41}	-1.571E-03	-1.232E-04	-1.781E-03	-1.256E-03
C_{42}	-8.890E-05	-1.638E-04	0.000E+00	-4.654E-04
C_{43}	4.836E-07	5.266E-06	-2.243E-06	3.091E-06
C_{44}	-7.803E-09	-3.037E-08	0.000E+00	-2.199E-08

4. Analysis and Findings

4.1. Simulation, Offset Variation, and Validation

The proposed model was developed in simulation and optimization package AnyLogic 7.2. Although this software is not traffic specific like VISSIM, etc., it does include some useful classes and functionalities for traffic studies along with the Road Traffic, Analysis, Presentation, Agent, Process modeling, and Statechart libraries that were applied in the current research. The road network with four coordinated intersections, timing plans for every intersection, turning volumes were discussed previously.

Values for deceleration and acceleration are set according to comfortable rate for vehicle deceleration and acceleration (3 m/s2 and 2 m/s2 respectively) [26] [27]). Each simulation continues for 900 seconds. Vehicles are generated from different carSources based on the rate of vehicles per unit time that are different for every carSource. When the simulation is started, the functional layer of the road (Figure 3) becomes animated. The numbers below the road segments display vehicles on this segment with each vehicle in its corresponding state (i.e. this many vehicles entered this particular road segment carMoveTo, this many vehicles are moving, this many vehicles left). Also, the physical layer shows car movement on the road network according to lane assignments and timing plans. The physical layer also shows traffic lights changing color. Some states on Statecharts of the intersections (Figure 4) are highlighted showing which state the traffic light is currently in.

For the current research, multiple simulations were performed with different offsets. In the technique called offset variation, offsets ranging from 0 to 120 seconds were varied in 20 second increments. Altogether, 343 simulations were run in order to find optimal offsets for particular inputs such as road network, set of timing plans, and HRD. As a result of these simulations, optimal offsets were found to be 110, 20 and 20 seconds, in good agreement with offsets reported in Day [21].

After every simulation, we get output data in HRD format. Emissions of every vehicle in every second on each road segment are calculated based on the VT-micro model described earlier and stored in logs, which are processed later to find possible patterns in inputs.

Multiple scenarios can be run depending on EV inclusion/exclusion and emissions from each of those scenarios can be compared later on. No-EV scenario is when there is no EV in the road network. This is the base case. Scenarios EVP and EVP with right-of-way consider EV. In EVP scenario an EV gets EVP and cars move normally. In scenario EVP with right-of-way, an EV gets EVP and cars yield right-of-way. Any one of the scenarios can be chosen along with offsets before the start of the simulation in the simulation window. Later in the report, the degree to which EV effects emissions in different scenarios is analyzed.

The group and individual behavior of vehicles were analyzed as a way to sanity check the validity of the developed model. The vehicle flow travelling on the road network on Figure 12 represents vehicle group behavior. A red square around one of the vehicles indicates which vehicle was selected for individual profile checking.

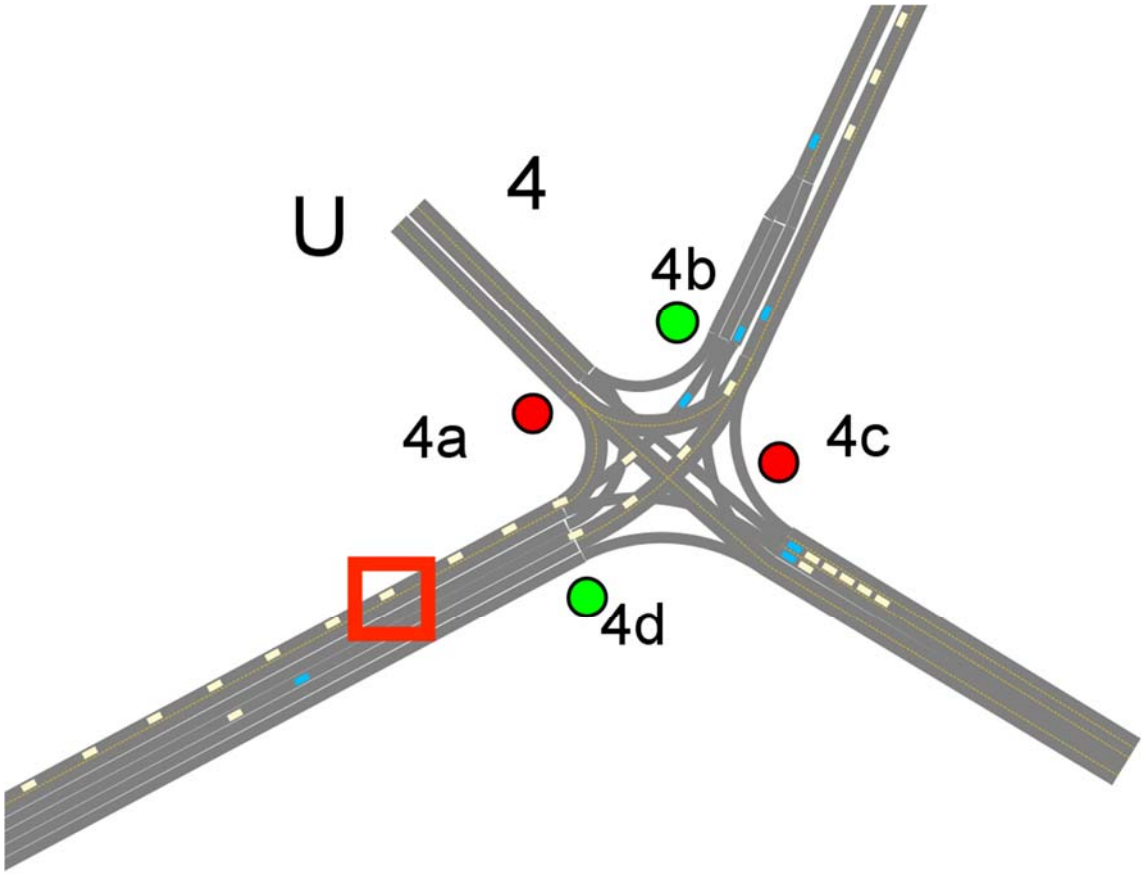

Figure 12 Group behavior of vehicles

An individual vehicle profile consisting of a time-space diagram, smoothed speed, and acceleration was extracted from a simulation shown on Figure 13, Figure 14, and Figure 15.

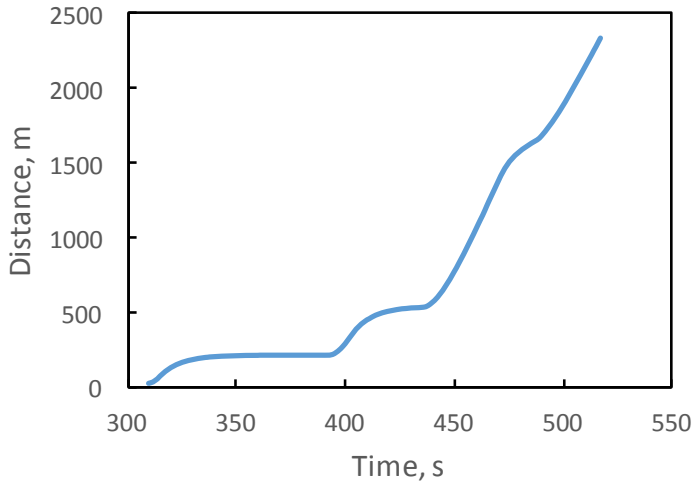

Figure 13 Time-space diagram of an individual vehicle

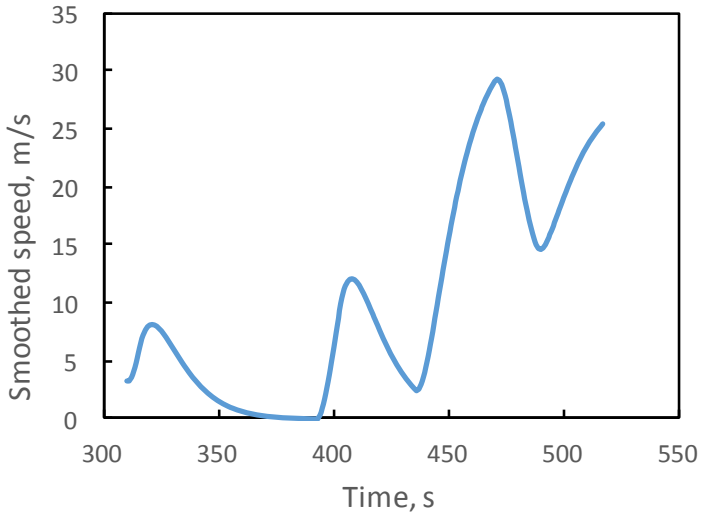

Figure 14 Smoothed speed of an individual vehicle

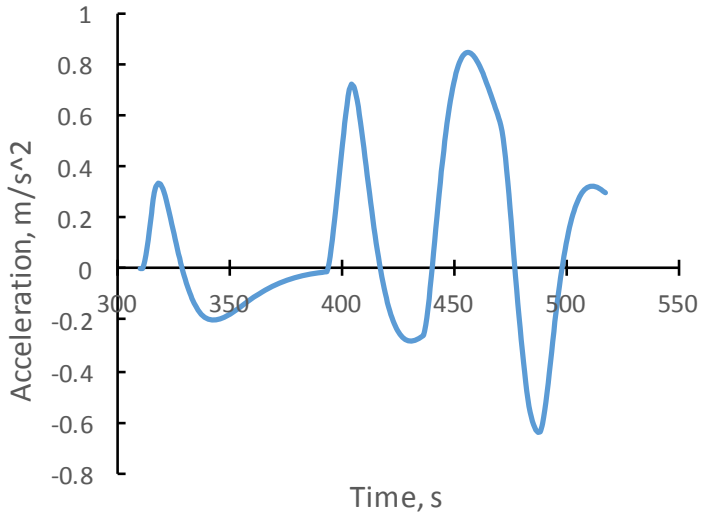

Figure 15 Acceleration of an individual vehicle

All four graphs display normal individual and group behavior of a vehicle, which, along with the good agreement of our offsets to literature values, indicates that the model is valid.

4.2. HRD Utilization in Emission Predication

There are two loop detectors in our model: 100 ft and 200 ft away from each intersection on the major approaches. The loop detectors are assumed to be 5 meters long.

There is a sample of HRD output from controllers of all 4 intersections in Table 2 and in Table 3. It consists of Signal ID, Timestamp, Event code ID and Parameter. The info of green, yellow and

red lights (Event code ID 1, 8 and 10) along with timeStamps are called signal phase info. The info about traffic moving on top of the detector and leaving it (EventCodeID 82 and 81) along with time stamps is called detector events info. From a combination of signal phase info and detector events info, the number of vehicles can be counted and their speeds and accelerations calculated.

Table 2 Sample of HRD from 200ft detector

Signal ID	Timestamp		Event code ID	Parameter
Intersection 1	6/11/15	30:00.0	1	2
Intersection 1	6/11/15	30:15.8	82	1
Intersection 1	6/11/15	30:16.0	81	1
Intersection 1	6/11/15	30:35.9	82	1
Intersection 1	6/11/15	30:36.1	81	1
Intersection 1	6/11/15	30:37.5	82	1
Intersection 1	6/11/15	30:37.7	81	1
Intersection 1	6/11/15	30:38.3	82	1
Intersection 1	6/11/15	30:38.5	81	1
Intersection 1	6/11/15	30:51.7	82	1
Intersection 1	6/11/15	30:51.9	81	1
Intersection 1	6/11/15	30:52.5	82	1
Intersection 1	6/11/15	30:52.7	81	1
Intersection 1	6/11/15	30:58.7	82	1
Intersection 1	6/11/15	30:59.0	81	1
Intersection 1	6/11/15	31:25.0	82	1
Intersection 1	6/11/15	31:25.2	81	1
Intersection 1	6/11/15	31:36.8	82	1
Intersection 1	6/11/15	31:37.0	81	1
Intersection 1	6/11/15	30:22.0	8	2

Table 3 Sample of HRD from 100ft detector

Signal ID	Timestamp		Event code ID	Parameter
Intersection 1	6/11/15	30:00.0	1	2
Intersection 1	6/11/15	30:16.6	82	2
Intersection 1	6/11/15	30:16.8	81	2
Intersection 1	6/11/15	30:36.8	82	2
Intersection 1	6/11/15	30:37.0	81	2
Intersection 1	6/11/15	30:38.3	82	2
Intersection 1	6/11/15	30:38.5	81	2
Intersection 1	6/11/15	30:39.2	82	2
Intersection 1	6/11/15	30:39.4	81	2
Intersection 1	6/11/15	30:52.5	82	2
Intersection 1	6/11/15	30:52.7	81	2
Intersection 1	6/11/15	30:53.3	82	2
Intersection 1	6/11/15	30:53.7	81	2

Intersection 1	6/11/15	30:59.8	82	2
Intersection 1	6/11/15	31:00.3	81	2
Intersection 1	6/11/15	31:25.7	82	2
Intersection 1	6/11/15	31:26.0	81	2
Intersection 1	6/11/15	31:37.5	82	2
Intersection 1	6/11/15	31:37.7	81	2
Intersection 1	6/11/15	30:22.0	8	2

HRD from Table 2 and Table 3 about loop detectors at 200ft and 100ft away from the intersection 2b was processed to generate the data shown in Table 4 and Table 5. For example, from Table 2 time ON (t1) and time OFF (t2) were collected that are first 2 columns in Table 4. Similarly, from Table 3 time ON (t3) and time OFF (t4) were collected that are first 2 columns in Table 5. Since the length of loop detector and vehicle occupancy are known (5 meters and (t2-t1)), speed V1 with which the vehicle was travelling on loop detector 200 ft and speed V2 with which the same vehicle was travelling on loop detector 100 ft can be calculated. Also, acceleration of a vehicle between these two loop detector can be calculated by dividing (V2-V1)/(t3-t1).

Table 4 200 ft loop detector data

t1	t2	V1
15.90	16.07	28.60
35.96	36.17	24.10
37.52	37.72	24.38
38.32	38.52	24.38
51.71	51.91	24.59
52.51	52.71	24.59
58.77	59.00	22.12
85.14	85.30	32.16
96.85	97.02	28.93

Table 5 100 ft loop detector data

t3	t4	V2
16.63	16.81	28.60
36.83	37.04	24.10
38.38	38.59	24.38
39.20	39.41	23.81
52.56	52.77	24.59
53.39	53.77	13.33
59.86	60.34	10.31
85.80	85.95	32.16
97.58	97.75	28.93

Using Table 4 and Table 5 (from 200 ft away and from 100ft away) we create Table 6.

Table 6 Data extracted from HRD

200 ft, t1	200 ft, t2	100 ft, t3	100 ft, t4	200 ft, V1	100 ft, V2	200-100ft,A
15.90 (82)	16.07 (81)	16.63 (82)	16.81(81)	28.60	28.60	0.00
35.96 (82)	36.17 (81)	36.83 (82)	37.04 (81)	24.10	24.10	0.00

Similarly, this table becomes filled with the data from all vehicles in all simulations. A separate table for each major approach is made (8 tables in total). As of now, the columns V1 and V2 are the most important ones. Then in every one of these 8 tables one more column named speed between 200ft and 100 ft was added so now the average speed for each approach is available with all simulations included. Now only cars that stopped anywhere on this particular approach that we are dealing with need to be selected. In the simulation this selection is done by a script to select stopped vehicles because we have full control over vehicles. In a reality only speeds and accelerations of the cars are available from HRD so a prediction based on speeds and accelerations must be made. It is known that stopped cars are the main contributors to vehicle emissions since when they accelerate they produce much more emissions than cruising cars. Therefore, the frequency distribution of the speeds between two detectors and accelerations of all stopped cars are plotted to identify the most frequent speeds and most frequent accelerations. In order to estimate the number of stopped cars in individual simulations, all cars that fall within the range of one standard deviation around the mean are selected. So, the most frequent speeds of the cars that will stop need to be considered. That is why the speed range of 1 standard deviation is selected and that should give good enough prediction. So, all vehicles on a particular road segment whose speeds fall within this range are counted. This is how stopped vehicles are predicted on the particular approach based on speed. Similarly, all vehicles on a particular road segment whose accelerations fall within identified range are counted. This is the way stopped vehicles are predicted on the particular approach based on accelerations. Also, cars that satisfy both speed-based ranges and acceleration-based ranges are selected. The number of stopped vehicles on a particular approach will be used for an analysis in the following sections.

4.3. Finding Classifier and Its Threshold

As stated in the introduction, vehicle emissions depend on timing plans, traffic volume and traffic characteristics. Hence, it makes sense to start searching for significant inputs approach-wise such average speed, average acceleration, standard deviation speed, standard deviation acceleration. Offset is insignificant so it is omitted.

As a result of all 343 simulations, a summary excel file with the essence of every simulation is produced. For example, intersection 4 has these outputs:

- total network emission within particular simulation
- offsets values
- westbound approach emission
- eastbound approach emission
- average speed on 4b
- average acceleration on 4b
- standard deviation in speeds on 4b
- standard deviation in acceleration on 4b

- average speed on 4d
- average acceleration on 4d
- standard deviation in speeds on 4d
- standard deviation in acceleration on 4d
- stopped vehicles on approach 4d based on speeds
- stopped vehicles on approach 4b based on speeds

There are three scenarios that have been simulated in this study, namely No EV, EVP, EVP with right-of-way. Thus, there are three summary excel files – one for every scenario.
In every scenario, CO emission, HC emission, NOx emission at the 4th intersection was sorted one after another. The 15 minimum and 15 maximum values were taken and used to produce graphs of number of stopped vehicles on two major approaches 4b and 4d of intersection 4. Figure 17 does not display a clear pattern as we see some overlap between minimum emission cases and maximum emission cases in No-EV scenario. In contrast, patterns in Figure 19 and Figure 21 are clear. EV makes scenarios more distinct. Regression analysis was applied to intersections 4 for all three scenarios with all available inputs. The predicted models shown in Figure 18, Figure 20, Figure 22 had R^2 values of 70%, 78%, 80% respectively.

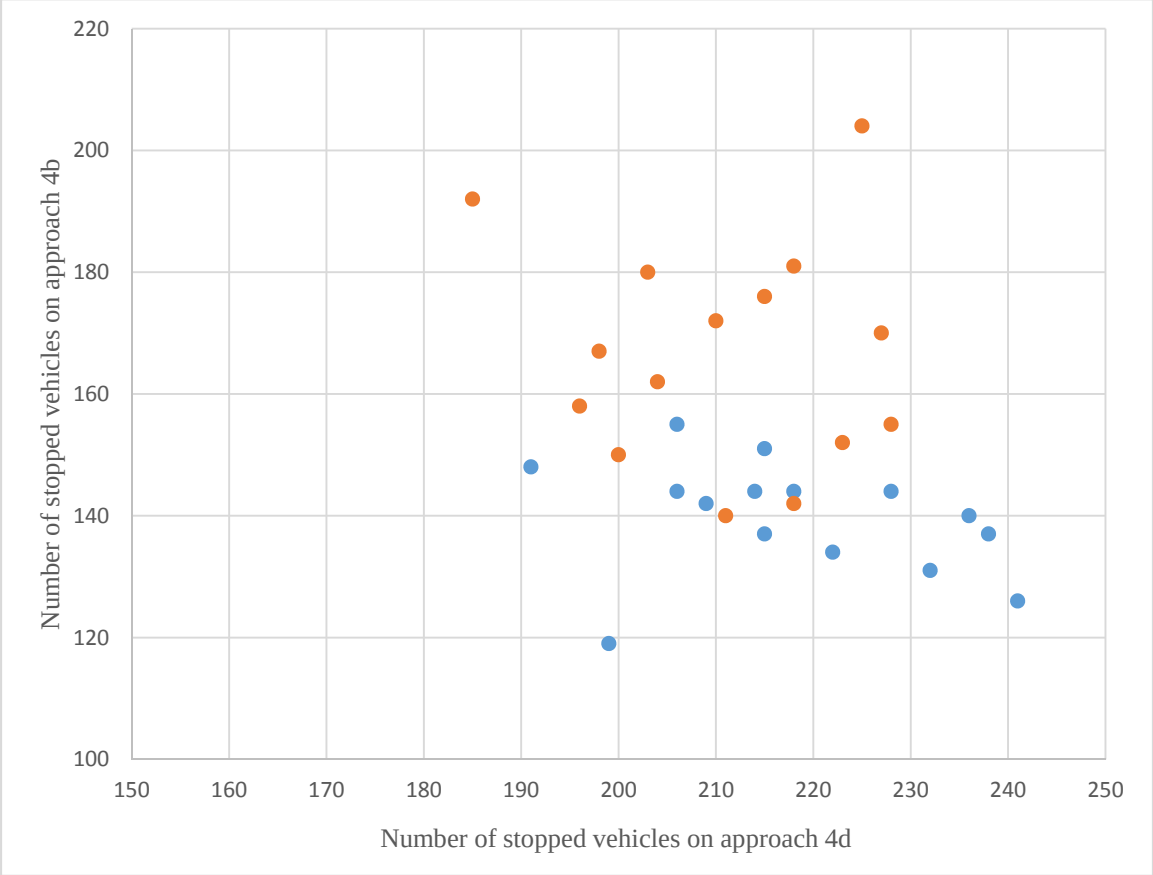

Figure 16 Stopped vehicles on approaches 4d and 4b in minimum emission no EV case (blue) vs maximum emission no EV case (red)

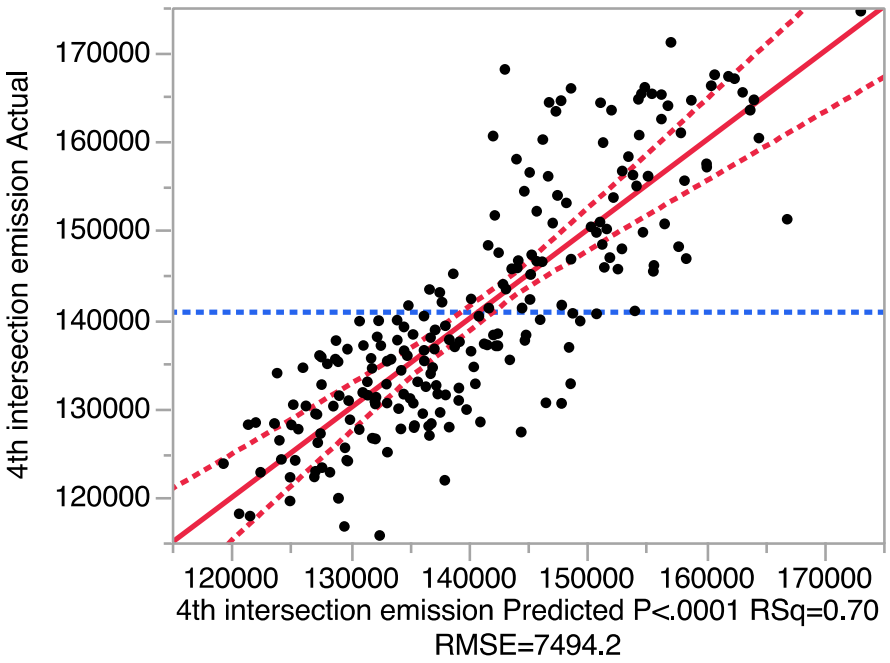

Figure 17 Prediction of the proposed model for intersection 4 in No-EV scenario

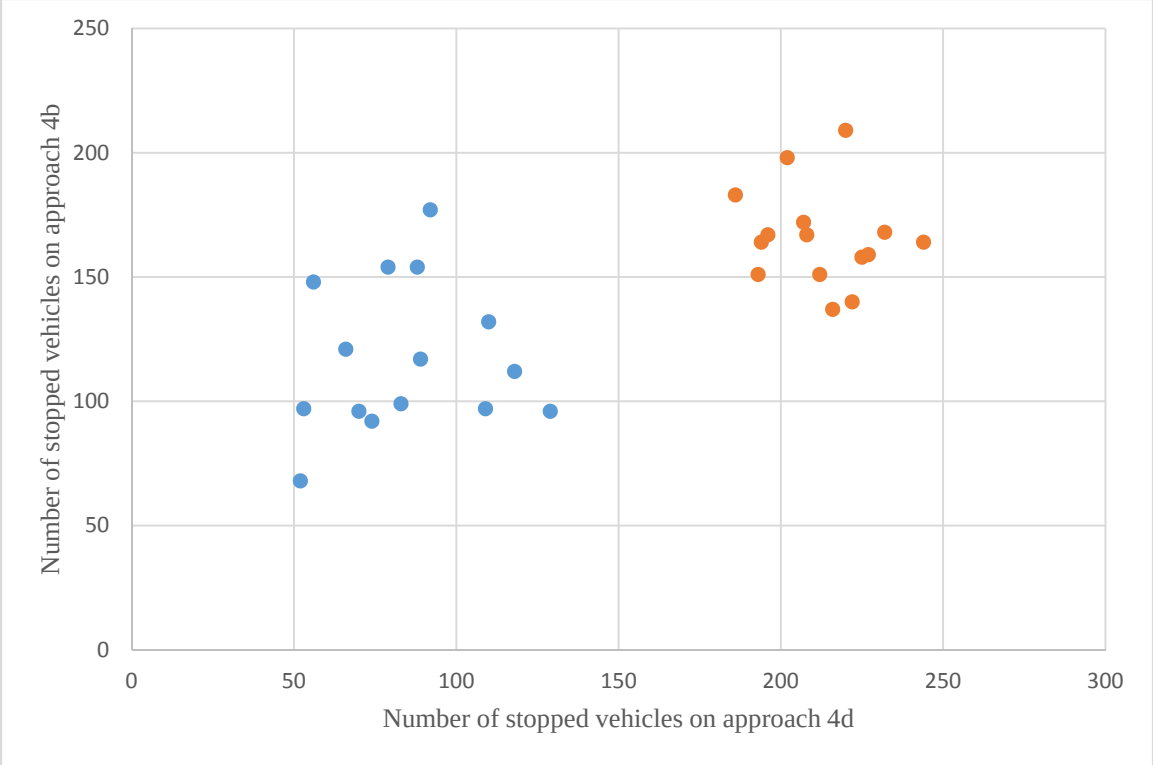

Figure 18 Stopped vehicles on approaches 4d and 4b in minimum emission EVP case (blue) vs maximum emission EVP case (red)

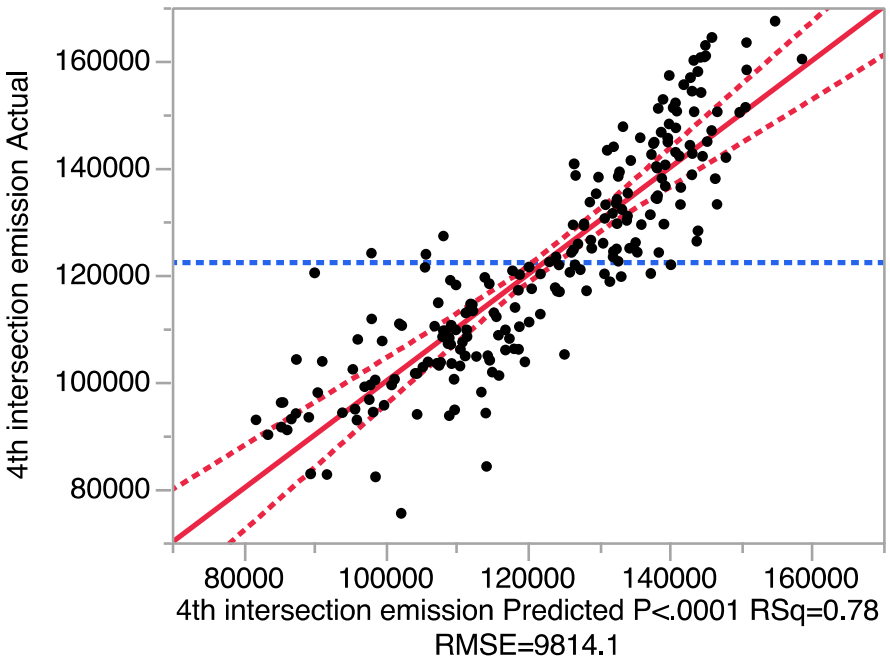

Figure 19 Prediction of the proposed model for intersection 4 in EVP scenario

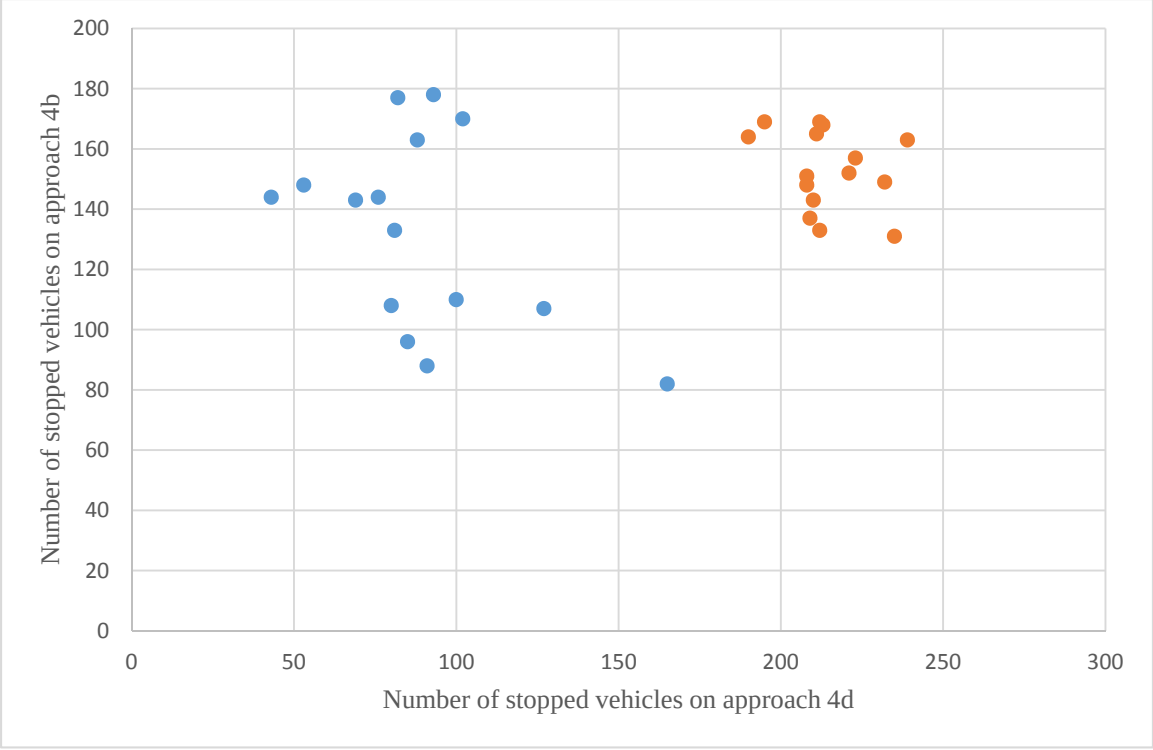

Figure 20 Stopped vehicles on approaches 4d and 4b in minimum emission EVP with right-of-way case (blue) vs maximum emission EVP with right-of-way case (red)

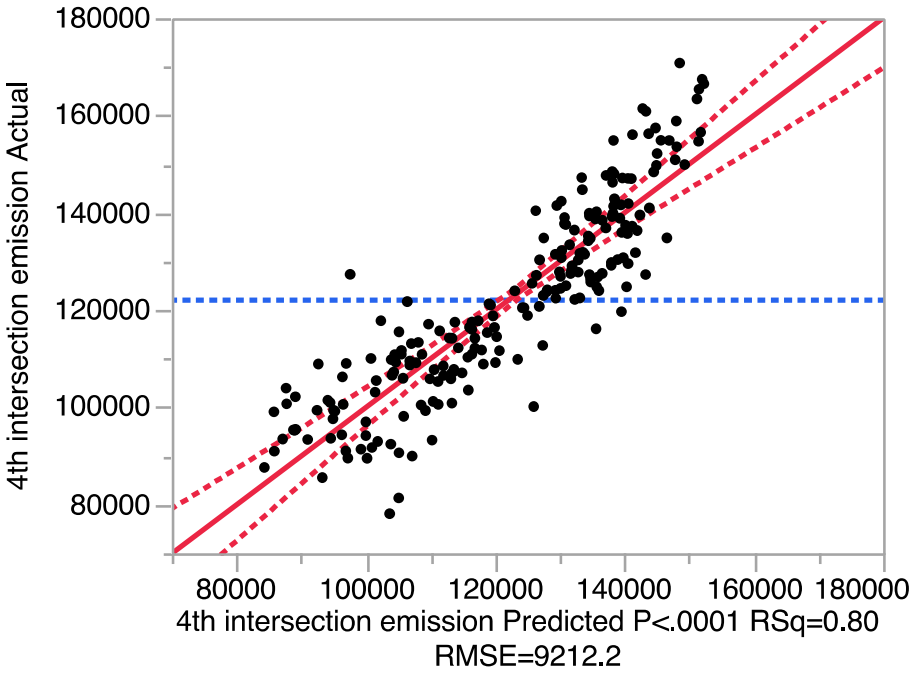

Figure 21 Prediction of the proposed model for intersection 4 in EVP with right-of-way scenario

Discriminant analysis has proved to be a useful tool for finding significance of the factors and the equation, that is why it was used to find a classifier for vehicle emissions based on HRD. Discriminant analysis was applied to intersection 4 based on stopped vehicles on 4b approach and stopped vehicles on 4d approach for No-EV, EVP and EVP with right-of-way scenarios. For every scenario, CO emission, HC emission, NOx emission was considered separately. Graphs for all 9 scenarios are shown on Figure 23 through Figure 31. The following figures show the reports generated by JMP statistical software.

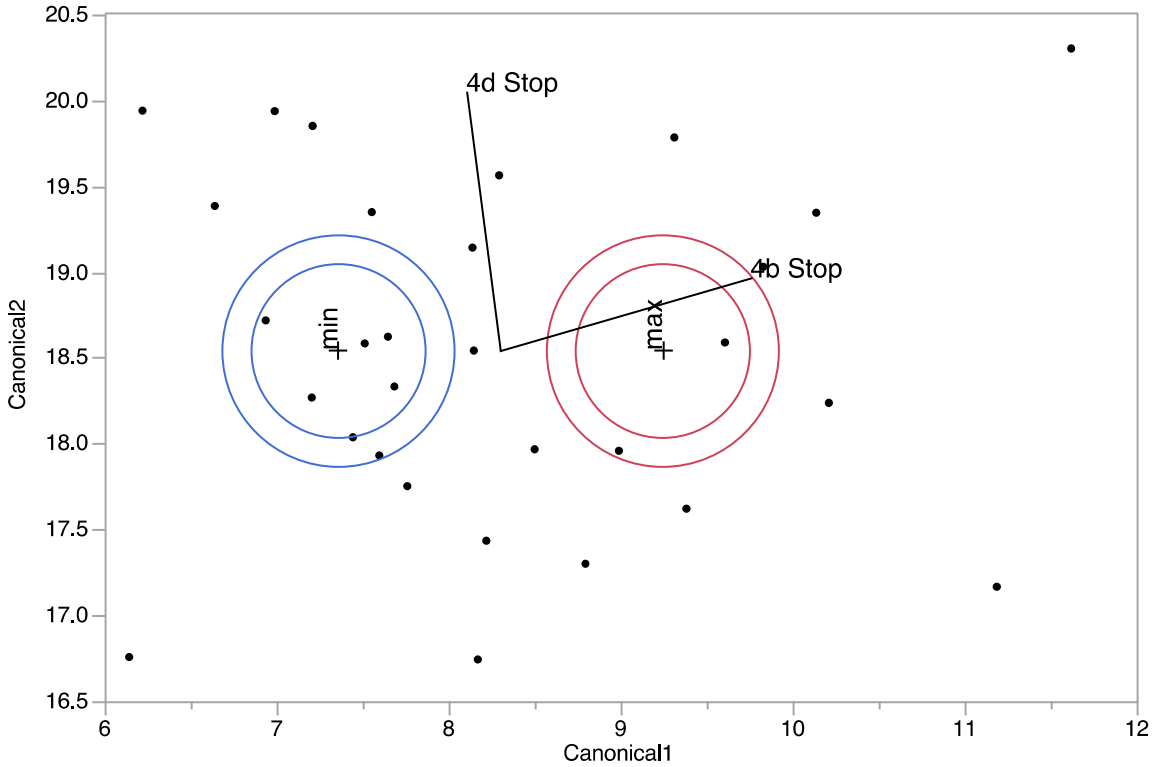

Figure 22 Discriminant analysis of intersection 4 based on stopped vehicles in No-EV scenario for CO emission

The equation for classifier for No-EV case for CO emission is provided below.
Canonical1 = -0.009*4d stopped cars + 0.067*4b stopped cars (1)

Calculated value of the classifier (threshold) less than 8.303 indicates acceptable level of emission at an intersection, greater than 8.303 belongs to unacceptable level of emission. Depending on the value for the classifier, decision can be make whether the emissions are within acceptable ranges or some changes are required for a particular intersection to bring down the emissions.

Minimum and maximum cases do not overlap and can be distinguished. Difference in CO emission between minimum average and maximum average cases in No-EV scenario is 36.1%.

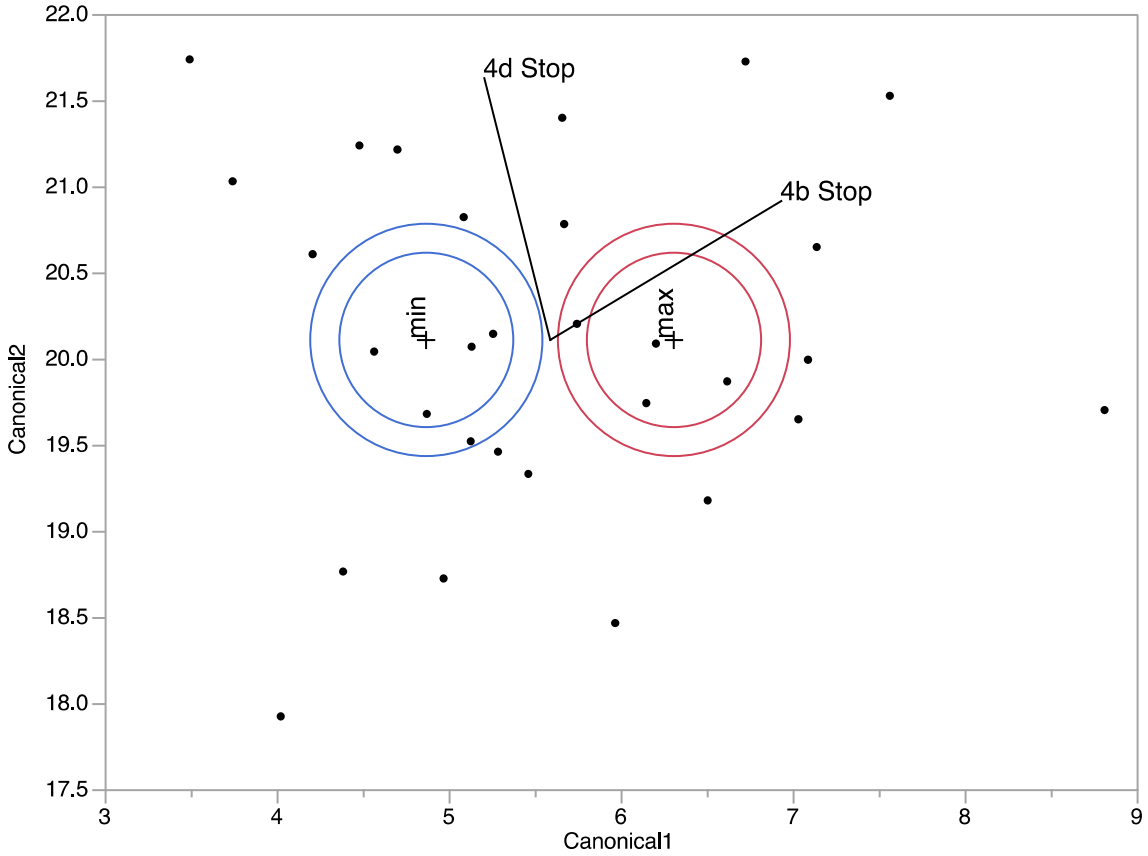

Figure 23 Discriminant analysis of intersection 4 based on stopped vehicles in No-EV scenario for HC emission

The equation for classifier for EVP case for HC emission is provided below.
Canonical1 = - 0.017*4d stopped cars + 0.062*4b stopped cars (2)

Threshold is 5.590.

Minimum and maximum cases do not overlap and can be distinguished. However, they are very close to one another. Difference in HC emission between minimum average and maximum average cases in No-EV scenario is 50.6%.

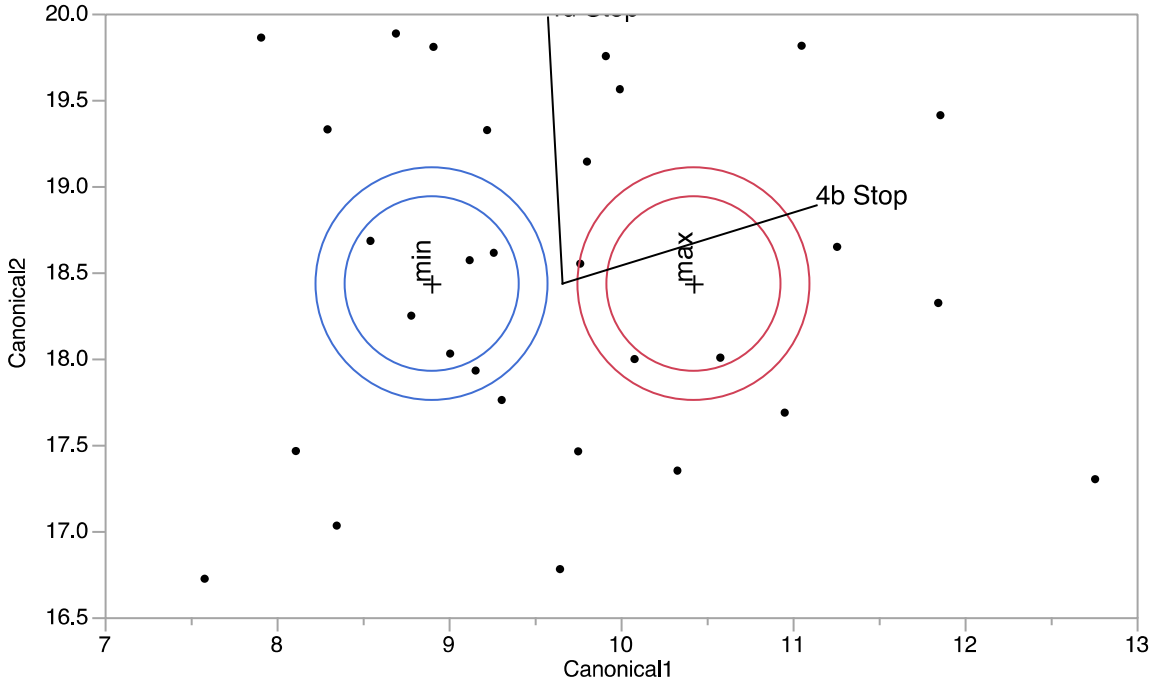

Figure 24 Discriminant analysis of intersection 4 based on stopped vehicles in No-EV scenario for NOx emission

The equation for classifier for EVP case for NOx emission is provided below.
Canonical1 = - 0.004*4d stopped cars + 0.070*4b stopped cars (3)

Threshold is 9.662.

Minimum and maximum cases do not overlap and can be distinguished. However, they are very close to one another. Difference in NOx emission between minimum average and maximum average cases in No-EV scenario is 41.0%.

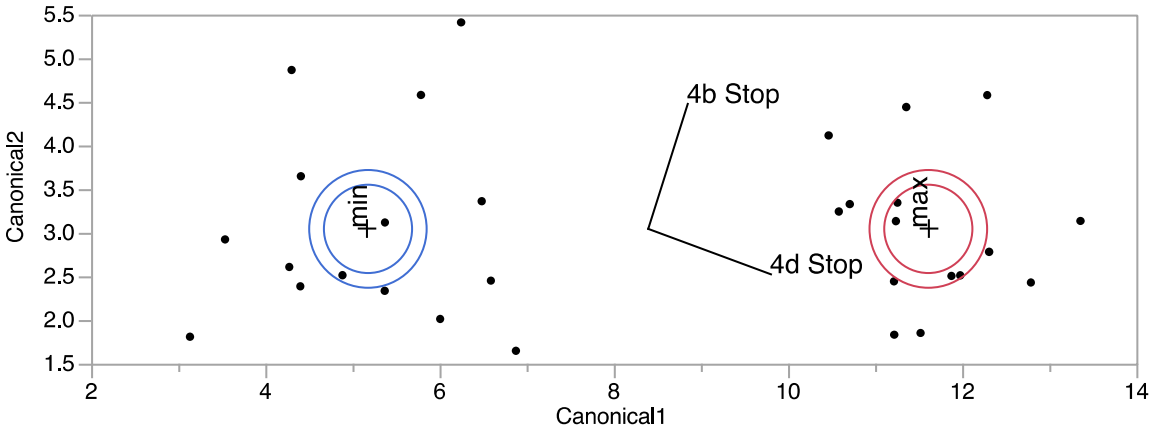

Figure 25 Discriminant analysis of intersection 4 based on stopped vehicles in EVP scenario for CO emission

The equation for classifier for EVP case for CO emission is provided below.
Canonical1 = 0.044*4d stopped cars + 0.012*4b stopped cars (4)

Threshold is 8.395.

Minimum and maximum cases do not overlap and can be well distinguished. Difference in CO emission between minimum average and maximum average cases in EVP scenario is 79.4%.

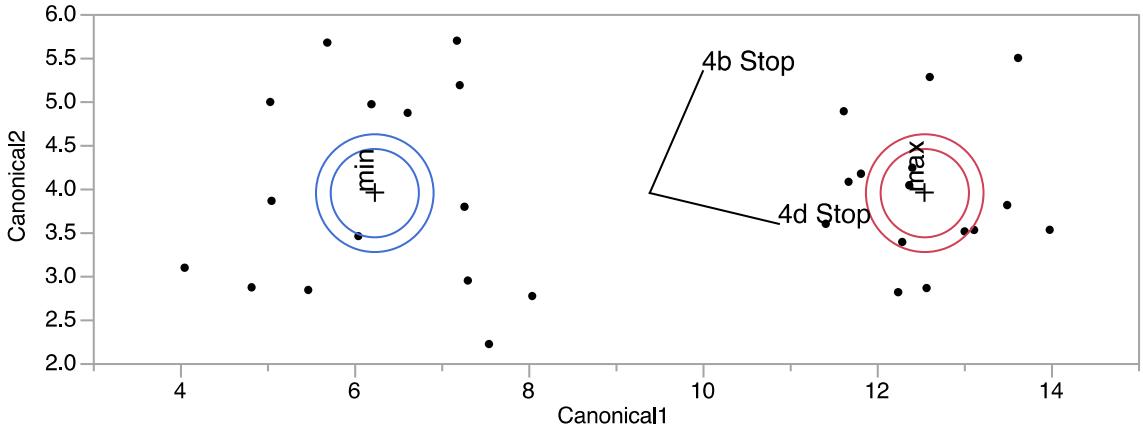

Figure 26 Discriminant analysis of intersection 4 based on stopped vehicles in EVP scenario for HC emission

The equation for classifier for EVP case for HC emission is provided below.
Canonical1 = 0.046*4d stopped cars + 0.017*4b stopped cars (5)

Threshold is 9.393.

Minimum and maximum cases do not overlap and can be well distinguished. Difference in HC emission between minimum average and maximum average cases in EVP scenario is 86.8%.

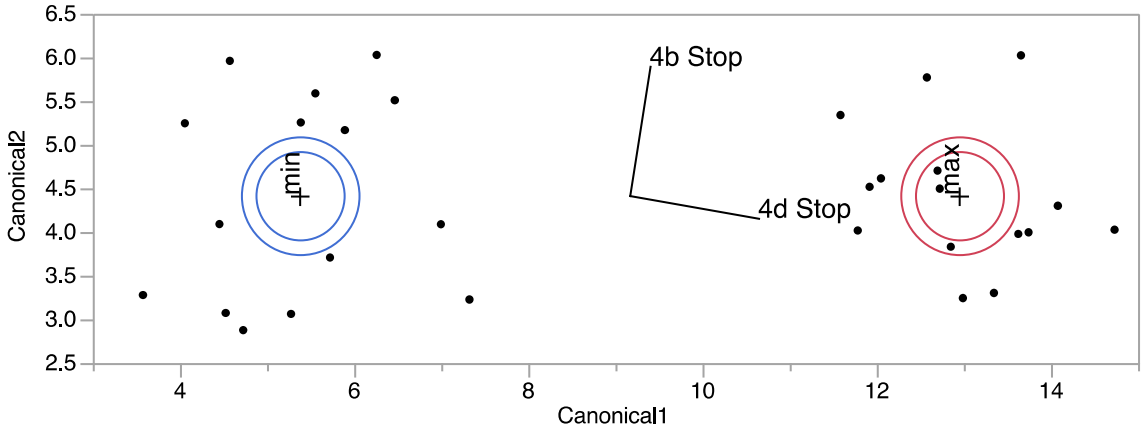

Figure 27 Discriminant analysis of intersection 4 based on stopped vehicles in EVP scenario for NOx emission

The equation for classifier for EVP case for NOx emission is provided below.
Canonical1 = 0.056*4d stopped cars + 0.006*4b stopped cars (6)

Threshold is 9.171.

Minimum and maximum cases do not overlap and can be well distinguished. Difference in NOx emission between minimum average and maximum average cases in EVP scenario is 81.2%.

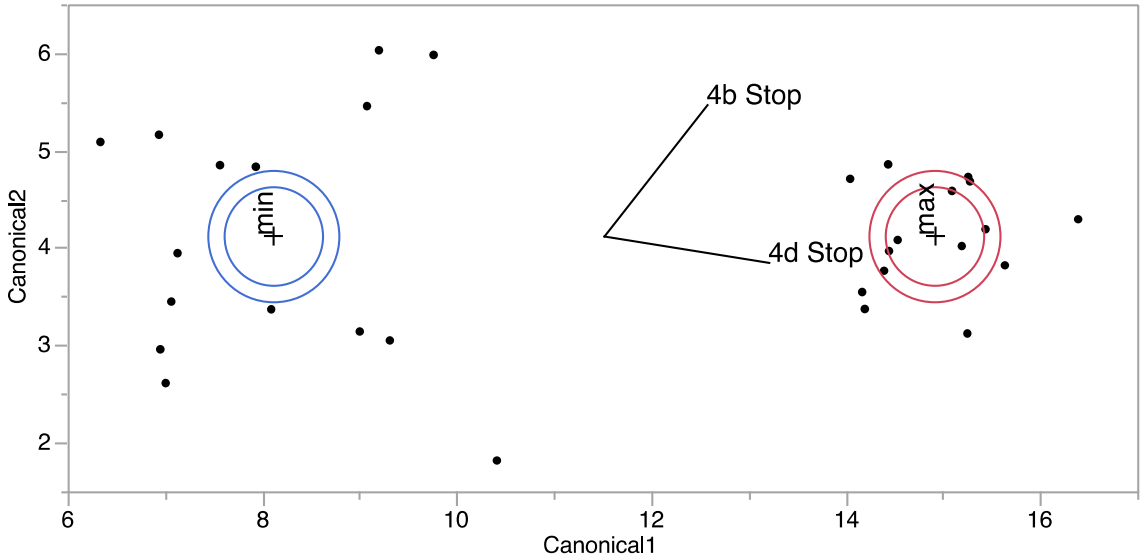

Figure 28 Discriminant analysis of intersection 4 based on stopped vehicles in EVP with right-of-way scenario CO emission

The equation for classifier for EVP case for CO emission is provided below.
Canonical1 = 0.048*4d stopped cars + 0.030*4b stopped cars (7)

Threshold is 11.520.

Minimum and maximum cases do not overlap and can be well distinguished. Difference in CO emission between minimum average and maximum average cases in EVP with right-of-way scenario is 78.6%.

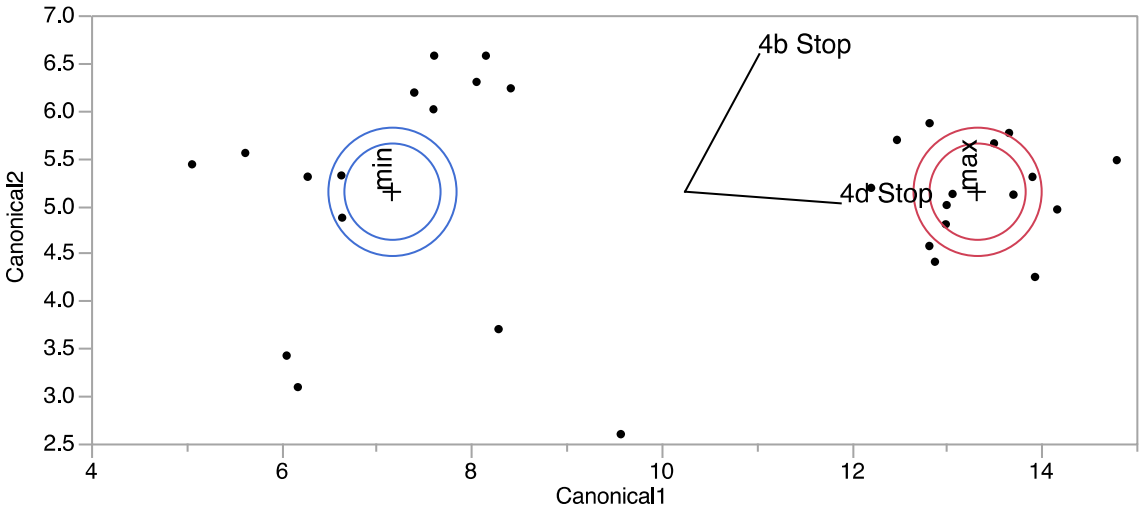

Figure 29 Discriminant analysis of intersection 4 based on stopped vehicles in EVP with right-of-way scenario CO emission

The equation for classifier for EVP case for HC emission is provided below.
Canonical1 = 0.048*4d stopped cars + 0.021*4b stopped cars (8)

Threshold is 10.250.

Minimum and maximum cases do not overlap and can be well distinguished. Difference in HC emission between minimum average and maximum average cases in EVP with right-of-way scenario is 90.8%.

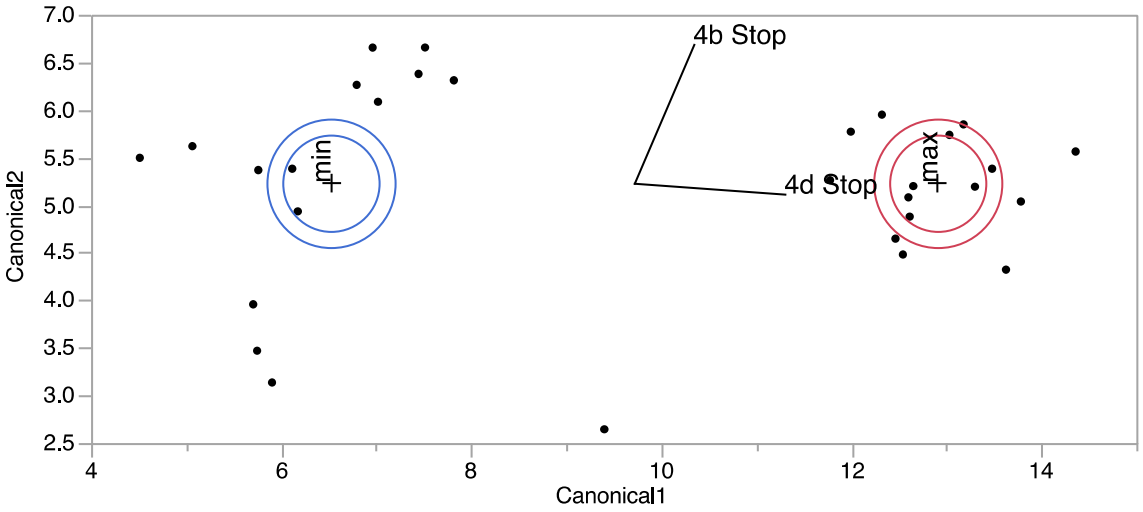

Figure 30 Discriminant analysis of intersection 4 based on stopped vehicles in EVP with right-of-way scenario CO emission

The equation for classifier for EVP with right-of-way case for NOx emission is provided below.
Canonical1 = 0.049*4d stopped cars + 0.017*4b stopped cars (9)

Threshold is 9.722.

Minimum and maximum cases do not overlap and can be well distinguished. Difference in NOx emission between minimum average and maximum average cases in EVP with right-of-way scenario is 82.8%.

Comparison of discriminants is provided in Table 7.

Table 7 Comparison of discriminants

	No-EV	EVP	EVP with right-of-way
CO	8.303	8.395	11.520
HC	5.590	9.393	10.250
NOx	9.662	9.171	9.722
Total emission	8.3	8.5	10.8

In No-EV scenario discriminant based on CO captures the difference between maximum and minimum cases. In EVP and EVP with right-of-way scenarios all three discriminants capture the difference between maximum and minimum cases.

CO discriminant is not sensitive to No-EV and EVP scenarios. However, CO discriminant is different in EVP with right-of-way scenarios. HC discriminant in all 3 scenarios is sensitive. It increased from 5.590 in No-EV scenario to 9.393 in EVP scenario and further increased to 10.250 in EVP with right-of-way scenario. NOx discriminant is not sensitive to any of the 3 scenarios. Total emission, that is a sum of CO, HC and NOx emissions, approximately reflects CO discriminant in all 3 scenarios.

NOx seems to be a good classifier since it does not change scenario to scenario and dos not depend on EV presence. NOx discriminant has average value of threshold around 9.5.

4.4. Impact of EV Presence on Emissions

As was mentioned earlier, there is an attempt to find out whether presence of EV changes emissions and if it does to what extent. Outputs from offset variation for No EV scenario found previously are compared to offset variation for EVP scenario (EVP is given and vehicles move normally) and EVP with right-of-way scenario (EVP is given and vehicles yield to EV). All three scenarios are plotted for the westbound approach on Figure 32.

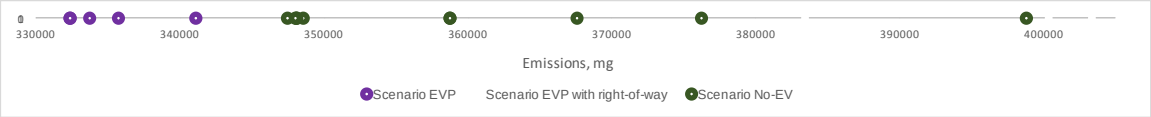

Figure 31 Comparison of maximum emissions in scenarios No-EV, EVP and EVP with right-of-way in westbound approach

Emissions observed for all scenarios are provided in Table 8. Emissions in EVP scenario are 9% less than in the No-EV scenario. Emissions in scenario EVP with right-of-way are 16.5% bigger than in No-EV scenario.

Table 8 Comparison of maximum emissions in all scenarios

Scenario EVP	Scenario No-EV	Scenario EVP with right-of-way
Emission on westbound approach	Emission on westbound approach	Emission on westbound approach
341187.33	398861.64	444058.0614
335803.21	376287.81	439058.0614
333821.21	367660.71	403429.9788
332428.35	358795.10	400429.9788
332428.35	358795.10	423429.9788
328813.58	348648.04	423429.9788
327171.11	348151.54	383429.9788
325216.41	348151.54	424429.9788
325216.41	348040.63	412429.9788
324342.04	347497.08	439429.9788

However, different relationships between scenarios may occur if compared at the intersections or at the individual approaches.

5. Conclusions

Previous research proved that stored HRD from traffic controllers can be an effective tool to estimate emissions for two reasons. First, if detectors are already installed near the intersections, HRD in form of controller's logs are most likely already stored and available for analysis. Utilizing this data saves the time and high costs involved in conducting a survey to obtain necessary data. Second, HRD is stored in a format that is widely-accepted and commonly-known. Thus it is relatively easy for engineers to understand the data and use it in traffic analysis. The above mentioned reasons justify the use of HRD. The HRD used in this study was taken from the Morristown WV-705 corridor. The number of stopped vehicles at an intersection in this corridor was determined based on event codes and timings from the controller's log. Also, speed and acceleration of the vehicles were calculated based on HRD to use later in emissions calculations with the VT-micro microscopic emission model. HRD and emission values from a few most and least optimal emission cases of one of the intersections were fed into statistical software and processed with discriminant analysis. A classifier threshold value of 14.2 along with its formula based on stopped vehicles were developed to help traffic engineers estimate emission at the intersection judging by HRD only. Besides analysis of normal traffic, HRD is an effective tool to process info about EVs, specifically EVP call ON and OFF events. This allows evaluation of the effect EVP has on emissions. This information is critical because EVs are a very important participant of a road network and should be given right-of-way over other cars if possible. The work presented in this study compared scenarios with and without EVP to test the hypothesis that EVP affects emissions.

The road network WV-705 with four intersections was implemented in AnyLogic 7.2 software and signals were coordinated. The VT-Micro emission model was incorporated in AnyLogic to calculate emission from the vehicles. Process for calculating individual vehicle speeds and accelerations from HRD and analyzing them to predict number of stopped vehicles was shown. Development of the classifier to predict emissions based on stopped vehicles from HRD was presented, its thresholds and equation were reported.

Results indicate that vehicle emissions in EVP case without other cars yielding to EV is 8% less compared to emission from No EV case. Vehicle emissions in EVP case with other cars giving right-of-way to EV is 16.5% more compared to No EV case emission.

With the methods described in this study, a Traffic Engineer may use the developed classifier to justify whether any changes are to be made to reduce emissions at intersections. As a result, intersections with excessive emissions can be quickly identified and given priority in efforts to improve performance just by utilizing HRD from an office instead of measuring emissions in the field. Our research is significant due to its potential in estimating vehicle emissions and pointing out any existing problems

6. Recommendations for Future Work

Future research should focus on developing and analyzing different road networks to refine the proposed set of classifiers and increase their precision. New ways of utilizing HRD to evaluate and improve the overall control scheme should also be explored.

Reference List

1. Paniati, J. and M. Amoni, Traffic Signal Preemption for Emergency Vehicle a Cross—Cutting Study. US Federal Highway Administration, 2006.
2. Louisell, C., et al., Simple worksheet method to evaluate emergency vehicle preemption and its impacts on safety. Transportation Research Record: Journal of the Transportation Research Board, 2004(1867): p. 151-162.
3. Qin, X. and A.M. Khan, Control strategies of traffic signal timing transition for emergency vehicle preemption. Transportation research part C: emerging technologies, 2012. 25: p. 1-17.
4. Nelson, E. and D. Bullock, Impact of emergency vehicle preemption on signalized corridor operation: An evaluation. Transportation Research Record: Journal of the Transportation Research Board, 2000(1727): p. 1-11.
5. Jordan, C.A. and M. Cetin. Signal Preemption Strategy for Emergency Vehicles Using Vehicle to Infrastructure Communication. in Transportation Research Board 94th Annual Meeting. 2015.
6. Chou, C.-S. and A.P. Nichols. Characterizing Emergency Vehicle Preemption Operation Using High-Resolution Traffic Signal Event Data. in Transportation Research Board 95th Annual Meeting. 2016.
7. Wang, Z., et al. Emission Mitigation via Longitudinal Control of Intelligent Vehicles in a Congested Platoon: An Exploratory Study. in Transportation Research Board 94th Annual Meeting. 2015.
8. Chang, M.-F. and R. Herman, Trip time versus stop time and fuel consumption characteristics in cities. Transportation Science, 1981. 15(3): p. 183-209.
9. Rakha, H. and Y. Ding, Impact of stops on vehicle fuel consumption and emissions. Journal of Transportation Engineering, 2003. 129(1): p. 23-32.
10. An, F., et al., Development of comprehensive modal emissions model: operating under hot-stabilized conditions. Transportation Research Record: Journal of the Transportation Research Board, 1997(1587): p. 52-62.
11. Rakha, H., K. Ahn, and A. Trani, Comparison of MOBILE5a, MOBILE6, VT-MICRO, and CMEM models for estimating hot-stabilized light-duty gasoline vehicle emissions. Canadian Journal of Civil Engineering, 2003. 30(6): p. 1010-1021.
12. Rakha, H., H. Yue, and F. Dion, VT-Meso model framework for estimating hot-stabilized light-duty vehicle fuel consumption and emission rates. Canadian Journal of Civil Engineering, 2011. 38(11): p. 1274-1286.
13. Akcelik, R., An interpretation of the parameters in the simple average travel speed model of fuel consumption. Australian Road Research, 1985. 15(1).
14. Bachman, W., et al., Modeling regional mobile source emissions in a geographic information system framework. Transportation Research Part C: Emerging Technologies, 2000. 8(1): p. 205-229.
15. Yue, H., Mesoscopic fuel consumption and emission modeling. 2008.
16. AnyLogic documentation. 2015.
17. Sturdevant, J.R., et al., Indiana Traffic Signal Hi Resolution Data Logger Enumerations. 2012.
18. Lavrenz, S.M., et al. Characterizing Signalized Intersection Performance Using Maximum Vehicle Delay. in Transportation Research Board 94th Annual Meeting. 2015.

19. Hainen, A., et al., High-Resolution Event-Based Data at Diamond Interchanges: Performance Measures and Optimization of Ring Displacement. Transportation Research Record: Journal of the Transportation Research Board, 2014(2439): p. 12-26.
20. Hainen, A.M., et al., Sequence Optimization at Signalized Diamond Interchanges Using High-Resolution Event-Based Data. Transportation Research Record: Journal of the Transportation Research Board, 2015(2487): p. 15-30.
21. Day, C., et al., Performance measures for adaptive signal control: Case study of system-in-the-loop simulation. Transportation Research Record: Journal of the Transportation Research Board, 2012(2311): p. 1-15.
22. Day, C. and D. Bullock, Arterial performance measures, volume 1: performance-based management of arterial traffic signal systems. Final report, NCHRP, 2011.
23. Day, C., J. Sturdevant, and D. Bullock, Outcome-oriented performance measures for management of signalized arterial capacity. Transportation Research Record: Journal of the Transportation Research Board, 2010(2192): p. 24-36.
24. Day, C., et al., Evaluation of arterial signal coordination: methodologies for visualizing high-resolution event data and measuring travel time. Transportation Research Record: Journal of the Transportation Research Board, 2010(2192): p. 37-49.
25. Rakha, H., K. Ahn, and A. Trani, Development of VT-Micro model for estimating hot stabilized light duty vehicle and truck emissions. Transportation Research Part D: Transport and Environment, 2004. 9(1): p. 49-74.
26. Hoberock, L., A survey of longitudinal acceleration comfort studies in ground transportation vehicles. Journal of Dynamic Systems, Measurement, and Control, 1977. 99(2): p. 76-84.
27. Maurya, A.K. and P.S. Bokare, Study of deceleration behaviour of different vehicle types. International Journal for Traffic and Transport Engineering, 2012. 2(3): p. 253-270.